

ALTERNATIVES TO INFLATION  
—  
NON-MINIMAL EKPYROSIS AND CONFLATION

D I S S E R T A T I O N

ZUR ERLANGUNG DES AKADEMISCHEN GRADES  
D O C T O R R E R U M N A T U R A L I U M  
(DR. RER. NAT.)  
IM FACH PHYSIK

EINGEREICHT AN DER  
MATHEMATISCHE-NATURWISSENSCHAFTLICHEN FAKULTÄT  
DER HUMBOLDT-UNIVERSITÄT ZU BERLIN

von  
ANGELIKA FERTIG

PRÄSIDENT DER HUMBOLDT-UNIVERSITÄT ZU BERLIN:  
PROF. DR. JAN-HENDRIK OLBERTZ

DEKAN DER MATHEMATISCHE-NATURWISSENSCHAFTLICHEN FAKULTÄT:  
PROF. DR. ELMAR KULKE

GUTACHTER:

1. PROF. DR. HERMANN NICOLAI HUMBOLDT-UNIVERSITÄT ZU BERLIN
2. PROF. DR. KAZUYA KOYAMA UNIVERSITY OF PORTSMOUTH
3. PROF. DR. JAN PLEFKA HUMBOLDT-UNIVERSITÄT ZU BERLIN

TAG DER MÜNDLICHEN PRÜFUNG: 22. JULI 2016



# Abstract

In this thesis we explore cosmological models of the early universe, in particular alternatives to the theory of inflation.

In the first part of this thesis, we derive the evolution equations for two scalar fields with non-canonical field space metric up to third order in perturbation theory, employing the covariant formalism. These equations can be used to derive predictions for local bi- and trispectra of multi-field cosmological models, e.g. in non-minimal ekpyrotic models. In these models, nearly scale-invariant entropy perturbations are generated first due to a non-minimal kinetic coupling between two scalar fields, and subsequently converted into curvature perturbations. Remarkably, the entropy perturbations have vanishing bi- and trispectra during the ekpyrotic phase. However, in order to obtain a large enough amplitude and small enough bispectrum of the curvature perturbations, as seen in current measurements, the conversion process must be very efficient, leading to a significant, negative trispectrum parameter.

As a second alternative to inflation, we construct a new kind of cosmological model that conflates inflation and ekpyrosis in the framework of scalar-tensor theories of gravity. During a phase of conflation, the universe undergoes accelerated expansion, but with negative potential energy. A distinguishing feature of the model is that it does not amplify adiabatic scalar and tensor fluctuations, and in particular does not lead to eternal inflation and the associated infinities. We also show how density fluctuations in accordance with current observations may be generated by adding a second scalar field to the model and making use of the entropic mechanism.

The distinguishing observational feature of both models compared to single-field slow-roll inflation is an absence of primordial gravitational waves, in agreement with current data from the PLANCK satellite.

**Keywords:** cosmology, alternatives to inflation, perturbation theory, non-Gaussianity

## Zusammenfassung

In dieser Arbeit untersuchen wir kosmologische Modelle des frühen Universums, insbesondere alternative Modelle zur Inflationstheorie.

Im ersten Teil leiten wir mithilfe des kovarianten Formalismus die Bewegungsgleichungen für zwei Skalarfelder mit nicht-kanonischem Feldraum bis zur dritten Ordnung in der Störtheorie her. Diese Gleichungen können dazu verwendet werden, Vorhersagen für die Bi- und Trispektren von Multi-Feldmodellen zu treffen, z.B. nicht-minimale ekpyrotische Modelle. In diesen Modellen werden zuerst aufgrund der nicht-minimalen kinetischen Kopplung zwischen den beiden Skalarfeldern nahezu skaleninvariante Entropiefluktuationen erzeugt, die dann anschließend in adiabatische Fluktuationen umgewandelt werden. Das Bi- sowie das Trispektrum der Entropiefluktuationen ist genau null während der ekpyrotischen Phase. Damit die Amplitude der adiabatischen Fluktuationen und das Bispektrum kompatibel mit derzeitigen Messungen sind, muss der Umwandlungsprozess effizient sein, was zu einem signifikanten, negativen Trispektrum-Parameter führt.

Als zweite Alternative zur Inflation konstruieren wir ein neues kosmologisches Modell, das im Rahmen der Skalar-Tensor-Gravitationstheorien Elemente der Inflation mit Elementen des ekpyrotischen Modells verbindet. Während einer Phase der Konflation expandiert das Universum beschleunigt, jedoch mit negativer potentieller Energie. Skalare und tensorielle Fluktuationen werden nicht verstärkt – die ewige Inflation und die damit einhergehenden Unendlichkeiten werden vermieden. Wir zeigen außerdem, wie Dichtefluktuationen in Übereinstimmung mit aktuellen Beobachtungen erzeugt werden können, indem wir mithilfe eines zweiten Skalarfeldes den entropischen Mechanismus einsetzen.

Beide Modelle unterscheiden sich von “slow-roll” Inflationstheorien basierend auf einem Skalarfeld darin, dass keine primordialen Gravitationswellen produziert werden, und sie folglich mit den aktuellen Daten des PLANCK-Satelliten übereinstimmen.

**Schlagwörter:** Kosmologie, Alternativen zur Inflation, Störtheorie, Nicht-Gaussianität

## Acknowledgements

I would like to thank my supervisor, Jean-Luc Lehners, for his guidance, enthusiasm and continuous support. I deeply appreciate the valuable discussions we had. He was always able to offer a helpful new perspective and taught me the importance of taking a step back to consider the bigger picture.

I would also like to express my gratitude to my official advisor, Hermann Nicolai, for giving me the opportunity to work at an excellent research institute. It has been a privilege and pleasure to be a part of the quantum gravity division.

I am grateful to Kazuya Koyama and Jan Plefka for agreeing to referee my thesis and to Dirk Kreimer and Marek Kowalski for serving on my thesis committee.

Furthermore, I have learned about a lot of different aspects of cosmology during the weekly theoretical cosmology group meetings. I would like to thank George Lavrelashvili, Michael Köhn, Lorenzo Battarra, Rhiannon Gwyn, Edward Wilson-Ewing, Enno Mallwitz, Esther Kähler, Clemens Hübner-Worseck, Shane Farnsworth and Sebastian Bramberger for inspiring discussions and broadening my horizon. I enjoyed collaborating with Enno Mallwitz, thank you for making even long Mathematica days endurable.

My PhD experience has been enriched by friendship and conversation with Parikshit Dutta, Marco Finocchiaro, Philipp Fleig, Nicolai Friedhoff, Filippo Guarnieri, Despoina Katsimpouri, Alexander Kegeles, Pan Kessel, Isha Kotecha, Olaf Krueger, Claudio Paganini, Seungjin Lee, Johannes Thürigen and many others. Special thanks to the best office mate one can hope for, Olof Ahlen.

Thank you Bonnie Chow, my identical particle that I am still entangled with even though we are too far apart. My best friend – what would I do without you?

I want to dedicate this thesis to my parents. Without you I would never have made it this far. I will forever be grateful for your love, encouragement and unconditional support. Thank you grandma for always thinking of me and always being there for me when I need you. My sister – I am grateful for all the advice you have given me over the years, thank you for sharing everything with me. I want to thank my brother for not being satisfied with one question about physics being answered but always asking for more, challenging the foundations of my knowledge. Last but not least, I give my deepest thanks to Nils for all your help, comfort and inspiration.



# Contents

Abstract . . . . .	iii
Acknowledgements . . . . .	vii
List of Figures . . . . .	xi
<b>1 Introduction</b>	<b>1</b>
<b>2 The early universe</b>	<b>6</b>
2.1 Friedmann-Lemaître-Robertson-Walker cosmology . . . . .	6
2.1.1 The Friedmann-Lemaître-Robertson-Walker metric . . . . .	7
2.1.2 The Einstein equations . . . . .	9
2.2 Puzzles . . . . .	13
2.2.1 Horizon problem . . . . .	14
2.2.2 Flatness problem . . . . .	17
2.3 Inflation . . . . .	19
2.3.1 Background dynamics . . . . .	22
2.3.2 Scalar perturbations . . . . .	26
2.3.3 Gravitational waves . . . . .	35
2.3.4 Problems . . . . .	37
2.4 Ekpyrosis and the cyclic model . . . . .	39
2.4.1 The ekpyrotic solution . . . . .	41
2.4.2 The entropic mechanism . . . . .	45
2.4.3 (No) gravitational waves . . . . .	53
2.5 The bounce . . . . .	54
<b>3 Covariant formalism and perturbation theory up to third order</b>	<b>57</b>
3.1 The covariant formalism . . . . .	58
3.2 Two scalar fields with non-trivial field space metric . . . . .	60
3.3 Perturbation theory . . . . .	63
3.3.1 Perturbation theory up to second order . . . . .	64
3.3.2 Perturbation theory at third order . . . . .	66
<b>4 The non-minimally coupled ekpyrotic model</b>	<b>72</b>
4.1 The ekpyrotic phase . . . . .	74
4.1.1 The background solution . . . . .	74

4.1.2	Linear perturbations . . . . .	75
4.1.3	Higher-order perturbations . . . . .	78
4.2	The conversion phase . . . . .	81
4.2.1	Linearly decaying field space metric . . . . .	84
4.2.2	Asymptotically flat field space metric . . . . .	86
4.3	Comparison to the minimally coupled entropic mechanism . . . . .	89
4.4	Gravitational waves . . . . .	90
<b>5</b>	<b>Conflation – a new type of accelerated expansion</b>	<b>92</b>
5.1	Conflation . . . . .	93
5.1.1	Jordan frame action . . . . .	93
5.1.2	A specific transformation . . . . .	94
5.1.3	Equations of motion in Jordan frame . . . . .	96
5.1.4	Initial conditions and evolution with a shifted potential . . .	97
5.1.5	Transforming an Einstein frame bounce . . . . .	99
5.2	Perturbations . . . . .	104
5.2.1	Perturbations for a single field . . . . .	105
5.2.2	Non-minimal entropic mechanism in Jordan frame . . . . .	107
<b>6</b>	<b>Conclusions</b>	<b>110</b>
<b>A</b>	<b>A new definition of the entropy perturbation <math>\delta s^{(3)}</math></b>	<b>116</b>
<b>B</b>	<b>Useful formulae for the covariant formalism</b>	<b>119</b>
<b>C</b>	<b>Simplifications for our specific non-minimal model</b>	<b>128</b>
	<b>Bibliography</b>	<b>131</b>

## List of Figures

1.1	The cosmic microwave background as seen by the PLANCK satellite [1]. At the time of last scattering the universe was about 380 000 years old. The small temperature fluctuations correspond to regions of slightly different densities, which form the seeds of all future structure.	2
2.1	The three possible shapes of the FLRW universe; a spherical or closed universe with $k = +1$ , a hyperbolic or open universe with $k = -1$ , or a flat universe with $k = 0$ . Reproduced from [2]. . . . .	10
2.2	Conformal diagram for the standard FLRW cosmology illustrating the horizon problem, based on [3]. The region of space which was in causal contact before recombination has a much smaller radius than the separation between two regions from which we receive CMB photons.	17
2.3	The shape of the effective potential depends on the temperature relative to the critical temperature. For high $T > T_c$ , there is only one minimum at $\phi = 0$ . Once the temperature drops below the critical temperature, another minimum is established at $\phi_0$ . <i>Left</i> : Old inflation is based on a first-order phase transition. The scalar field starts out at $\phi = 0$ , which becomes a false vacuum when $T < T_c$ . This phase of inflation lasts until the universe tunnels to the true vacuum at the global minimum $\phi_0$ . <i>Right</i> : The important phase in the new inflationary model happens after a second-order phase transition: when $T < T_c$ , the field slowly rolls from zero to the minimum at $\phi_0$ . . . .	21
2.4	Conformal diagram for the inflationary cosmology illustrating the solution to the horizon problem, based on [3]. Causal contact between two regions separated by more than about two degrees in the CMB is achieved by increasing the amount of conformal time between the big bang, now at $\tau_i = -\infty$ , and recombination at $\tau_{\text{rec}}$ , such that their past light cones overlap in the shaded region. The time $\tau = 0$ becomes the time of reheating. . . . .	23
2.5	A simple inflationary model: on the plateau the potential is sufficiently flat allowing the field to roll very slowly and inflation to occurs. . . .	25

2.6	Perturbations exit the horizon during inflation: the horizon is almost constant while the fluctuations are stretched to such an extent that they exit the horizon when their wavelength becomes comparable to the horizon size. . . . .	31
2.7	Tensor-to-scalar ratio $r_{0.002}$ versus scalar spectral index $n_s$ from PLANCK in combination with other data sets, compared to the theoretical predictions of selected inflationary models [4]. . . . .	37
2.8	The braneworld picture of our universe, based on [5]. Gravity can propagate in the whole spacetime while other forces and matter are localised on the $(3 + 1)$ -dimensional branes. There is an attractive force between the two branes across the bulk spacetime that makes them collide at regular intervals. The collision corresponds to the big bang as seen from the brane. . . . .	40
2.9	A scalar field rolling down a steep, negative potential leads to an ekpyrotic phase. . . . .	42
2.10	Perturbations exit the horizon during ekpyrosis: the fluctuations stay almost constant while the horizon shrinks. . . . .	45
2.11	The decomposition into the adiabatic direction, $\sigma$ , and the transverse direction, $s$ , is shown. Perturbations along the direction of the background trajectory are adiabatic/curvature perturbations, whereas perturbations orthogonal to the trajectory represent entropy/isocurvature perturbations. Based on [6]. . . . .	46
2.12	After a rotation in field space, the two-field ekpyrotic potential decomposes into the adiabatic direction, $\sigma$ , and the transverse tachyonic direction, $s$ . The ekpyrotic scaling solution corresponds to motion along the ridge of the potential. Based on [7]. . . . .	47
4.1	After a rotation in field space, the two-field ekpyrotic potential can be viewed as composed of an ekpyrotic direction ( $\sigma$ ) and a transverse direction ( $s$ ). The ekpyrotic scaling solution corresponds to motion along the adiabatic direction. Perturbations along the direction of the trajectory are adiabatic/curvature perturbations, while perturbations transverse to the trajectory are entropy/isocurvature perturbations. . .	73
4.2	<i>Left:</i> The repulsive potentials ( $V_{1,2}$ with $r = 0, 1$ ) given in Eq. (4.47). <i>Right:</i> The field space trajectory in the repulsive potential $V_1(r = 0)$ . . . . .	83
4.3	The evolution of the fields ( <i>left</i> ), the field space metric and the scalar (Ricci) curvature ( <i>right</i> ) during one e-fold of conversion (from $t = -275$ to $t = -47$ ), plotted for the specific case with $V_2(r = 1) = v \left[ (\sinh x)^{-2} + (\sinh x)^{-4} \right]$ , and $\Omega (c = 1, b = d = \frac{1}{10}) = 1 - \frac{1}{10} I_0 \left( \frac{1}{10} e^{\phi/2} \right)$ , giving $f_{NL} = -1.3$ and $g_{NL} = -544$ . . . . .	85

4.4	Non-Gaussianity plotted against different slopes of the scalar curvature ( $\dot{R}$ ) for different durations of the conversion ( $N = 1/2, 2/3, 3/4, 1$ ) for the repulsive potential $V_2$ with $r = 1$ . The slope $\dot{R}$ is varied by choosing different values for $d = 1/10, 1/20, 1/50$ . Note that the magnitudes of $f_{NL}$ and $g_{NL}$ are significantly reduced for smoother conversion processes. . . . .	85
4.5	Non-Gaussianity plotted against different slopes of the scalar curvature ( $\dot{R}$ ) for different potentials ( $V_{1,2}$ with $r = 0, 1$ ) for a conversion duration of one e-fold. The two $r = 0$ lines happen to be virtually coincident. Note that the values for $f_{NL}$ are clustered around zero, while the values for $g_{NL}$ are always appreciably negative. This is a characteristic feature of current ekpyrotic models. . . . .	86
4.6	The evolution of the fields, the field space metric and the scalar curvature during one e-fold of conversion (from $t = -304$ to $t = -46$ ), plotted for the specific case with $V_2(r = 1) = v \left[ (\sinh x)^{-2} + (\sinh x)^{-4} \right]$ , and $\Omega(b = d = \frac{1}{50}) = 1 - \frac{1}{50} e^{\phi/100}$ , giving $f_{NL} = 1.0$ and $g_{NL} = -235$ . . . . .	87
4.7	Non-Gaussianity plotted against different field space metrics ( $\Omega = 1 - be^{d\phi/2}$ with $b = d$ ) for different durations of the conversion ( $N = 1/2, 2/3, 3/4, 1$ ) for the potential $V_2$ with $r = 0$ . Note that as in the case with a linearly decaying field space curvature, the magnitudes of $f_{NL}$ and $g_{NL}$ are significantly reduced for smoother conversion processes. . . . .	88
4.8	Non-Gaussianity plotted against different field space metrics ( $\Omega = 1 - be^{d\phi/2}$ with $b = d$ ) for different potentials ( $V_{1,2}$ with $r = 0, 1$ ) for a conversion duration of one e-fold. . . . .	88
4.9	Non-Gaussianity plotted against different potentials ( $V_{1,2}$ with $r = 0, 1$ ) for a conversion duration of one e-fold for the minimal entropic mechanism. . . . .	90
5.1	<i>Left:</i> The original Jordan frame potential $V_J$ is shown in blue, the shifted potential $U_J$ in dashed red. <i>Right:</i> The equation of state in Jordan frame, for the shifted potential. . . . .	98
5.2	Scalar field and scale factor in Jordan frame: the blue curves show the transformed ekpyrotic scaling solution and the red dashed curves correspond to the field evolutions in the shifted potential. . . . .	99
5.3	The Einstein frame scalar potential used in the bounce model (5.32). . . . .	100
5.4	<i>Left:</i> Scalar field and scale factor for the bounce solution in Einstein frame. <i>Right:</i> Parametric plot of the scalar field and scale factor in Einstein frame. This plot nicely illustrates the smoothness of the bounce. . . . .	101

5.5 Full evolution of the scale factor for the transformed solution in Jordan frame. The conflationary phase lasts while the scalar field rolls up the potential towards  $\Phi \sim 10^{-9}$ . During this period the scale factor increases by many orders of magnitude. During the exit of the conflationary phase the scale factor and scalar field undergo non-trivial evolution which is hard to see in the present figure and is shown in detail in Fig. 5.6 . . . . . 103

5.6 *Left:* Scalar field and scale factor for the transformed solution in Jordan frame towards the end of the evolution. *Right:* Parametric plot of the scalar field and scale factor in Jordan frame. Note that initially the scalar field decreases in value very rapidly. Later on, as the scalar field stabilises, the scale factor goes through oscillations, but eventually increases monotonically. . . . . 103

# Chapter 1

## Introduction

When we look at the night sky we see an uncountable number of bright points – planets, stars and galaxies. And yet, the sky is much darker during the night than during the day. The overall relative darkness seems inconsistent with an infinite, static and eternal universe, as pointed out by astronomer Heinrich Wilhelm Olbers in the early 19th century: such a universe should be populated by an infinite number of stars and hence any line of sight from Earth would end in a star leading to an infinitely bright night sky. The resolution of the paradox is brought about by the big bang theory. Not only is the universe of finite age, but it also expands causing the energy of emitted starlight to be reduced via redshift.

Moreover, since the speed of light is finite as well, observing distant objects allows us to study the universe when it was much younger. The oldest photons we can detect originate from the time when, after the hot big bang, the expanding universe had cooled enough for neutral atoms to form and light to not be scattered anymore. This surface of last scattering is called the cosmic microwave background (CMB) as the photons that arrive at earth today have been redshifted to microwave wavelengths. Discovered by Arno A. Penzias and Robert W. Wilson [8] in 1965 as isotropic radiation with a uniform temperature of about 2.7 K, recent observations by the PLANCK satellite (see Fig. 1.1) [9, 4, 10] show tiny temperature fluctuations with an amplitude of order one in  $10^5$ . The statistics of these small anisotropies constitutes the main source of information about the early universe. Hot spots correspond to overdense regions representing the seeds of all the structure we observe in the universe, like stars and galaxies.

Large-scale structure surveys, which observe the distribution of galaxies and galaxy clusters as the universe evolves in time, might lead to valuable new insights.

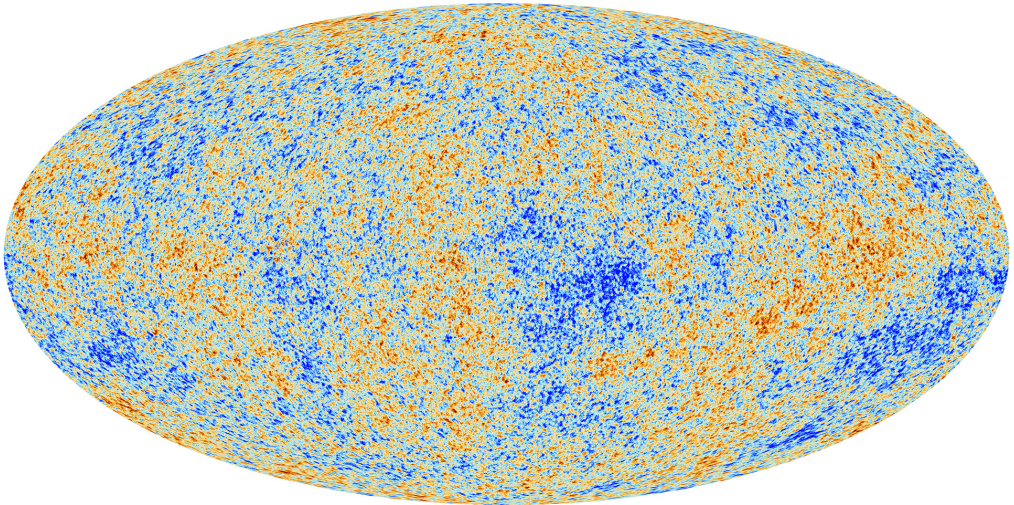


Figure 1.1: The cosmic microwave background as seen by the PLANCK satellite [1]. At the time of last scattering the universe was about 380 000 years old. The small temperature fluctuations correspond to regions of slightly different densities, which form the seeds of all future structure.

In the future, they might be able to rival the precision of the CMB maps, as our understanding of structure formation is continually improving [11]. While Einstein’s theory of gravity has been probed to extremely high precision in our solar system (see [12] for a review), it cannot account for the recently discovered acceleration of the universe [13]. We either have to assume a new form of energy density called dark energy that effectively acts as repulsive gravity, or gravity has to be modified on cosmological scales such that it allows for self-accelerating solutions [14].

Similarly to this late-time acceleration in the expansion of the universe a phase of inflation (see [3] for a review) during very early times has been postulated, yet at a much higher energy scale. A subsequent period of reheating would have slowed the expansion down while filling the universe with radiation and matter. Emerging from the big bang with typical initial conditions some regions of space supposedly have the properties required to undergo a period of inflation that smooths and flattens the universe, accounting for the homogeneity and isotropy of the CMB at the background level. Moreover, inflation provides an explanation for the small temperature anisotropies by stretching quantum fluctuations to cosmological distances. Simple scalar-field models of inflation lead to rather clear predictions for these perturbations: the so-called inflaton must roll down a very flat potential which implies that it is approximately a free field. This in turn leads to a spectrum of density perturba-

tions that is Gaussian to high accuracy, implying that both the bispectrum/3-point correlation function and trispectrum/4-point function are expected to be very small. More complicated models can however be designed, involving multiple fields and/or higher-derivative kinetic terms, such that essentially all potential combinations of observations can be matched. One may hope that this uncomfortable fact could be circumvented if additional constraints on model building, arising from the combination with particle physics or eventually quantum gravity, become available. In the meantime, it is interesting to observe that simple inflationary models also typically predict primordial gravitational waves at observable levels, so that the current non-observation already starts to rule out a number of long-favoured models [4]. Experiments like the BICEP / KECK observatories at the south pole search for a primordial gravitational wave signal in the B-mode polarisation of the CMB [15]. A joint analysis with PLANCK showed that a significant contribution to the polarisation comes from galactic dust [16]. Measurements in the next few years operating at increased sensitivity will further constrain the origin of the observed signal.

From a theoretical point of view, single-field models of inflation present important challenges (see e.g. [17]): for one, inflation does not provide a complete history of the universe, and one may ask what happened before inflation and how the inflationary phase started. In fact, the initial conditions need to be very special: the scalar field has to start out at large potential energy with negligible initial velocity, everywhere within a region of the universe that is a billion times larger than the Planck scale. This requirement clashes somewhat with the motivation for inflation, which is to explain the specialness of the early universe in a dynamical fashion. A second complicating feature of (most) inflationary models is that they typically lead to the runaway behaviour of eternal inflation: large quantum fluctuations can momentarily disrupt the inflationary dynamics and create an infinite number of causally disconnected pocket universes containing all possible values for the amplitude, the spectrum and the Gaussianity of the perturbations. In the absence of a measure (which the theory does not provide) the theory then loses all its predictive power and the naive predictions quoted above become questionable.

This situation suggests two possible approaches: the first is to try and understand the above-mentioned challenges better and to resolve them. On the other hand, we may look for alternative theories which might be able to explain the same cosmological data without however presenting us with such conceptual conundrums. Evidently it is interesting to pursue both approaches – here, we will be concerned with the second approach.

The thesis is organised as follows: In the next chapter we follow the progress that has been made in describing the evolution of the universe, beginning with the old big bang theory based on Einstein’s theory of general relativity and Hubble’s observation that the universe expands. We show how inflation solves most of the puzzles connected with the hot big bang theory, most notably the horizon and flatness problem. Moreover, we add quantum perturbations, which become the temperature fluctuations observed in the cosmic microwave background. Inflation contains problems of its own though, which we outline and take as motivation to investigate alternative theories such as the ekpyrotic / cyclic model. We then discuss how the big bang can be replaced with a bounce linking a contracting phase to the currently expanding phase in order to make these models viable.

Chapter 3 contains our main technical developments based on published work [18] in collaboration with Jean-Luc Lehners. Employing the covariant formalism, we derive the evolution equations for two scalar fields with a non-minimal kinetic coupling up to third order in perturbation theory. Even though the scalar-field space is endowed with a non-trivial metric, the model does not contain higher-derivative kinetic terms. For this reason, only the non-Gaussianities of local form are relevant, and these can be calculated from the classical evolution on large scales. This will extend the existing treatment up to second order in perturbation theory by Renaux-Petel and Tasinato [19], as well as the existing development of third-order perturbation theory for trivial field space metrics [20]. These equations will be used to calculate the non-Gaussian corrections to the primordial density fluctuations in terms of the bispectrum and the trispectrum.

The results are applied to a new mechanism for generating ekpyrotic density perturbations in chapter 4. The model we are interested in, non-minimal ekpyrosis, was first proposed by Qiu, Gao and Saridakis [21] and Li [22], and generalised in [23]. It contains two scalar fields, but only one has a steep negative potential, whereas the potential of the other is negligible or even precisely zero. The first field dominates the energy density and thus drives the ekpyrotic phase. In the non-minimally coupled entropic mechanism, nearly scale-invariant entropy perturbations are then generated by a field-dependent coupling between the two scalar field kinetic terms. Subsequently, these entropy perturbations are converted into curvature perturbations. We show that this model leads to vanishing bi- and trispectrum during the ekpyrotic phase. Moreover, we investigate the effect of the conversion mechanism on both the bispectrum and trispectrum in detail. We show that the conversion process has a crucial impact on the final predictions for the bispectrum and trispectrum of

the curvature perturbations. In particular, we find that the conversion process must be very efficient in order for these models to be in agreement with current limits on the bispectrum parameter  $f_{NL}$ . Interestingly, such efficient conversions then lead to a non-trivial prediction for the trispectrum non-linearity parameter  $g_{NL}$ , which is expected to be negative and of a magnitude of several hundred typically. The spectrum and bispectrum during the ekpyrotic phase were calculated in collaboration with Enno Mallwitz and Jean-Luc Lehners in [24], and the extension to the trispectrum and detailed analysis of the conversion were carried out together with Jean-Luc Lehners in [18].

Inflation and ekpyrosis share a number of features: they are the only dynamical mechanisms known to smoothen the universe's curvature (both the homogeneous part and the anisotropies) [25, 26]. They can also amplify scalar quantum fluctuations into classical curvature perturbations which may form the seeds for all the large-scale structure in the universe today [27, 28]. Moreover, they can explain how space and time became classical in the first place [29]. With a number of assumptions, in both frameworks models can be constructed that agree well with current cosmological observations, see e.g. [30, 31]. But in other ways, the two models are really quite different: inflation corresponds to accelerated expansion and requires a significant negative pressure, while ekpyrosis corresponds to slow contraction in the presence of a large positive pressure. Inflation typically leads to eternal inflation and the associated ambiguities about its actual predictions [17], while ekpyrosis requires a null energy violating (or a classically singular) bounce into the expanding phase of the universe [32]. In chapter 5 we introduce the idea of conflation, which corresponds to a phase of accelerated expansion in a scalar-tensor theory of gravity and which combines elements from both inflation and ekpyrosis. In the inflationary model, the universe is rendered smooth by a phase of accelerated expansion, like in inflation. However, the potential is negative, and adiabatic scalar and tensor fluctuations are not amplified, just as for ekpyrosis. Hence eternal inflation and the associated infinities are avoided. As we will show, one can obtain nearly scale-invariant curvature perturbations by adding a second scalar field and employing an entropic mechanism analogous to the one used in ekpyrotic models. This chapter is based on work [33] done in collaboration with Enno Mallwitz and Jean-Luc Lehners.

# Chapter 2

## The early universe

In this chapter we will set the scene for the following ones in terms of the structure of the theories we study as well as notation. We describe the historical development of early universe cosmology, including the hot big bang model as well as the inflationary theory designed to resolve the puzzles that arose with the former. We then discuss problems of inflation which motivate the investigation of alternative theories of the early universe. We work in reduced Planck units,  $c = \hbar = 1$  and  $8\pi G = M_{\text{Pl}}^{-2} = 1$ , which eliminates the factor  $8\pi G$  from the Einstein field equations, unless stated otherwise.

### 2.1 Friedmann-Lemaître-Robertson-Walker cosmology

The fact that the universe expands was probably the most important discovery in cosmology in the last century. In 1917 Albert Einstein [34, 35] realised that according to general relativity the universe had to either expand or contract. However, to match the absence of observational evidence for any form of dynamical evolution of the universe, he added a positive cosmological constant<sup>1</sup>, even though a static universe is not a stable solution. Alexander A. Friedmann [36, 37] then found the full set of solutions for models of the universe with positive, zero and negative curvature. In 1927 George Lemaître [38, 39] was the first to take the implications of an expanding universe seriously. He concluded that the universe must have had an origin, which he later called the “primeval atom”. In 1929 Edwin P. Hubble [40] discovered that

---

<sup>1</sup>In later years Einstein declared the introduction of the cosmological constant his “biggest blunder”. As a matter of fact, there is no a priori reason for the constant to vanish – the constant can indeed be used to model dark energy. Einstein’s mistake consisted in overlooking the instability of his solution.

the further away a galaxy is from us, the more redshifted it is. This proportionality between the recession speed of galaxies and their distance from us is called Hubble's law, and admits the interpretation that the universe does indeed expand. Moreover, in the 1940s George Gamow [41, 42] laid the foundation for our present understanding of hot big bang nucleosynthesis. He explained the observed relative abundance of light elements like helium, deuterium and lithium by taking into account how the temperature of the universe decreased due to its expansion after starting out in a very hot and dense state. Lastly, in 1965 Arno A. Penzias and Robert W. Wilson [8] discovered the cosmic microwave background, the afterglow of the big bang. The isotropic black body radiation (today at about 2.73K) was emitted around 380,000 years after the big bang from the so-called "surface of last scattering" when the universe had cooled enough to form neutral atoms and photons decoupled from matter.

Over the last decades these observations have been confirmed, and more and more detail of the CMB and large scale structure (LSS) has been obtained, establishing the hot Big Bang as the preferred model of the universe<sup>2</sup>. However, there are certain issues which make it unlikely that this is a complete model – they will be discussed in section 2.2.

### 2.1.1 The Friedmann-Lemaître-Robertson-Walker metric

According to the Cosmological Principle (CP) the universe is homogeneous and isotropic on large scales. Homogeneity means that, if the evolution of the universe is represented as a time-ordered sequence of 3D space-like hypersurfaces, the physical conditions are the same at each point of a given hypersurface. For a spacetime to be isotropic, the physical conditions have to be identical in all directions when viewed from a given point on the hypersurface, i.e. there are no preferred directions in space. The CP is a generalisation of the Copernican Principle at the cosmological level. The latter assumes that we do not occupy a privileged position in our universe. Since the universe is isotropic around us, it should thus be isotropic everywhere, automatically implying homogeneity<sup>3</sup>.

On scales smaller than about 100 Mpc<sup>4</sup>, the CP is no longer valid. Clearly, the

---

<sup>2</sup>According to the current understanding of the evolution of our universe, there are two dark components that have to be included: (cold) Dark Matter and Dark Energy, potentially in the form of the cosmological constant  $\Lambda$ . The preferred model of the universe is thus referred to as  $\Lambda$ CDM – see section 2.1.2.

<sup>3</sup>Note that isotropy at every spacetime point implies homogeneity but not vice versa.

<sup>4</sup>One parsec (pc), an abbreviation of the *parallax* of one arcsecond, is the distance at which one

centre of the sun or our galaxy is very different from interstellar or intergalactic space, respectively. The largest known structures are galaxy filaments that consist of gravitationally bound galaxies and form the boundaries between large voids in the universe. Beyond those structures it has been confirmed by modern observations that local variations in matter are averaged out, and we can assume that the CP is applicable. Not only are radio galaxies randomly distributed across the entire sky, the distribution of the observed redshift in the spectra of distant galaxies is also isotropic, implying a uniform Hubble flow, i.e. expansion of the universe, in all directions. In addition to observations from LSS, the most important source is the CMB; temperature anisotropies at the time of last scattering are only of the order of one part in  $10^5$ <sup>5</sup>, as shown for the first time by the COsmic Background Explorer (COBE) satellite in 1992 [43].

In general relativity, the CP implies that we can foliate the 4D manifold of the universe as  $\mathbb{R} \times \Sigma$ , where  $\mathbb{R}$  represents the time direction and  $\Sigma$  is a maximally symmetric 3-space – the universe is homogeneous and isotropic in space, but not in time. The metric can thus be taken to be of the form

$$ds^2 = -dt^2 + a^2(t)\gamma_{ij}(x)dx^i dx^j, \quad (2.1)$$

where  $t$  is a time-like coordinate, labelling cosmological events in the 3-surface  $\Sigma(x)$ , and the metric  $\gamma_{ij}$  is maximally symmetric in  $\Sigma$ . The scale factor  $a(t)$  represents the relative size of spatial sections of  $\Sigma$  at time  $t$ . Note that  $g_{0i} = 0$  due to the isotropy requirement, as it would otherwise introduce a preferred direction.

Isotropy further implies that the maximally symmetric spatial metric  $d\ell^2 = \gamma_{ij}(x)dx^i dx^j$  has to be spherically symmetric, and can therefore be written as

$$d\ell^2 = e^{2\beta(r)}dr^2 + r^2(d\theta^2 + \sin^2\theta d\phi^2), \quad (2.2)$$

where the form of the function  $g_{rr}(r) = e^{2\beta(r)}$  has been chosen for convenience. The

---

astronomical unit (the average distance between the Earth and the sun, 150 million kilometres) subtends an angle of one arcsecond. 100 Mpc equals about  $3.26 \cdot 10^8$  light-years, or about  $3.08 \cdot 10^{21}$  km in length.

<sup>5</sup>Actually, due to the peculiar motion of the Earth w.r.t. the cosmological rest frame of the CMB (around the sun, around the galactic centre, within the motion of our galaxy cluster), there is a dipole anisotropy of  $\delta T/T \sim 10^{-3}$ , which has to be subtracted off.

components of the Ricci tensor for this metric are

$$\begin{aligned} {}^{(3)}R_{rr} &= \frac{2}{r}\partial_r\beta \\ {}^{(3)}R_{\theta\theta} &= e^{-2\beta}(r\partial_r\beta - 1) + 1 \\ {}^{(3)}R_{\phi\phi} &= \left[e^{-2\beta}(r\partial_r\beta - 1) + 1\right]\sin^2\theta \end{aligned} \quad (2.3)$$

Moreover, maximally symmetric metrics obey

$${}^{(3)}R_{ikjl} = k(\gamma_{ij}\gamma_{kl} - \gamma_{il}\gamma_{kj}), \quad (2.4)$$

where  $k$  is a constant due to homogeneity. The Ricci tensor is then given by

$${}^{(3)}R_{ij} = 2k\gamma_{ij}. \quad (2.5)$$

Equating the two expressions for the Ricci tensor, (2.3) with (2.5), we can solve for  $\beta(r)$ , obtaining

$$\beta = -\frac{1}{2}\ln(1 - kr^2). \quad (2.6)$$

Thus, the spacetime metric becomes

$$ds^2 = -dt^2 + a^2(t) \left[ \frac{dr^2}{1 - kr^2} + r^2(d\theta^2 + \sin^2\theta d\phi^2) \right], \quad (2.7)$$

which is the famous Friedmann-Lemaître-Robertson-Walker metric (FLRW). Note that this metric is invariant under the redefinition

$$k \rightarrow \frac{k}{|k|}, \quad r \rightarrow r\sqrt{|k|}, \quad a \rightarrow \frac{a}{\sqrt{|k|}}, \quad (2.8)$$

so that the only relevant parameter is  $k/|k|$ . There are three cases of interest: a closed universe, with constant positive curvature,  $k = +1$ ; a flat universe of vanishing spatial curvature,  $k = 0$ ; and an open universe, with constant negative curvature,  $k = -1$  (see Fig. 2.1).

### 2.1.2 The Einstein equations

As outlined in the beginning of the section, modern cosmology began as a quantitative science with the advent of Einstein's general relativity. He showed that gravitation is a distortion of the structure of spacetime by matter, affecting the

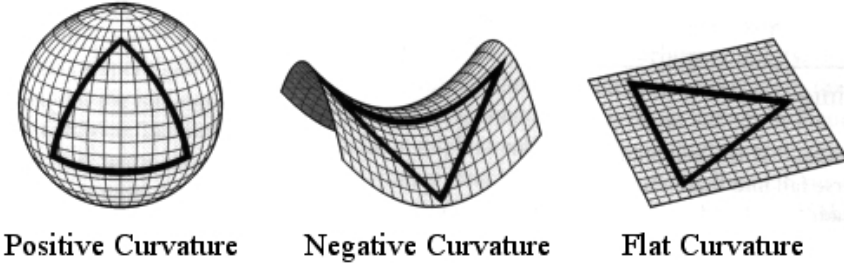


Figure 2.1: The three possible shapes of the FLRW universe; a spherical or closed universe with  $k = +1$ , a hyperbolic or open universe with  $k = -1$ , or a flat universe with  $k = 0$ . Reproduced from [2].

inertial motion of other matter. The Einstein field equations relate the spacetime geometry, given in terms of the Einstein tensor  $G_{\mu\nu}$ , to the energy density in terms of the stress-energy tensor  $T_{\mu\nu}$ ,

$$G_{\mu\nu} \equiv R_{\mu\nu} - \frac{1}{2}g_{\mu\nu}R = 8\pi G T_{\mu\nu}, \quad (2.9)$$

where we have temporarily reinserted the factor  $8\pi G$ .

In addition to the FLRW metric from the last section, which determines the left-hand side, we need to model the matter and energy in the universe. The most general matter fluid consistent with the CP is a perfect fluid, where an observer comoving with the fluid would see the universe around it as spatially isotropic. The energy-momentum tensor associated with a perfect fluid can be written as

$$T^{\mu\nu} = pg^{\mu\nu} + (p + \rho)u^\mu u^\nu, \quad (2.10)$$

where  $p(t)$  and  $\rho(t)$  are the pressure and energy density of the fluid, respectively, and  $u^\mu$  is the comoving four-velocity, satisfying  $u_\mu u^\mu = -1$ . With the four-velocity for a fluid at rest in comoving coordinates given by  $u^\mu = (1, 0, 0, 0)$ , the energy-momentum tensor becomes

$$T_\nu^\mu = \text{diag}(-\rho(t), p(t), p(t), p(t)). \quad (2.11)$$

The  $\mu = \nu = 0$  component of the Einstein equations (2.9) and its combination with

the  $\mu=\nu=i$  component then lead to the so-called Friedmann equations

$$3\left(\frac{\dot{a}}{a}\right)^2 = \rho - \frac{3k}{a^2}, \quad (2.12)$$

$$3\frac{\ddot{a}}{a} = -\frac{\rho + 3p}{2}. \quad (2.13)$$

In order to find explicit solutions, it is necessary to choose an equation of state, a relationship between energy density and pressure. The most relevant fluids in cosmology obey the simple equation of state

$$p = w\rho, \quad (2.14)$$

where  $w$  is a constant.

The  $\nu = 0$  component of the covariant conservation of the energy-momentum tensor,  $T_{\nu;\mu}^\mu = 0$ , gives

$$T_{0;\mu}^\mu = 0 = -\dot{\rho} - 3\frac{\dot{a}}{a}(\rho + p). \quad (2.15)$$

Substituting the expression for the equation of state parameter  $w$  from (2.14), we obtain the continuity equation

$$\frac{\dot{\rho}}{\rho} = -3\frac{\dot{a}}{a}(1+w), \quad (2.16)$$

which can be integrated to give

$$\rho \propto a^{-3(1+w)}. \quad (2.17)$$

There are several fluids which are of particular interest in cosmology: Dust is collisionless, nonrelativistic matter, whose equation of state obeys  $w_m = 0$ . Hence from (2.17), the energy density in matter, which is proportional to the number density of particles, falls off as  $\rho(\text{matter}) \propto a^{-3}$  with the expansion of the universe. Examples include ordinary stars and galaxies as well as dark matter, for which the pressure is negligible in comparison with the energy density.

Radiation has an equation of state given by  $w_r = 1/3$ , and is associated with relativistic degrees of freedom, i.e. not only photons, but also nearly massless particles like for example neutrinos. In an expanding universe the energy density of radiation decays as  $\rho(\text{radiation}) \propto a^{-4}$ : in addition to the decrease in number density, individual photons also lose energy in proportion to  $a^{-1}$  as they redshift.

Einstein's cosmological constant can be given in terms of the energy-momentum tensor as  $T_{\mu\nu}^{\text{vac}} = -\Lambda g_{\mu\nu}$ , and is perhaps associated with the energy of the vacuum itself<sup>6</sup>. The vacuum energy density has an equation of state  $w_\Lambda = -1$ , and remains constant with the expansion of the universe, providing a possible explanation for the observed late time accelerated expansion of the universe due to dark energy.

The energy density of anisotropies in the curvature of the universe can be shown to scale as  $\rho(\text{anisotropies}) \propto a^{-6}$  [5]: We consider a metric of the Kasner type (a special case of the Bianchi I metric) with negligible initial curvature,

$$ds^2 = -dt^2 + a(t)^2 \sum_i e^{2\beta_i(t)} dx^i dx_i \quad \text{with} \quad \sum_i \beta_i = 0. \quad (2.18)$$

The Friedmann equations become

$$H^2 = \frac{1}{3}\rho + \frac{1}{6} \sum_i \dot{\beta}_i^2, \quad (2.19)$$

$$\dot{H} = -\frac{1}{2}(\rho + p) - \frac{1}{2} \sum_i \dot{\beta}_i^2, \quad (2.20)$$

where we have introduced the Hubble parameter,  $H(t) = \frac{\dot{a}}{a}$ . Together with the condition on the Kasner exponents in (2.18) they imply

$$\ddot{\beta}_i + 3H\dot{\beta}_i = 0, \quad (2.21)$$

which has the growing mode solution  $\dot{\beta}_i \propto a^{-3}$ . Hence the energy density in the anisotropies scales as  $\frac{1}{2} \sum_i \dot{\beta}_i^2 \propto a^{-6}$ , where we will denote the constant of proportionality by  $\sigma^2$ .

The first Friedmann equation (2.12) can then be rewritten in the following form

$$3H^2 = \Lambda - \frac{3k}{a^2} + \frac{\rho_m}{a^3} + \frac{\rho_r}{a^4} + \frac{\sigma^2}{a^6} + \dots + \frac{\rho_\phi}{a^{3(1+w_\phi)}}, \quad (2.22)$$

where we have added the scaling for a scalar field  $\phi$ , which will become important later. We can infer the energy density content of the universe by combining measurements of the CMB, LSS and Type Ia supernovae. In terms of the fraction of the total energy density,  $\Omega_{i,0} \equiv \rho_{i,0}/3H^2$ , it consists of radiation ( $\Omega_{r,0} \approx \mathcal{O}(10^{-5})$ ), baryonic and dark matter ( $\Omega_{m,0} \approx 0.31$ ), and dark energy ( $\Omega_{\Lambda,0} \approx 0.69$ ), which can

---

<sup>6</sup>A naive estimate of the contribution of the energy associated with quantum vacuum fluctuations over-estimates the vacuum energy relative to the observational constraint by more than  $\sim 120$  orders of magnitude [44].

be modelled by  $\Lambda$  if it is constant. Nearly all the energy density today is contained in the latter two, such that this parametrisation of the standard big bang cosmology is called the  $\Lambda$ CDM (Lambda cold dark matter) model. The Friedmann equation then shows how the different components scale with the expansion of the universe due to their dependence on  $a$ . Radiation dominated during early times, before matter and finally dark energy took over. The first two imply decelerated expansion of the universe, with the scale factor going like  $t^{1/2}$  and  $t^{2/3}$ , respectively, whereas dark energy domination implies accelerated expansion.

## 2.2 Puzzles

Due to its successes in describing our universe the  $\Lambda$ CDM model is also referred to as the standard model of cosmology. It not only predicts the existence of the cosmic microwave background, but also the observed abundances of hydrogen, helium and lithium in interstellar gas produced during primordial nucleosynthesis. Moreover, the cosmological parameters (including dark energy) are such that the age of the universe comes out larger than the age of the oldest objects we can observe, like stars in globular clusters. Dark matter plays a key role in structure formation since it begins to collapse into a complex network of dark matter halos well before ordinary matter, which is impeded by radiation pressure. Without dark matter, the epoch of galaxy formation would occur substantially later in the universe than is observed.

Despite these achievements, there are some aspects of the model which require further consideration. From precise measurements of the CMB we know that the early universe was extraordinarily simple: not only approximately flat, homogeneous and isotropic, but also containing nearly scale-invariant and Gaussian density fluctuations. A major goal of cosmology is to find a convincing explanation for this initial state. For the standard model of cosmology to provide a consistent theory to explain the state of the observable universe, we have to assume very particular initial conditions whose origin is not explained. Instead of putting them in by hand, we want to explain dynamically why the universe looks the way it does. The specialness of the initial state can be quantified in terms of the horizon problem and the flatness problem, which we discuss in more detail in sections 2.2.1 and 2.2.2, respectively.

Another problem is related to the very high temperatures in the early universe. Grand unified theories (GUTs) propose that at high temperatures (above  $T_{\text{GUT}} \sim 10^{15} \text{ GeV}$ ) the electromagnetic, the weak and the strong interactions are not actually fundamental forces but arise due to spontaneous symmetry breaking (SSB) from

a single gauge theory. As the temperature drops through the GUT threshold, a phase transition associated with SSB occurs. Depending on the properties of the symmetry breaking, the phase transition can produce topological defects such as magnetic monopoles, strings, domain walls or textures via the Kibble mechanism [45, 46]. Different regions of the universe fall into different minima in the set of possible states. Topological defects are then precisely the “boundaries” between these regions with different choices of minima. Their formation is an inevitable consequence of the fact that different regions cannot agree on their choices since the correlation length cannot be larger than causality would allow, i.e. it must be at least as big as the horizon size. Accordingly, in the case of the GUT phase transition, at least one magnetic monopole should be produced per horizon volume (determined at the time when the symmetry breaking took place) [47, 48]. They should have persisted until the present day, to such an extent that the resulting monopole number density would be some ten orders of magnitude bigger than the critical density of the universe [49, 50]. Not only is that not the case, but all searches of them have failed, placing tight limits on the density of relic magnetic monopoles in the universe [51].

The observation of the expansion of the universe brought about another puzzle, namely the big bang singularity. Extrapolating backwards in time, the density and temperature of matter as well as the spacetime curvature diverge and general relativity predicts its own breakdown. According to the singularity theorems of Hawking and Penrose [52] such a singularity, at which time and space are supposed to begin, is unavoidable. The theorems are based on certain assumptions that translate into the condition that the null energy condition has to be satisfied in a flat FLRW universe – the known matter and energy density content of the universe including dark energy fulfil this condition. A full theory of quantum gravity, which remains to be found, is generally expected to resolve the singularity and provide a physical description of the big bang event.

### 2.2.1 Horizon problem

In this subsection we will show that the fact that the universe is homogeneous and isotropic on large scales constitutes a problem. When we evolve the universe back in time using GR, the finiteness of the speed of light implies that there are regions in the CMB that have never been in causal contact since the big bang. Yet, they have nearly the same temperature. It is basically a strong initial conditions problem: the big bang must have occurred simultaneously in at least  $10^5$  adjacent regions – it did

not originate from a single point.

The problem can be studied in some more detail by looking at the FLRW metric (2.7) for radial propagation of light in a flat universe, with  $k = d\theta = d\phi = 0$ , which simplifies to

$$ds^2 = -dt^2 + a(t)^2 dr^2 = a(\tau)^2 [-d\tau^2 + dr^2], \quad (2.23)$$

where we have introduced the conformal time  $\tau$  via the relation

$$d\tau = \frac{dt}{a(t)}. \quad (2.24)$$

For null geodesics the line element vanishes:  $ds^2 = 0$ . We can thus integrate (2.23) to give the maximal distance a photon can travel between an initial time  $t_i$  and a later time  $t > t_i$

$$\Delta r = \Delta\tau = \tau - \tau_i = \int_{t_i}^t \frac{dt}{a(t)}, \quad (2.25)$$

which is equal to the amount of conformal time elapsed during the interval  $\Delta t = t - t_i$ . The so-called *comoving particle horizon*,  $\Delta r_{\max}$ , is then defined as the greatest comoving distance from which an observer at time  $t$  will be able to receive signals travelling at the speed of light since the big bang started, defined formally by the initial singularity at  $a_i = a(t_i = 0) = 0$ . In other words, causal influences have to come from within this region.

The integral (2.25) can be rewritten in terms of the *comoving Hubble radius*  $(aH)^{-1}$  as

$$\Delta r = \int \frac{dt}{a(t)} = \int (aH)^{-1} d\ln a. \quad (2.26)$$

For a universe dominated by a perfect fluid with  $p = w\rho$ , as described in the previous subsection, the scale factor goes like

$$a \sim t^{\frac{2}{3(1+w)}}, \quad (2.27)$$

which can be obtained from integrating the Friedmann equation (2.12) together with the continuity equation (2.17). Thus, the comoving Hubble radius evolves as

$$(aH)^{-1} \sim a^{\frac{1}{2}(1+3w)}. \quad (2.28)$$

Performing the integral in (2.26), we obtain

$$\tau \sim \frac{2}{(1+3w)} a^{\frac{1}{2}(1+3w)}. \quad (2.29)$$

All familiar matter sources satisfy the strong energy condition (SEC),  $1+3w > 0$ . The comoving horizon (2.25) is thus finite as  $\tau_i = \tau(a_i = 0) = 0$ :

$$\Delta r_{\max} = \tau - 0 \sim a(t)^{\frac{1}{2}(1+3w)}, \quad \text{for } w > -\frac{1}{3}. \quad (2.30)$$

We can show that this implies that most spots in the CMB have non-overlapping past light-cones and hence never were in causal contact by calculating the angle subtended by a causal patch in the CMB. The horizon length at recombination corresponds to an angular size on the sky of

$$\theta_{\text{hor, rec}} = \frac{\Delta r_{\max}(z_{\text{rec}})}{d_A(z_{\text{rec}})}, \quad (2.31)$$

which is the ratio of the comoving particle horizon at recombination and the comoving angular diameter distance from us (at redshift  $z_0 = 0$ ) to recombination ( $z_{\text{rec}} \approx 1100$ ).<sup>7</sup> The cosmological redshift  $z$  of a source observed from Earth (at  $a_0 = 1$ ) is defined via

$$a = (1+z)^{-1}. \quad (2.32)$$

Thus, the comoving particle horizon (2.26) at the time of last scattering becomes

$$\Delta r_{\max}(z_{\text{rec}}) = \int_{a_i=0}^{a_{\text{rec}}} \frac{da}{a^2 H} \stackrel{\text{MD}}{\approx} \int_0^{(1+z_{\text{rec}})^{-1}} \frac{da}{a^{1/2} H_0} = \frac{2}{H_0} (1+z_{\text{rec}})^{-1/2}, \quad (2.33)$$

where the main contribution to the integral comes from times in which pressureless matter dominates (MD) the Hubble expansion rate  $H \stackrel{\text{MD}}{=} \frac{2}{3t} = H_0 a^{-3/2}$  since  $a \sim t^{2/3}$ , which can be inferred from the Friedmann equation (2.22).

The comoving angular diameter distance is defined as the ratio of the assumed comoving size of an object,  $D$ , and the measured angular diameter,  $\Delta\theta$ , and can be determined from the angular part of the metric (2.7) with  $dt = dr = d\phi = 0$  and hence  $aD = ar\Delta\theta$ , such that

$$d_A = \frac{D}{\Delta\theta} = r, \quad (2.34)$$

---

<sup>7</sup>Notice that the definition of the subtended angle does not change if instead we used the proper particle horizon and proper angular diameter distance, as the factors of  $a$  would cancel each other.

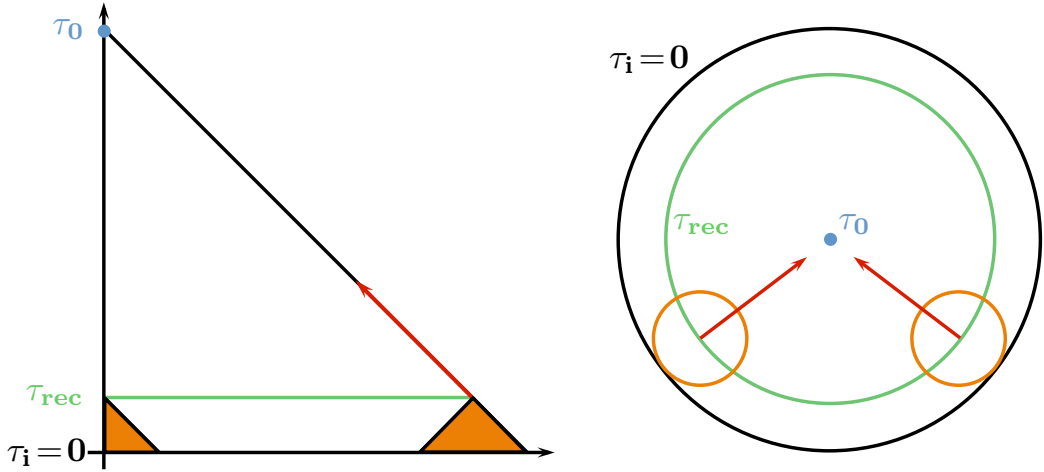


Figure 2.2: Conformal diagram for the standard FLRW cosmology illustrating the horizon problem, based on [3]. The region of space which was in causal contact before recombination has a much smaller radius than the separation between two regions from which we receive CMB photons.

where we have to integrate from the scale factor at recombination,  $a(z_{\text{rec}})$ , to the one today,  $a_0$ . Hence,

$$d_A(z_{\text{rec}}) \stackrel{\text{MD}}{\approx} \int_{(1+z_{\text{rec}})^{-1}}^{a_0=1} \frac{da}{a^{1/2} H_0} = \frac{2}{H_0} \left[ 1 - (1+z_{\text{rec}})^{-1/2} \right] \stackrel{z_{\text{rec}} \gg 1}{\approx} \frac{2}{H_0}, \quad (2.35)$$

where we have again assumed matter domination.

We finally obtain the angular size on the sky of the horizon length at recombination<sup>8</sup>:

$$\theta_{\text{hor, rec}} = \frac{\Delta r_{\text{max}}(z_{\text{rec}})}{d_A(z_{\text{rec}})} \approx (1+z_{\text{rec}})^{-1/2} \approx 0.03 \approx 1.7^\circ. \quad (2.36)$$

We conclude that regions in the CMB separated by more than about two degrees have never been in causal contact. Nevertheless, their temperature is the same up to one part in ten thousand, giving rise to the horizon problem.

### 2.2.2 Flatness problem

From the scaling of the different energy density components with the scale factor in the Friedmann equation (2.22), we can deduce that after a phase of radiation-

---

<sup>8</sup>The actual value is a bit smaller,  $\theta_{\text{hor, rec}} \approx 1.2^\circ$ , as the universe has not been matter-dominated throughout its whole evolution.

and matter-domination, the curvature should come to dominate in an expanding universe. Dividing the Friedmann equation by the critical density  $\rho_{\text{crit}} = 3H^2$ , we can define the density parameters  $\Omega_i$  as

$$\Omega_i \equiv \frac{\rho_i}{\rho_{\text{crit}}}, \quad (2.37)$$

and thus Eq. (2.22) becomes

$$1 = \Omega_\Lambda + \Omega_k + \Omega_m + \Omega_r + \Omega_{\sigma^2} + \dots \quad (2.38)$$

However, from observations we know that our universe is very close to spatially flat today, i.e. the energy density in curvature is in fact negligible, [9]

$$\Omega_k \equiv \frac{-k}{(aH)^2} \stackrel{t_0}{=} 0.000 \pm 0.005 \quad (2\sigma). \quad (2.39)$$

In other words, the energy density in dark energy, baryonic and dark matter, radiation and anisotropies – where the contribution from the latter two is also insignificant – approximately adds up to unity,

$$1 \approx \Omega_\Lambda + \Omega_m. \quad (2.40)$$

Assuming that the expansion is dominated by some form of matter with equation of state  $w$ , the change in the curvature density parameter is given by

$$\dot{\Omega}_k = H\Omega_k(1 + 3w) \quad \Omega_{k,N} = \pm\Omega_k(1 + 3w), \quad (2.41)$$

where we have used (2.27), allowing both for the universe to expand (with  $H > 0$ ) and to contract (with  $H < 0$ ). We have introduced the number of e-folds of evolution of the universe,  $N$ , defined via

$$dN = d\ln a = Hdt, \quad (2.42)$$

where the dependence on the Hubble rate explains the appearance of the minus sign in the second equation of (2.41). For matter satisfying the SEC, i.e.  $w > -1/3$ , the solution  $\Omega_k = 0$  is then an unstable point in an expanding universe – if  $\Omega_k > 0$  at some point, it keeps growing, whereas if  $\Omega_k < 0$ , it keeps decreasing. On the other hand, any matter satisfying the SEC in a contracting universe will drive the universe to spatial flatness  $\Omega_k \rightarrow 0$ .

Assuming we can simply extrapolate back to the Planck time, the curvature density would go like

$$\frac{\Omega_{k,\text{Pl}}}{\Omega_{k,0}} = \frac{(aH)_0^2}{(aH)_{\text{Pl}}^2}. \quad (2.43)$$

For a rough estimate we can assume radiation-domination as most of the e-folds of evolution of the universe occur during that phase. From the scaling of  $a$  with time (2.27) and  $w_r = 1/3$ , we have  $a \propto t^{1/2}$  and hence  $(aH)^2 \propto t^{-1}$ . Thus,

$$\frac{\Omega_{k,\text{Pl}}}{\Omega_{k,0}} = \frac{t_{\text{Pl}}}{t_0} \sim 10^{-60}. \quad (2.44)$$

Not only is the curvature observed today very close to zero (2.39), at the Planck time, it must have been 60 orders of magnitude smaller still! Even though we might not be able to trust the extrapolation all the way back to the Planck time, this simple estimate shows that the universe must have been extremely flat at early times.

### 2.3 Inflation

In 1979 Robert H. Dicke and Phillip J. E. Peebles [53] were the first to draw real attention to the puzzles described in the last section, in particular the flatness problem. In the same year, Robert Brout, Francois Englert and Edgard Gunzig proposed a model in which the matter emerging from quantum fluctuations had a large negative pressure, giving rise to “an open universe that closely resembles a de Sitter space” [54]. They were interested in this inflationary phase as a means to create a universe out of nothing, however, and not as a way to solve the hot big bang problems. By semi-classically incorporating quantum corrections to general relativity, Alexei A. Starobinsky [55, 56] found a class of cosmological solutions that begin with a de Sitter phase, evolve through an oscillatory phase, and eventually make a transition into the standard FLRW expanding solution. The backreaction generically leads to  $R^2$ -corrections to the Einstein-Hilbert action. Moreover, he predicted a large gravitational wave amplitude when compared to a radiation-dominated phase – the amplitude is small compared to other, subsequent inflationary models. His approach required choosing a special state for the early universe, namely the maximally symmetric de Sitter spacetime, rather than an arbitrary initial state. In that sense Starobinsky’s original motivation was quite different from the goals of inflationary cosmology.

In 1980, two papers were published that addressed the horizon problem: Kat-

suhiko Sato [57] suggested that a phase of exponential expansion could increase the region between domain walls to a size larger than the observable universe, making them unobservable today. Furthermore, Demosthenes Kazanas [58] proposed that during a phase transition in the early universe the expansion can be exponential, potentially accounting for the observed isotropy of the universe if the phase lasts long enough.

In his seminal paper [25], Alan H. Guth was very clear in his motivation to solve the horizon and flatness problems, and finally coined the term inflation. He proposed that the universe underwent a phase of accelerated expansion during a false vacuum phase before decaying to the true vacuum via a bubble nucleation. The model, now called “old inflation”, suffers from a *graceful exit* problem though. All the energy after the nucleation of a bubble is transferred to its walls, and can only be thermalised through many collisions with other bubble walls. However, if inflation lasts long enough to solve the initial conditions problems, collisions between bubbles become exceedingly rare. Thus, in any one causal patch too little reheating takes place, leading to large inhomogeneities in contradiction with observations.

To overcome the graceful exit problem Andrei D. Linde [59] and independently Andreas Albrecht and Paul J. Steinhardt [60] effectively replaced the first-order phase transition with a second-order one – see Fig 2.3. Both models of the GUT phase transition were based on a Coleman-Weinberg [61] effective potential for the Higgs field.

Expressed in terms of a scalar field (called the inflaton) in a symmetry-breaking potential below the critical temperature  $T < T_c$ , old inflation takes place while the field sits in the local, metastable minimum at  $\phi = 0$  – the false vacuum – before tunnelling through the barrier to the true vacuum at  $\phi_0$ . In “new inflation” the crucial ultra-rapid expansion phase no longer takes place while the field sits at the now unstable equilibrium at  $\phi = 0$ , but during the time that it slowly rolls on an extremely flat effective potential towards the symmetry-breaking minimum  $\phi_0$ . Reheating takes place once the potential energy stored in the scalar field is converted to radiation when the field starts rolling faster and eventually oscillates around the minimum.

These models are also called small-field inflationary models as the inflaton is displaced by less than a Planck mass, and they face several issues of their own. It becomes necessary to severely fine-tune the shape of the Coleman-Weinberg type potential such that there is a very flat plateau near  $\phi = 0$  in order to satisfy the slow-roll conditions. A further problem for many slow-field models is that the slow-

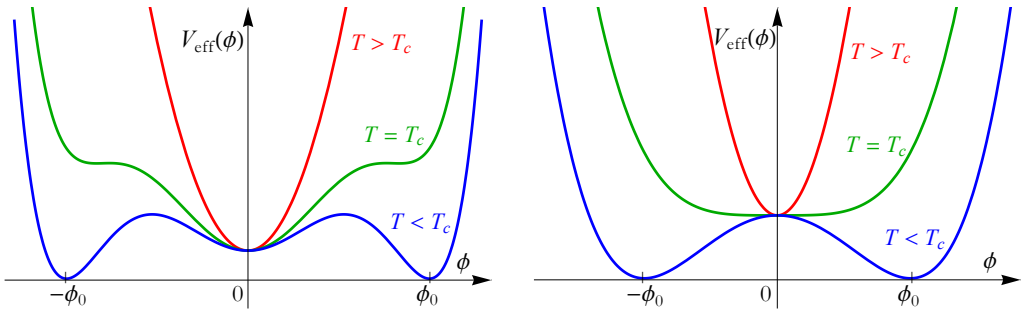


Figure 2.3: The shape of the effective potential depends on the temperature relative to the critical temperature. For high  $T > T_c$ , there is only one minimum at  $\phi = 0$ . Once the temperature drops below the critical temperature, another minimum is established at  $\phi_0$ . *Left:* Old inflation is based on a first-order phase transition. The scalar field starts out at  $\phi = 0$ , which becomes a false vacuum when  $T < T_c$ . This phase of inflation lasts until the universe tunnels to the true vacuum at the global minimum  $\phi_0$ . *Right:* The important phase in the new inflationary model happens after a second-order phase transition: when  $T < T_c$ , the field slowly rolls from zero to the minimum at  $\phi_0$ .

roll trajectory is not an attractor in phase space; the initial field velocity must be constrained to be very small. Furthermore, in order to obtain a sufficiently small amplitude of density perturbations, the inflaton field must have a very small coupling constant. However, this implies that the inflaton could not be in thermal equilibrium with other matter fields. In the absence of thermal equilibrium, the phase space of initial conditions is much larger for large values of the field, i.e. it is unlikely that the scalar field would begin rolling close to its symmetric point at  $\phi = 0$ .

In 1983 Linde proposed the first large-field model, which he called “chaotic inflation” [62]. He abandoned the idea that the universe was in a state of thermal equilibrium from the very beginning, but considered a universe that initially consisted of many domains with a chaotically distributed scalar field. Different scalar field potentials are then possible, where it is assumed that inflation takes place while the scalar field slowly rolls towards the origin from large values of  $\phi \gtrsim M_{\text{Pl}}$ . Domains in which the scalar field is too small never inflate, whereas those domains that originally contained large field values in the slow-roll regime of the potential do and hence make up the main contribution to the total volume of the universe.

If the inflationary phase lasts for long enough, it can solve the horizon, flatness and magnetic monopole problems by smoothing out inhomogeneities, anisotropies and the curvature of space, and diluting topological defects. However, in addition to the background the CMB contains small temperature fluctuations – the seeds for

all the structure in the universe. Including quantum fluctuations of the scalar field, Viatcheslav F. Mukhanov and Gennady V. Chibisov [27] calculated the spectrum of the resulting density perturbations after a phase of Starobinsky inflation in 1981. The generation of density perturbations in the new inflationary model was addressed a year later at the Nuffield Workshop on the Very Early Universe, held at the University of Cambridge. Independently of the work of Mukhanov and Chibisov the fluctuations were calculated by the following groups attending the workshop: Stephen Hawking [63], Starobinsky [64], Guth and So-Young Pi [65], and Bardeen, Steinhardt and Turner [66]. In section 2.3.2 we will show in detail how quantum fluctuations in a quasi-de Sitter space produce a spectrum of perturbations that accurately matches the observations.

### 2.3.1 Background dynamics

Both the flatness and the horizon problem arise because the comoving Hubble radius  $(aH)^{-1}$  always (except for the recent dark energy dominated phase) grows during the evolution of the universe in the standard big bang cosmology. Their solution can thus be conjectured as a phase of decreasing Hubble radius in the early universe called inflation,

$$\frac{d}{dt}(aH)^{-1} < 0. \quad (2.45)$$

If the comoving Hubble radius decreases so does  $|\Omega_k| \propto (aH)^{-2}$ , driving the universe toward flatness. The unstable solution  $\Omega_k = 0$  is turned into an attractor during such a phase. In terms of the equation of state parameter  $w$  it becomes clear from (2.41) that we require a violation of the SEC, or equivalently energy density with negative pressure: for  $w = p/\rho < -1/3$ , we obtain the desired behaviour  $\dot{\Omega}_k, \Omega_{k,N} < 0$ . Moreover, the big bang singularity is now pushed to negative conformal time, see Fig. 2.4. From (2.29) we have

$$\tau_i \propto \frac{2}{(1+3w)} a_i^{\frac{1}{2}(1+3w)} = -\infty, \quad \text{for } w < -\frac{1}{3}. \quad (2.46)$$

In the standard FLRW cosmology the integral determining the comoving particle horizon (2.25) is dominated by late times – see (2.30). However, if  $(aH)^{-1}$  is large in the past, then the integral is dominated by early times and offers a resolution to the horizon problem:  $\Delta r_{\max}$ , the distance beyond which particles could never have communicated with each other, is much larger than the Hubble radius  $(aH)^{-1}$  today. Hence, particles that cannot communicate at present were in causal contact early on.

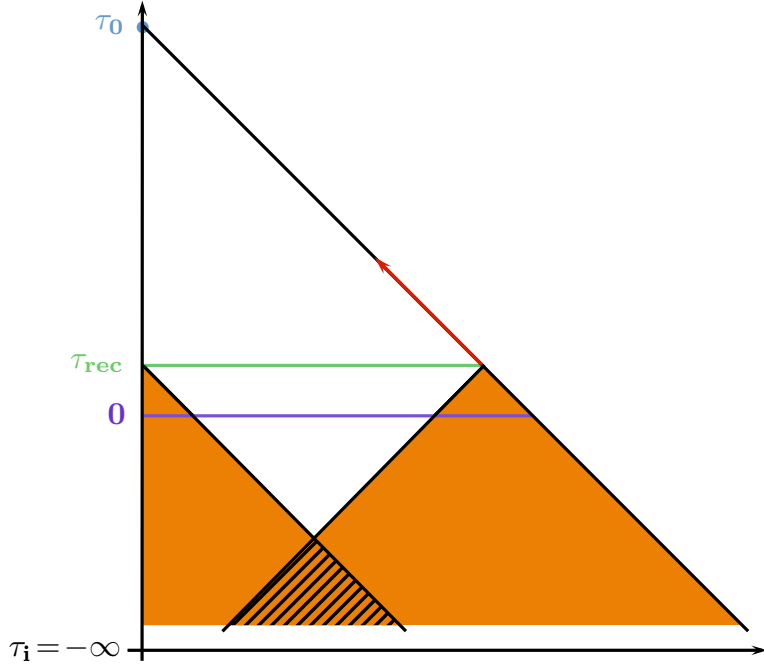


Figure 2.4: Conformal diagram for the inflationary cosmology illustrating the solution to the horizon problem, based on [3]. Causal contact between two regions separated by more than about two degrees in the CMB is achieved by increasing the amount of conformal time between the big bang, now at  $\tau_i = -\infty$ , and recombination at  $\tau_{\text{rec}}$ , such that their past light cones overlap in the shaded region. The time  $\tau = 0$  becomes the time of reheating.

The phase of decreasing comoving Hubble horizon (2.45) can be rewritten in the following way,

$$\frac{d}{dt}(aH)^{-1} = \frac{d}{dt}(\dot{a})^{-1} = -\frac{\ddot{a}}{\dot{a}^2} < 0. \quad (2.47)$$

Hence, a shrinking comoving Hubble radius (for positive coordinate time  $t$ ) implies accelerated expansion

$$\ddot{a} > 0. \quad (2.48)$$

We have already noted that for inflation to occur, we need  $w < -\frac{1}{3}$ . Equivalently, this condition can be expressed in terms of the *slow-roll parameter*  $\epsilon$ ,

$$\epsilon \equiv -\frac{\dot{H}}{H^2} = -\frac{d \ln H}{dN} = \frac{3}{2}(1+w) < 1. \quad (2.49)$$

In other words, while the scale factor  $a$  grows rapidly, the Hubble parameter  $H$  is approximately constant. Moreover, inflation has to last for a sufficiently long time in order to solve the puzzles. A simple estimate shows that in order to solve the flatness problem, the relative density in curvature has to decrease by 60 orders of magnitude (2.44). For an approximately constant Hubble parameter we thus need

$$\frac{\Omega_{k, \text{infl-beg}}}{\Omega_{k, \text{infl-end}}} \approx \frac{a_{\text{infl-end}}^2}{a_{\text{infl-beg}}^2} = e^{-2N} \gtrsim 10^{-60}, \quad (2.50)$$

and hence inflation has to last for around 70 e-folds of evolution,

$$N \gtrsim 70. \quad (2.51)$$

Thus, the slow-roll parameter has to remain small for a sufficiently large number of Hubble times. This translates into the following condition on the second slow-roll parameter,  $\eta$ :

$$\eta \equiv \frac{d \ln \epsilon}{d N} = \frac{\dot{\epsilon}}{H\epsilon}, \quad |\eta| < 1. \quad (2.52)$$

In addition to inflation there is a second way to solve the horizon and flatness problems dynamically. Instead of a phase of accelerated expansion, a phase of ultra-slow contraction also accomplishes the task. During ekpyrosis  $a$  stays approximately constant while  $H$  grows rapidly, as will be presented in detail in section 2.4.

The simplest way to model a matter component with the required equation of state is to employ a scalar field  $\phi$ , called the inflaton, with canonical kinetic energy and with a very flat potential  $V(\phi)$ . The dynamics of such a scalar field minimally coupled to gravity is then governed by the action

$$S = S_{\text{EH}} + S_\phi = \int d^4x \sqrt{-g} \left[ \frac{1}{2}R + \frac{1}{2}g^{\mu\nu}\partial_\mu\phi\partial_\nu\phi - V(\phi) \right], \quad (2.53)$$

which is the sum of the gravitational Einstein-Hilbert action  $S_{\text{EH}}$  and the action of a scalar field  $S_\phi$ . The self-interaction of the scalar field is described by the potential  $V(\phi)$ . The energy-momentum tensor for the scalar field is obtained by varying the scalar field action w.r.t. the metric,

$$T_{\mu\nu}^{(\phi)} = -\frac{2}{\sqrt{-g}} \frac{\delta S_\phi}{\delta g^{\mu\nu}} = \partial_\mu\phi\partial_\nu\phi - g_{\mu\nu} \left( \frac{1}{2}\partial_\rho\phi\partial^\rho\phi + V(\phi) \right). \quad (2.54)$$

In the case of the FLRW metric (2.7), and restricting to the case of a homogeneous

field  $\phi(t, x) = \phi(t)$ , the scalar energy-momentum tensor takes the form of a perfect fluid (2.11) with

$$\rho_\phi = \frac{1}{2}\dot{\phi}^2 + V(\phi), \quad (2.55)$$

$$p_\phi = \frac{1}{2}\dot{\phi}^2 - V(\phi). \quad (2.56)$$

The resulting equation of state is given by

$$w_\phi = \frac{p_\phi}{\rho_\phi} = \frac{\frac{1}{2}\dot{\phi}^2 - V(\phi)}{\frac{1}{2}\dot{\phi}^2 + V(\phi)}, \quad (2.57)$$

which is close to  $-1$  if the potential is sufficiently flat such that the field rolls very slowly, i.e.

$$\frac{1}{2}\dot{\phi}^2 \ll V(\phi) \quad \Rightarrow \quad w_\phi \simeq -1. \quad (2.58)$$

Hence, such a scalar field can lead to negative pressure ( $w_\phi < 0$ ) and accelerated expansion ( $w_\phi < -1/3$ ). Notice that this implies a very small slow-roll parameter,

$$\epsilon = -\frac{\dot{H}}{H^2} = \frac{1}{2} \left( \frac{\dot{\phi}}{H} \right)^2 \approx \frac{3}{2} \frac{\dot{\phi}^2}{V} \ll 1. \quad (2.59)$$

Fig. 2.5 depicts a potential where inflation happens on a flat plateau before rolling into a minimum.

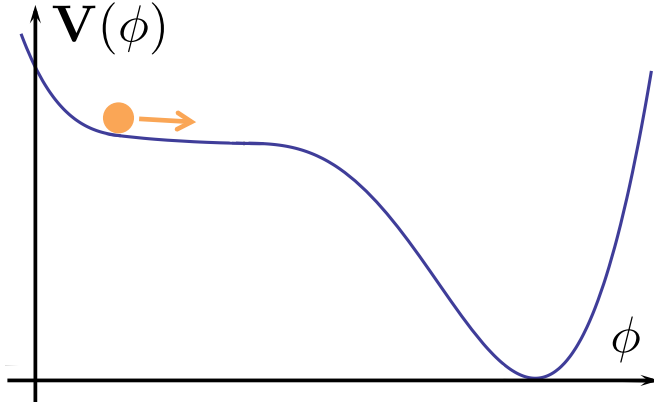


Figure 2.5: A simple inflationary model: on the plateau the potential is sufficiently flat allowing the field to roll very slowly and inflation to occurs.

Varying  $S_\phi$  w.r.t. the scalar field leads to the following equation of motion,

$$\frac{\delta S_\phi}{\delta \phi} = \frac{1}{\sqrt{-g}} \partial_\mu (\sqrt{-g} \partial^\mu \phi) + V_{,\phi} = 0. \quad (2.60)$$

The background dynamics of the scalar field in the FLRW geometry are then determined by

$$\ddot{\phi} + 3H\dot{\phi} + V_{,\phi} = 0, \quad (2.61)$$

$$3H^2 = \rho_\phi = \frac{1}{2}\dot{\phi}^2 + V(\phi), \quad (2.62)$$

$$\dot{H} = -\frac{1}{2}\dot{\phi}^2, \quad (2.63)$$

where the latter two equations, (2.62) and (2.63), are simply the Friedmann equations for a scalar field. The equation of motion (2.61) matches the one for a particle rolling down its potential, where the  $H\dot{\phi}$  term acts as friction. In order for slow-roll inflation to persist, the acceleration of the scalar field has to be small, i.e. we require a small dimensionless acceleration per Hubble time:

$$\delta \equiv -\frac{\ddot{\phi}}{H\dot{\phi}} \ll 1. \quad (2.64)$$

Expressed in terms of the second slow-roll parameter we then have

$$\eta = \frac{\dot{\epsilon}}{H\epsilon} = 2\frac{\ddot{\phi}}{H\dot{\phi}} - 2\frac{\dot{H}}{H^2} = 2(\epsilon - \delta) \ll 1, \quad (2.65)$$

where we have used the second expression for  $\epsilon$  in (2.59) to rewrite  $\dot{\epsilon}$ .

By definition, inflation ends when  $w$  ceases to be close to  $-1$ , implying

$$\epsilon \sim \eta \sim 1. \quad (2.66)$$

More concretely, the field will stop rolling slowly when the Hubble parameter has decreased, providing less friction, and the potential has become too steep to guarantee that the kinetic energy is negligible with respect to the potential energy.

### 2.3.2 Scalar perturbations

As outlined in the beginning of this section, it was realised shortly after the formulation of the theory of inflation that it could also source primordial perturbations. At

that time, temperature variations in the CMB had not yet been observed, but the fact that we observe galaxies today, and the fact that the density contrast of matter<sup>9</sup> grows proportional to the scale factor in a matter-dominated universe implied that some perturbations had to exist at the time of last scattering. During inflation the scalar field evolution  $\phi(t)$  governs the energy density of the early universe and hence controls the end of inflation. However, due to the uncertainty principle the inflaton has a quantum mechanical variance, i.e. spacetime-dependent perturbations

$$\delta\phi(t, \mathbf{x}) \equiv \phi(t, \mathbf{x}) - \bar{\phi}(t), \quad (2.67)$$

where the over-bar denotes the homogeneous background value of the scalar field which only depends on time. It follows that in some regions inflation ends later than in others, such that different regions of space inflate by different amounts. These differences in the local expansion history lead to differences in the local densities after inflation and ultimately to the CMB temperature fluctuations. In addition to the perturbation in the field, the metric is split into the background plus small perturbations,

$$g_{\mu\nu}(t, \mathbf{x}) = \bar{g}_{\mu\nu}(t) + \delta g_{\mu\nu}(t, \mathbf{x}), \quad (2.68)$$

as well. Since the perturbations are small,  $\frac{\delta\phi}{\phi}, \frac{\delta g_{\mu\nu}}{\bar{g}_{\mu\nu}} \ll 1$ , expanding the Einstein field equations at linear order in perturbations approximates the full non-linear solution to high accuracy,

$$\delta G_{\mu\nu} = 8\pi G \delta T_{\mu\nu}. \quad (2.69)$$

In the following we calculate in detail the spectrum of fluctuations obtained from single-field slow-roll models of inflation, and compare it with observations.

The fluctuations in the CMB are directly related to the scalar perturbations, whereas tensor fluctuations give rise to primordial gravitational waves. Vector perturbations can be neglected as they decay in an expanding universe. For concreteness, we will consider single-field slow-roll models of inflation with action (2.53). For the scalar modes there is only one physical degrees of freedom. A priori, there are five scalar modes: four metric perturbations  $(A, B, \psi, E)$ ,

$$ds^2 = -(1 + 2A) dt^2 + 2a(t) B_{,i} dx^i dt + a(t)^2 [(1 - 2\psi) \delta_{ij} - 2E_{,ij}] dx^i dx^j, \quad (2.70)$$

---

<sup>9</sup>The density contrast is defined as the ratio between the density difference of some region  $\delta\rho$  over the average background density  $\rho$ :  $\Delta \equiv \delta\rho/\rho \propto 1/(\rho a^3)$ . In a matter-dominated universe  $\rho \propto a^{-3}$  and hence  $\Delta \propto a$ , whereas  $\Delta \propto a^2$  in a radiation-dominated universe with  $\rho \propto a^{-4}$ .

and one scalar field perturbation,  $\delta\phi$ . However, two modes are removed by gauge invariances associated with the invariance of the action (2.53) under scalar coordinate transformations,  $x^\mu \rightarrow x^\mu + \xi^\mu$ , and another two by the Einstein constraint equations. In order to derive the quadratic action for this mode we make use of the Arnowitt-Deser-Misner (ADM) decomposition [67], where the metric fluctuations become non-dynamical Lagrange multipliers. In the following, all perturbations are first-order quantities and depend on both time and space. Spacetime is sliced into three-dimensional hypersurfaces,

$$ds^2 = -N^2 dt^2 + \gamma_{ij} (dx^i + N^i dt) (dx^j + N^j dt), \quad (2.71)$$

where  $N$  and  $N^i$  are the lapse function and shift vector respectively, and  $\gamma_{ij}$  is the spatial 3-metric. The action (2.53) becomes [68]

$$S = \frac{1}{2} \int d^4x \sqrt{\gamma} \left[ N^{(3)}R + N^{-1} (E_{ij}E^{ij} - E^2) + N^{-1} (\dot{\phi} - N^i \partial_i \phi)^2 - N\gamma^{ij} \partial_i \phi \partial_j \phi - 2NV \right], \quad (2.72)$$

where  $K_{ij} = N^{-1}E_{ij}$  is the extrinsic curvature of the three-dimensional spatial slices, and

$$E_{ij} \equiv \frac{1}{2} (\dot{\gamma}_{ij} - \nabla_i N_j - \nabla_j N_i), \quad E = E^i_i. \quad (2.73)$$

We choose to go to *comoving gauge*, defined by the vanishing of the momentum density,  $\delta T_{0i} = 0$ , implying

$$\delta\phi = 0, \quad \gamma_{ij} = a^2 e^{2\zeta} \delta_{ij} \approx a^2 (1 + 2\zeta) \delta_{ij}, \quad (2.74)$$

where  $\zeta$  is the comoving curvature perturbation – the physical scalar degree of freedom. The ADM action (2.72) implies the momentum and Hamiltonian constraint equations for the Lagrange multipliers  $N$  and  $N^i$ :

$$\nabla_i [N^{-1} (E_j^i - \delta_j^i E)] = 0, \quad (2.75)$$

$${}^{(3)}R - N^{-2} (E_{ij}E^{ij} - E^2) - N^{-2} \dot{\phi}^2 - 2V = 0. \quad (2.76)$$

To solve these constraint equations, we define the lapse function as

$$N \equiv 1 + A, \quad (2.77)$$

and split the shift vector into scalar ( $\psi$ ) and vector ( $\tilde{N}_i$ ) parts

$$N_i \equiv \partial_i \psi + \tilde{N}_i, \quad \text{where} \quad \partial_i \tilde{N}^i = 0. \quad (2.78)$$

The momentum constraint equation (2.75) admits the solution

$$A = \frac{\dot{\zeta}}{H} \quad \text{and} \quad \partial^2 \tilde{N}_i = 0, \quad (2.79)$$

where, together with an appropriate choice of boundary conditions, the second equation allows for  $\tilde{N}_i \equiv 0$ . From the Hamiltonian constraint (2.76) we then have

$$\psi = -\frac{\zeta}{H} + \frac{a^2 \dot{\phi}^2}{2H^2} \partial^{-2} \dot{\zeta}, \quad (2.80)$$

where the operator  $\partial^{-2}$  is the solution operator for the Laplacian, defined by  $\partial^{-2}(\partial^2 f) = f$ . Substituting the first-order solutions for the lapse and shift back into (2.72), integrating by parts and using the background equations of motion, the second-order action becomes

$$S^{(2)} = \frac{1}{2} \int d^4x a^3 \frac{\dot{\phi}^2}{H^2} \left[ \dot{\zeta}^2 - a^{-2} (\partial_i \zeta)^2 \right]. \quad (2.81)$$

We introduce the canonically normalised Mukhanov-Sasaki variable [69, 70]

$$v = z\zeta, \quad (2.82)$$

where we have defined

$$z^2 \equiv a^2 \frac{\dot{\phi}^2}{H^2} = 2a^2 \epsilon. \quad (2.83)$$

In conformal time, the action (2.81) becomes

$$S^{(2)} = \frac{1}{2} \int d\tau d^3x \left[ v'^2 - (\partial_i v)^2 + \frac{z''}{z} v^2 \right], \quad (2.84)$$

where a prime denotes a derivative w.r.t. conformal time. This is equivalent to the action of a harmonic oscillator with a time-dependent mass  $m_{\text{eff}}^2(\tau) \equiv \frac{z''}{z}$ , which accounts for the interaction of the scalar field  $\zeta$  with the gravitational background.

Expanding the fluctuation field  $v$  into Fourier modes, given by

$$v_{\mathbf{k}}(\tau) \equiv \int d^3x e^{-i\mathbf{k}\cdot\mathbf{x}} v(\tau, \mathbf{x}), \quad (2.85)$$

we obtain the following equation of motion for the mode functions, called the Mukhanov-Sasaki equation, by varying the action (2.84),

$$v''_{\mathbf{k}} + \left( k^2 - \frac{z''}{z} \right) v_{\mathbf{k}} = 0. \quad (2.86)$$

The general solution reads

$$v_{\mathbf{k}} \equiv a_{\mathbf{k}} v_k(\tau) + a_{\mathbf{k}}^\dagger v_{-k}^*(\tau), \quad (2.87)$$

where the mode functions  $v_k(\tau)$  and  $v_{-k}^*(\tau)$  depend only on the magnitude  $k = |\mathbf{k}|$  due to the assumed cosmological symmetries. With appropriate normalisation and by making use of the fact that the fluctuation field  $v$  is real, the solution is then given by

$$v(\tau, \mathbf{x}) = \int \frac{d^3 k}{(2\pi)^3} \left[ a_{\mathbf{k}} v_k(\tau) e^{i\mathbf{k}\cdot\mathbf{x}} + a_{\mathbf{k}}^\dagger v_k^*(\tau) e^{-i\mathbf{k}\cdot\mathbf{x}} \right]. \quad (2.88)$$

We proceed to quantise the field by imposing the canonical commutation relations

$$\left[ a_{\mathbf{k}_1}, a_{\mathbf{k}_2}^\dagger \right] = (2\pi)^3 \delta^3(\mathbf{k}_1 - \mathbf{k}_2), \quad [a_{\mathbf{k}_1}, a_{\mathbf{k}_2}] = \left[ a_{\mathbf{k}_1}^\dagger, a_{\mathbf{k}_2}^\dagger \right] = 0. \quad (2.89)$$

In the process,  $a_{\mathbf{k}}$  and  $a_{\mathbf{k}}^\dagger$  have been promoted to annihilation and creation operators, respectively (where we have dropped the hats  $\hat{\cdot}$ ), and the vacuum state  $|0\rangle$  is defined by

$$a_{\mathbf{k}}|0\rangle = 0. \quad (2.90)$$

In an exact de Sitter solution the Mukhanov-Sasaki equation (2.86) can be solved as follows. The effective mass reduces to  $\frac{z''}{z} = \frac{a''}{a}$  as  $\dot{\phi}$  and  $H$  are constant. Integrating the relation for conformal time (2.24) with  $a \propto e^{Ht}$ , we obtain  $a = -\frac{1}{H\tau}$  and hence

$$\frac{z''}{z} = \frac{a''}{a} = \frac{2}{\tau^2} \quad (\text{de Sitter}). \quad (2.91)$$

The solution to the equation of motion (2.86) is then

$$v_k(\tau) = \alpha \frac{e^{-ik\tau}}{\sqrt{2k}} \left( 1 - \frac{i}{k\tau} \right) + \beta \frac{e^{ik\tau}}{\sqrt{2k}} \left( 1 + \frac{i}{k\tau} \right). \quad (2.92)$$

In the far past  $|\tau|$  is large, and hence the modes are not affected by gravity and should asymptote to the Minkowski space free particle state. We have  $|k\tau| \gg 1$ , which physically means that the relevant modes have wavelengths much smaller than the horizon. In terms of initial conditions, this corresponds to imposing the

*Bunch-Davies vacuum* as the unique physical vacuum,

$$\lim_{k\tau \rightarrow -\infty} v_k(\tau) = \frac{e^{-ik\tau}}{\sqrt{2k}} \quad (\text{subhorizon}), \quad (2.93)$$

which is an oscillatory solution. This fixes  $\alpha = 1$  and  $\beta = 0$  in (2.92) and the solution becomes

$$v_k(\tau) = \frac{e^{-ik\tau}}{\sqrt{2k}} \left( 1 - \frac{i}{k\tau} \right). \quad (2.94)$$

In the opposite limit, for modes with wavelengths much larger than the horizon,  $|k\tau| \ll 1$ , we then find the growing solution

$$\lim_{k\tau \rightarrow 0^-} v_k(\tau) = -\frac{i}{\sqrt{2k^3\tau}} \propto \tau^{-1} \quad (\text{superhorizon}). \quad (2.95)$$

From (2.82) we therefore have  $\zeta_k \propto z^{-1}v_k \propto \text{const}$ , i.e. the comoving curvature perturbation freezes on superhorizon scales. Fig. 2.6 shows how the fluctuations are stretched during inflation such that they exit the horizon when  $k = |\tau|^{-1} = aH$ .

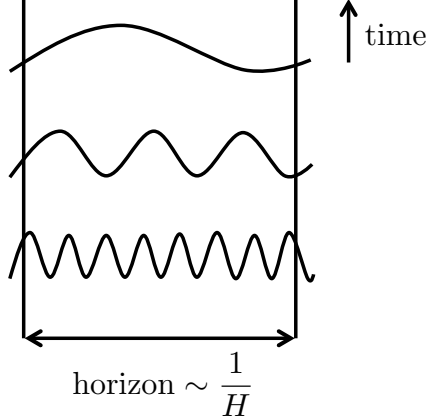


Figure 2.6: Perturbations exit the horizon during inflation: the horizon is almost constant while the fluctuations are stretched to such an extent that they exit the horizon when their wavelength becomes comparable to the horizon size.

We are now in a position to evaluate the *power spectrum*  $P_\zeta(k)$  of the perturbations. It is defined as the Fourier transform of the 2-point correlation function,

$$\langle \zeta_{\mathbf{k}_1} \zeta_{\mathbf{k}_2} \rangle \equiv (2\pi)^3 P_\zeta(k_1) \delta^3(\mathbf{k}_1 + \mathbf{k}_2), \quad (2.96)$$

where isotropy dictates that  $P_\zeta$  only depends on  $k = |\mathbf{k}|$ . Expressed in terms of the

Mukhanov-Sasaki mode functions we have

$$\langle v_{\mathbf{k}_1} v_{\mathbf{k}_2} \rangle = \langle 0 | v_{\mathbf{k}_1} v_{\mathbf{k}_2} | 0 \rangle = (2\pi)^3 |v_{k_1}|^2 \delta^3(\mathbf{k}_1 + \mathbf{k}_2), \quad (2.97)$$

where we have used (2.87) and the commutation relations (2.89) to arrive at the last equality. Thus, on superhorizon scales (2.95) the power spectrum approaches

$$P_v(k) = |v_k|^2 = \frac{1}{2k^3 \tau^2} \quad (\text{superhorizon}), \quad (2.98)$$

and hence

$$P_\zeta(k) = z^{-2} P_v(k) = \frac{H^2}{4k^3 \epsilon} \quad (\text{superhorizon}). \quad (2.99)$$

Note that in the exact de Sitter limit the curvature fluctuations  $\zeta = z^{-1}v$  are ill-defined since  $z^2 = 2a^2\epsilon \rightarrow 0$  as the slow-roll parameter vanishes. In fact, in this case  $\zeta$  is meaningless as inflation never ends. The deviation from perfect de Sitter in a realistic scenario is described by the small but finite slow-roll parameter  $\epsilon$ .

The variance of the curvature perturbations,  $\Delta_s^2(k)$ , is related to the power spectrum via

$$\Delta_s^2(k) \equiv \frac{k^3}{2\pi^2} P_\zeta(k) = \frac{H^2}{8\pi^2 \epsilon}, \quad (2.100)$$

which deviates slightly from a scale-invariant spectrum with  $\Delta_s^2 \sim k^0$  since  $H$  and  $\epsilon$  are functions of time. The deviation from scale-invariance can be quantified in terms of the scalar spectral index  $n_s$ , which is defined as

$$n_s - 1 \equiv \frac{d \ln \Delta_s^2}{d \ln k}. \quad (2.101)$$

Using the fact that the comoving curvature perturbation freezes at horizon crossing  $k = aH$ , we can then evaluate the spectral index to first order in the slow-roll parameters  $\epsilon$  (2.49) and  $\eta$  (2.52),

$$n_s - 1 = \frac{d \ln \Delta_s^2}{d N} \frac{d N}{d \ln k} \bigg|_{k=aH} = -2\epsilon - \eta. \quad (2.102)$$

In the de Sitter limit the spectrum is perfectly scale-invariant. While inflation takes place for  $\epsilon, |\eta| < 1$ , a nearly scale-invariant spectrum with a red tilt can be produced under the additional assumption that the field slowly rolls which implies that  $\epsilon, |\eta| \ll 1$  and  $\eta$  is not too negative. Such a spectrum, which has slowly increasing power at longer wavelengths, agrees with current observational limits from the PLANCK

satellite on the scalar spectral index [9],

$$n_s = 0.9667 \pm 0.0040 \quad (1\sigma). \quad (2.103)$$

If we stop at linear order in perturbation theory, then the equations of motion can be derived from the quadratic action  $S$  (2.81). Hence, the fluctuation modes obey Gaussian statistics as the probability goes like  $e^S$ . In this sense the higher-order corrections provide a measure of non-Gaussianity in the distribution of cosmological perturbations. Simple single-field inflationary models predict a small amount of non-Gaussianity, due to the fact that the potential is very flat and self-interactions of the inflaton are negligible. In contrast, as we will see in 2.4.2 and in more detail in chapter 4, due to a steep potential giving rise to substantial self-interaction, ekpyrotic models predict larger amounts of non-Gaussianity which ought to be observable in the near future.

We have seen that linear (Gaussian) perturbations are related to observations of the power spectrum,  $P(k)$ , defined by the 2-point correlation function (2.97). We can then expand the comoving curvature perturbation to higher orders in perturbation theory,

$$\zeta = \zeta^{(1)} + \zeta^{(2)} + \zeta^{(3)} + \dots \quad (2.104)$$

Quadratic and cubic corrections to these perturbations are related to observations of the 3- and 4-point functions, respectively. For an exactly Gaussian probability distribution all information is contained in the 2-point correlation function. In particular this implies that for odd  $n$ , all  $n$ -point functions are zero, while for even  $n$  the  $n$ -point functions can be written as products of 2-point functions. The bispectrum, i.e. the 3-point correlation function, is defined as

$$\langle \zeta_{k_1} \zeta_{k_2} \zeta_{k_3} \rangle = (2\pi)^3 B(k_1, k_2, k_3) \delta^3(\mathbf{k}_1 + \mathbf{k}_2 + \mathbf{k}_3). \quad (2.105)$$

The connected part of the 4-point function which is not already captured by the product of two 2-point functions is given by the trispectrum,

$$\langle \zeta_{k_1} \zeta_{k_2} \zeta_{k_3} \zeta_{k_4} \rangle = (2\pi)^3 T(k_1, k_2, k_3, k_4) \delta^3(\mathbf{k}_1 + \mathbf{k}_2 + \mathbf{k}_3 + \mathbf{k}_4). \quad (2.106)$$

The  $\delta$ -functions result from momentum conservation, while  $B$  and  $T$  are shape functions for a closed triangle and a quadrangle, respectively.

In momentum space,  $B$  is then parametrised by the shape function  $f_{NL}$ , via

$$B = \frac{6}{5} f_{NL} [P(k_1)P(k_2) + 2 \text{ permutations}] . \quad (2.107)$$

$T$  describes two different shape functions parametrised by  $\tau_{NL}$  and  $g_{NL}$ , see e.g. [71] for additional details. These are defined by

$$T = \tau_{NL} [P(k_{13})P(k_3)P(k_4) + 11 \text{ permut.s}] + \frac{54}{25} g_{NL} [P(k_2)P(k_3)P(k_4) + 3 \text{ permut.s}], \quad (2.108)$$

where  $\mathbf{k}_{ij} = \mathbf{k}_i + \mathbf{k}_j$ .

For the local types of non-Gaussianity that are relevant for the models we consider in this thesis, the parameters  $f_{NL}$  and  $g_{NL}$  can also be related to the (real space) expansion of the curvature perturbation on uniform energy density surfaces in terms of its Gaussian component  $\zeta_L$ , via

$$\zeta = \zeta_L + \frac{3}{5} f_{NL} \zeta_L^2 + \frac{9}{25} g_{NL} \zeta_L^3, \quad (2.109)$$

which is related to the Bardeen space-space metric perturbation  $\Phi_H = \Phi_L + f_{NL} \Phi_L^2 + g_{NL} \Phi_L^3$  [72] through  $\zeta_L = \frac{5}{3} \Phi_L$  during the era of matter domination. For completeness, for models in which the density perturbations originate from the dynamics of a single field<sup>10</sup>,  $\tau_{NL}$  is directly related to the square of  $f_{NL}$  – explicitly we have

$$\tau_{NL} = \frac{36}{25} f_{NL}^2. \quad (2.110)$$

For future reference, it is useful to rewrite Eq. (2.109) in terms of an integral of  $\zeta'$  at the respective order in perturbation theory, which yields the local non-linearity parameters directly:

$$f_{NL} = \frac{5}{3} \frac{\int_{t_{\text{beg}}}^{t_{\text{end}}} \zeta^{(2)'} dt}{\left( \int_{t_{\text{beg}}}^{t_{\text{end}}} \zeta^{(1)'} dt \right)^2}, \quad (2.111)$$

$$g_{NL} = \frac{25}{9} \frac{\int_{t_{\text{beg}}}^{t_{\text{end}}} \zeta^{(3)'} dt}{\left( \int_{t_{\text{beg}}}^{t_{\text{end}}} \zeta^{(1)'} dt \right)^3}, \quad (2.112)$$

where the integrals are evaluated until the time  $\zeta$  has evolved to a constant value.

---

<sup>10</sup>This is also the case for the non-minimal ekpyrotic phase considered in chapter 4, where the perturbations originate solely from the entropy field.

As already mentioned, single-field models of inflation predict small non-Gaussianity of order  $|f_{NL}|, |g_{NL}|, |\tau_{NL}| \sim \mathcal{O}(1)$  due to the non-linear evolution after inflation during reheating [68, 73, 71]. This compares to the observation of the local non-Gaussianity parameters from the PLANCK data [10],

$$f_{NL}^{\text{local}} = 0.8 \pm 5.0 \quad (1\sigma), \quad (2.113)$$

for the bispectrum parameter, and

$$g_{NL}^{\text{local}} = (-9.0 \pm 7.7) \times 10^4 \quad (1\sigma), \quad (2.114)$$

for the trispectrum parameter. These observations are compatible with no significant deviation from Gaussianity.

### 2.3.3 Gravitational waves

Tensor perturbations generated during inflation give rise to primordial gravitational waves. We can apply the formalism just introduced for the scalar fluctuations to compute the quantum generation of tensor perturbations and their resulting spectrum. There is only one tensor contribution in the perturbed ADM metric (2.71), which is already gauge-invariant,

$$\gamma_{ij} = a^2 (\delta_{ij} + h_{ij}), \quad (2.115)$$

where the perturbation is traceless and transverse,

$$h_{ii} = 0, \quad \partial_i h_{ij} = 0. \quad (2.116)$$

Expanding the Einstein-Hilbert action we obtain the second-order action for tensor fluctuations,

$$S_t^{(2)} = \frac{1}{8} \int d\tau d^3x a^2 \left[ (h'_{ij})^2 - (\partial_l h_{ij})^2 \right]. \quad (2.117)$$

We then define the Fourier representation as follows

$$h_{ij}(\tau, \mathbf{x}) = \int \frac{d^3k}{(2\pi)^3} \sum_{\lambda=+,\times} \epsilon_{ij}^\lambda(k) h_{\mathbf{k}}^\lambda(\tau) e^{i\mathbf{k}\cdot\mathbf{x}}, \quad (2.118)$$

where

$$\epsilon_{ii} = 0 \quad \text{and} \quad \epsilon_{ij}^\lambda(k) \epsilon_{ij}^{\lambda'}(k) = 2\delta_{\lambda\lambda'}. \quad (2.119)$$

The fields  $h_{\mathbf{k}}^{\lambda}$  describe the two polarization modes of the gravitational waves (+ and  $\times$ ). In terms of the canonically-normalized fields,

$$f_{\mathbf{k}}^{\lambda} \equiv \frac{a}{2} h_{\mathbf{k}}^{\lambda}, \quad (2.120)$$

the action (2.117) becomes

$$S_t^{(2)} = \sum_{\lambda} \frac{1}{2} \int d\tau d^3x \left[ \left( f_{\mathbf{k}}^{\lambda'} \right)^2 - \left( k^2 - \frac{a''}{a} \right) \left( f_{\mathbf{k}}^{\lambda} \right)^2 \right]. \quad (2.121)$$

Essentially, this corresponds to two copies of the action for the scalar perturbations (2.84) in the de Sitter limit  $\left( \frac{z''}{z} = \frac{a''}{a} \right)$ . Thus, we can infer the power spectrum for the field  $f_{\mathbf{k}}^{\lambda}$  in the de Sitter limit on large scales directly from (2.98),

$$P_f(k) = \frac{1}{2k^3\tau^2} = \frac{1}{2k^3} (aH)^2 \quad (\text{superhorizon}). \quad (2.122)$$

The tensor power spectrum,  $P_t$ , is given by the sum of the power spectra for each polarization mode of  $h_{ij}$ ,

$$P_t(k) = 2 \left( \frac{a}{2} \right)^{-2} P_f(k) = \frac{4H^2}{k^3}. \quad (2.123)$$

In terms of the variance of the tensor perturbations we obtain

$$\Delta_t^2(k) \equiv \frac{k^3}{2\pi^2} P_t(k) = \frac{2H^2}{\pi^2} \Big|_{k=aH}, \quad (2.124)$$

evaluated at horizon crossing. Note that due to historical convention the tensor spectral index is defined as

$$n_t \equiv \frac{d \ln \Delta_t^2}{d \ln k}, \quad (2.125)$$

such that  $n_t = 0$  corresponds to scale-invariance.

Observations of the power in primordial gravitational waves are usually provided as a ratio to the power in the scalar modes, defined as the *tensor-to-scalar ratio*

$$r \equiv \frac{\Delta_t^2(k)}{\Delta_s^2(k)}. \quad (2.126)$$

For single-field slow-roll inflationary models we then get from (2.101) and (2.125),

$$r = 16\epsilon. \quad (2.127)$$

As we have seen already, for slow-roll inflation to take place we require  $\epsilon \ll 1$ . The simplest estimate for the tensor-to-scalar ratio for these models is obtained by imposing the condition  $\epsilon \gg \frac{d \ln \epsilon}{dN} = \eta$  during most of the slow-roll period such that  $\epsilon$  is not only small but also nearly constant. From observations of the spectral tilt (2.103), the first slow-roll parameter then takes the value  $\epsilon \approx 0.017$ , giving  $r \approx 0.27 \pm 0.03 (1\sigma)$ . Compared to the upper bound on the tensor-to-scalar ratio from the PLANCK satellite [4],

$$r_{0.002} < 0.11 \quad (2\sigma), \quad (2.128)$$

this simple estimate demonstrates why some inflationary potentials are disfavoured, as can be seen in Fig. 2.7.

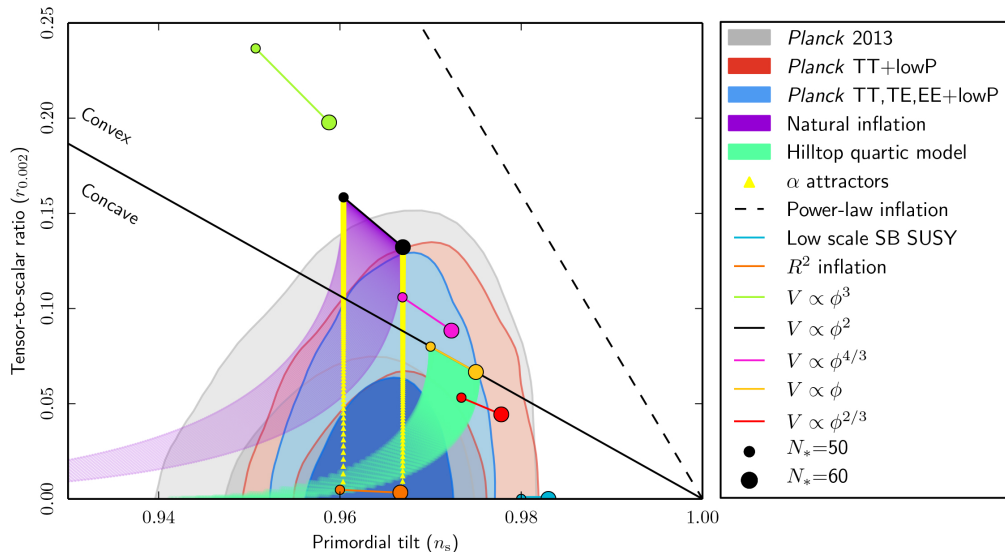


Figure 2.7: Tensor-to-scalar ratio  $r_{0.002}$  versus scalar spectral index  $n_s$  from PLANCK in combination with other data sets, compared to the theoretical predictions of selected inflationary models [4].

### 2.3.4 Problems

In this subsection we will motivate the investigation of alternative models to inflation. From a theoretical point of view, single-field plateau models of inflation present important challenges (see e.g. [17]). For one, inflation does not provide a complete history of the universe, and one may ask what happened before inflation and how the inflationary phase started. In fact, the initial conditions need to be very special: the

scalar field needs to start out at large potential values (e.g. on top of a high plateau) with negligible initial velocity, everywhere within a region of the universe that is a billion times larger than the Planck scale. This requirement clashes somewhat with the motivation for inflation, which is to explain the specialness of the early universe in a dynamical fashion. Several attempts have been made to quantify how unlikely the initial conditions for inflation have to be. There is an entropy argument by Roger Penrose [74] in which he considers the universe in terms of its entropy, i.e. the number of different configurations with different properties. The entropy of the universe today is much smaller than the maximum, and hence we live in a special state. However, in terms of entropy the initial conditions required for inflation are even less likely. Gary Gibbons and Neil Turok [75] have shown that although inflation is an attractor, short durations for inflation are exponentially preferred such that the horizon and flatness problems are not solved. The universe is supposed to start out with potential energy dominance, that is the scalar field should sit high on the potential nearly at rest. Since its kinetic energy scales as  $\sim 1/a^6$ , it becomes large when going back in time as the scale factor approaches zero. However, the potential energy remains essentially constant on the plateau, such that it is very unlikely to find the field at rest anywhere. In fact, it is exponentially rarer than the conditions we tried to explain in the first place. These arguments lead to the conclusion that our universe is more likely to have achieved its current conditions without inflation than with it.

Note that it might be possible to realise inflation in string theory based on certain assumptions [76]. Typically, there are many contributions to the effective potential. Parameters have to be fine-tuned quite carefully to find some region of the potential that is just flat enough where inflation can then occur. Moreover, string theory seems to prefer negative potentials and it is in fact hard to construct reliable standard inflationary models with positive potentials [77].

Inflation is very sensitive to parameters: for example, there are enough parameters to tweak in the theory that one can match either the initial BICEP2 results claiming a detection of gravitational waves with a tensor-to-scalar ratio of  $r = 0.20^{+0.07}_{-0.05} (1\sigma)$  [15], or the revised BICEP2 & PLANCK results with only an upper bound  $r_{0.05} < 0.12 (2\sigma)$  [16] (resulting from taking the effects of dust in our galaxy into account).

Another challenge is that most inflationary models lead to the runaway behaviour of eternal inflation [78, 79]. Small quantum fluctuations are the origin of the temperature fluctuations and the seeds for the large-scale structure. However, rare, large

quantum fluctuations can momentarily disrupt the inflationary dynamics such that in some regions inflation ends much later. These regions will blow up in volume leading to more rare fluctuations which lead to more inflation and so on. In this way an infinite number of causally disconnected pocket universes is created, containing all possible values for the amplitude, the spectrum and the Gaussianity of the perturbations. To complete the theory of inflation, an additional measure is necessary to regularise these infinities. In the absence of a measure the theory loses all its predictive power and the naive predictions in section 2.3 become questionable. Applying the volume measure as just outlined fails to explain why our universe looks the way it does. Different measures are possible (see e.g. [80, 81]), however, the question remains why one measure should be favoured over another.

Inflation does not solve the big bang singularity problem. A theorem by Börde, Guth and Vilenkin [82] shows that ever-expanding cosmologies are past incomplete, so that a classical universe – even if it includes a phase of inflation – must have started out with an initial singularity. In the context of the inflationary framework this problem has to be addressed since its predictions depend on the physical conditions at the onset of the inflationary stage. It is not fully understood yet whether phases preceding inflation, which ought to be governed by a full theory of quantum gravity, do not decisively influence the physics on scales of observational relevance today.

This situation suggests two possible approaches: the first is to try and understand the above-mentioned challenges better and to resolve them. A second approach is to look for alternative theories which might be able to explain the same cosmological data without however presenting us with such conceptual conundrums. Evidently it is interesting to pursue both approaches. In this thesis we will be concerned with the second approach. In particular, the kind of multiverse problem just described is evaded in ekpyrosis. Regions with large quantum fluctuations continue to contract slowly and do not compete in volume. Moreover, as we show in subsection 2.4.3 the cyclic model is falsifiable by detection of primordial tensor perturbations.

## 2.4 Ekpyrosis and the cyclic model

The original proposal of the ekpyrotic<sup>11</sup> and cyclic cosmology by Justin Khoury, Burt A. Ovrut, Paul J. Steinhardt and Neil Turok [83] is based on the braneworld picture of the universe, see Fig. 2.8. In addition to our  $(3 + 1)$ -dimensional brane there is a

---

<sup>11</sup>The term ekpyrosis is adopted from the Stoic model of cosmic evolution in which the universe is consumed by and reconstituted out of a fire, called ekpyrosis, at regular intervals [83].

second such boundary brane connected to ours via a 1-dimensional line segment, such that spacetime is effectively 5-dimensional. In the heterotic M-theory embedding, which motivated this scenario, there are 6 additional internal dimensions wrapped in a Calabi-Yau manifold at each spacetime point. The cyclic model proposes that

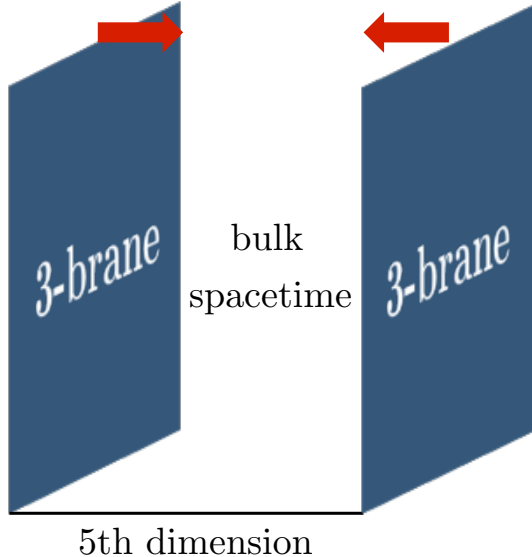


Figure 2.8: The braneworld picture of our universe, based on [5]. Gravity can propagate in the whole spacetime while other forces and matter are localised on the  $(3 + 1)$ -dimensional branes. There is an attractive force between the two branes across the bulk spacetime that makes them collide at regular intervals. The collision corresponds to the big bang as seen from the brane.

there is an attractive force between the branes, which causes them to approach each other. If this ekpyrotic phase lasts long enough the branes are flattened to such a degree that the horizon and flatness problems are solved. As seen from an observer on the brane, the eventual collision of the two branes corresponds to the reversal from contraction to expansion, identified with the big bang. It creates hot matter and radiation and triggers an epoch of expansion, cooling and structure formation. The seeds for the latter are due to quantum fluctuations during the ekpyrotic phase; the branes become slightly rippled and hence some regions collide at slightly different times leading to slightly different temperatures. While the branes are separated far from each other the potential energy associated with the interbrane force responsible for drawing the branes together again acts as dark energy. The cycle then starts to repeat once the branes become closer again, initiating a new ekpyrotic phase and eventually a new brane collision (big bang).

It has to be pointed out that this higher-dimensional description relies on the unproven reality of branes, extra dimensions and string theory. However, it is important to appreciate that the distinct phases of the colliding brane picture can also be discussed purely in a 4-dimensional effective theory, and in fact could have a different origin than the brane motion just described. In particular, the ekpyrotic phase uses the same ingredients as inflationary models but with different details. For a comprehensive review of the higher-dimensional and effective picture see [5]. In the following we will focus on the 4-dimensional effective ekpyrotic phase and first show how the background solution solves the puzzles described in 2.2, before going into detail on how to produce nearly scale-invariant and Gaussian density perturbations via the entropic mechanism. A main part of this thesis explores a variant of this mechanism, to be introduced in chapter 4.

### 2.4.1 The ekpyrotic solution

Instead of an inflationary phase, the puzzles described in section 2.2 can also be solved dynamically through a phase of ultra-slow contraction. For convenience we reproduce the Friedmann equation (2.22) here,

$$3H^2 = \Lambda - \frac{3k}{a^2} + \frac{\rho_m}{a^3} + \frac{\rho_r}{a^4} + \frac{\sigma^2}{a^6} + \dots + \frac{\rho_\phi}{a^{3(1+w_\phi)}}, \quad (2.129)$$

which relates the Hubble parameter to the total energy density in the universe. In a contracting universe it becomes clear that the anisotropy term comes to dominate the cosmic evolution, as it scales as  $a^{-6}$ . For the scalar field  $\phi$  to dominate the dynamics instead implies an equation of state parameter  $w_\phi > 1$ . From the expression for  $w_\phi$  in Eq. (2.57) we deduce that this bound can be achieved with a steep negative potential such that the field rolls fast enough for the denominator to be positive. A typical realisation is plotted in Fig. 2.9 where the ekpyrotic phase lasts while the potential is a negative exponential which can be written as

$$V(\phi) = -V_0 e^{-c\phi}, \quad (2.130)$$

where  $V_0$  and  $c$  are positive constants. In a flat FLRW universe, with metric (2.7) and  $k = 0$ , the equation of motion for the field and the Friedmann equations are

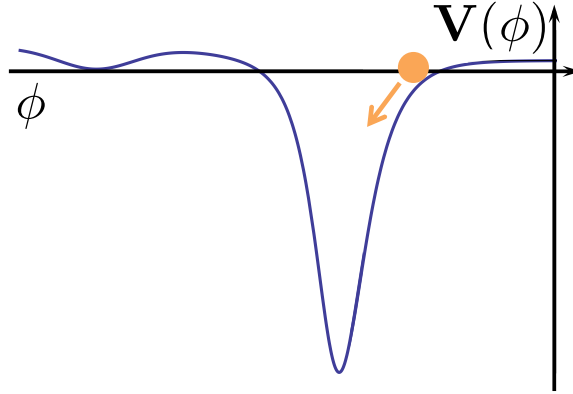


Figure 2.9: A scalar field rolling down a steep, negative potential leads to an ekpyrotic phase.

given by

$$\ddot{\phi} + 3H\dot{\phi} + V_{,\phi} = 0, \quad (2.131)$$

$$3H^2 = \rho_\phi = \frac{1}{2}\dot{\phi}^2 + V(\phi), \quad (2.132)$$

$$\dot{H} = -\frac{1}{2}(\rho_\phi + p_\phi) = -\frac{1}{2}\dot{\phi}^2, \quad (2.133)$$

which differ from the equations for inflation, (2.61) - (2.63), in the form of the potential (2.130). The set of equations admits the *scaling solution*

$$a \propto (-t)^{1/\epsilon}, \quad \phi = \sqrt{\frac{2}{\epsilon}} \ln \left[ -\sqrt{\epsilon V_0} t \right], \quad \epsilon = \frac{c^2}{2}, \quad \text{for } c \gg 1, \quad (2.134)$$

where  $t$  is negative and runs from large negative values to small negative values. Hence, the universe contracts very slowly with equation of state (2.57)

$$w_\phi = \frac{2\epsilon}{3} - 1 \gg 1. \quad (2.135)$$

In the ekpyrotic scenario  $\epsilon$  is the *fast-roll* parameter and its definition is identical with the slow-roll parameter in inflation. Thus, for a successful ekpyrotic phase where the universe becomes flat and anisotropies are suppressed we need  $\epsilon \gg 3$  (i.e.  $c^2 \gg 6$ ). Note that the scaling solution is such that in the Friedmann equation (2.132) each term scales as  $1/t^2$  and thus the relative importance of the various terms remains unchanged over time.

In order to solve the flatness problem described in section 2.2.2 we know from

(2.44) that the relative density in curvature has to decrease by 60 orders of magnitude. From the scaling solution (2.134) we see that the scale factor  $a$  is approximately constant while the Hubble parameter decreases like  $H = \frac{1}{\epsilon t} \propto t^{-1}$  during ekpyrosis. Since the energy density in curvature goes like  $(aH)^{-2}$ , we have

$$\frac{\Omega_{k, \text{ek-beg}}}{\Omega_{k, \text{ek-end}}} \propto \frac{(aH)_{\text{ek-end}}^2}{(aH)_{\text{ek-beg}}^2} \propto \frac{t_{\text{ek-beg}}^2}{t_{\text{ek-end}}^2} \gtrsim 10^{60}, \quad (2.136)$$

and hence

$$|t_{\text{ek-beg}}| \gtrsim 10^{30} |t_{\text{ek-end}}| \quad (2.137)$$

where ek-beg and ek-end refer to the beginning and end of the ekpyrotic phase, respectively. This corresponds to about 70 e-folds of evolution (cf. the 70 e-folds of inflation it takes to solve this puzzle in 2.51). In order to obtain the observed amplitude of cosmological perturbations, we require the minimum of the potential to be roughly at the grand unified scale,  $V_{\text{ek-end}} \approx (10^{-2} M_{\text{Pl}})^4$ , given by Eq. (2.169) in the next subsection. Plugging the scaling solution into the expression for the potential,  $V = -\frac{1}{\epsilon t^2}$ , we can determine the time ekpyrosis has to end,

$$t_{\text{ek-end}} \approx -10^3 M_{\text{Pl}}^{-1}. \quad (2.138)$$

Thus,

$$|t_{\text{ek-beg}}| \gtrsim 10^{33} M_{\text{Pl}}^{-1} \approx 10^{-10} \text{s}, \quad (2.139)$$

which is the minimum time the ekpyrotic phase has to last in order to solve the flatness puzzle – a very short time in cosmological terms, demonstrating the effectiveness of the ekpyrotic phase. We can also compare this time scale to the duration of the ekpyrotic phase in the cyclic theory. There, the potential interpolates between the dark energy scale at positive values on the right in Fig. 2.9 and the GUT scale at the bottom of the potential. Since  $V \propto t^{-2}$ , we obtain [5]

$$|t_{\text{ek-beg}}| = \sqrt{\frac{V_{\text{ek-end}}}{V_{\text{ek-beg}}}} |t_{\text{ek-end}}| \approx \sqrt{10^{112}} 10^3 M_{\text{Pl}}^{-1} \approx 10^{16} \text{s}, \quad (2.140)$$

which corresponds to a duration on the order of billion years, and hence the ekpyrotic phase easily resolves the flatness problem.

As we have already seen from the Friedmann equation, it is not the curvature but the anisotropy term that would dictate the dynamics in a contracting universe.

Belinsky, Khalatnikov and Lifshitz (BKL) showed in 1970 that if in a contracting universe all the energy density components have an equation of state  $w < 1$ , chaos ensues due to the instability of the universe w.r.t. small perturbations [84]. As the overall volume shrinks, the metric becomes highly anisotropic, which causes the universe to expand along one axis and contract along the others. This state can be approximated by the anisotropic Kasner solution, given in (2.18), however, the metric jumps from one Kasner form to another repeatedly, an effect known as BKL oscillations or ‘‘chaotic mixmaster’’ behaviour [85, 86]. This loss of all predictability in going towards the big crunch singularity can be avoided by the addition of the ekpyrotic scalar field with  $w_\phi > 1$ . The relative importance of the energy density in anisotropies scales as  $1/(a^6 H^2)$  from (2.22). Since to first approximation the scale factor is constant, the anisotropies scale in the same way as the curvature term and are hence exponentially suppressed, as seen from (2.137). Thus, at the end of the ekpyrotic phase the chaotic behaviour is suppressed and the universe contracts homogeneously and isotropically [26].

Before the bounce of the contracting universe to the expanding one we observe today, the ekpyrotic potential has to turn off and become irrelevant. The universe enters a kinetic-energy dominated phase, characterised by an equation of state  $w = 1$ . The equations of motion (2.131) - (2.133) then simplify to

$$3H^2 = -\dot{H} = \frac{1}{2}\dot{\phi}^2, \quad \ddot{\phi} + 3H\dot{\phi} = 0. \quad (2.141)$$

Integrating the first equation, we obtain  $a \propto e^{\phi/\sqrt{6}}$  and the solution

$$a = a_0(-t)^{\frac{1}{3}}, \quad \phi = \sqrt{\frac{2}{3}} \ln(-t) + \phi_0, \quad (2.142)$$

where  $a_0$  and  $\phi_0$  are constants. It is immediately clear that the energy density in the scalar field, i.e. the kinetic energy, scales as  $\dot{\phi}^2 \propto a^{-6}$  – the same way as the anisotropic term. Thus, the anisotropies do not regrow after the ekpyrosis is over, as their relative importance remains constant during the kinetic phase.

Lastly, the horizon problem is automatically solved in ekpyrotic and cyclic models, as there is enough time before the big bang for different parts of the currently observable universe to have been in causal contact with each other.

### 2.4.2 The entropic mechanism

In this subsection, we show how a spectrum of adiabatic, nearly scale-invariant and Gaussian scalar perturbations, that can account for the temperature anisotropy of the CMB and seed large-scale structure formation, may arise during the ekpyrotic phase. Quantum fluctuations added to the classical evolution just discussed are amplified into classical density perturbations. Besides inflation, the only other way this can be achieved dynamically is during ekpyrosis. Here, the horizon – the region of causal contact – shrinks rapidly while the fluctuation modes themselves remain roughly constant in size since the background approximates Minkowski with  $a \approx \text{const}$  as shown in Fig. 2.10.

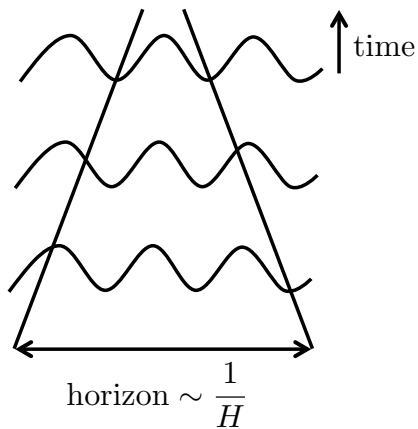


Figure 2.10: Perturbations exit the horizon during ekpyrosis: the fluctuations stay almost constant while the horizon shrinks.

There is one subtlety: ekpyrotic models require two scalar fields in order to produce a spectrum compatible with observations [87]. The so-called *entropic mechanism* is a two-stage process: first, as soon as there is more than one scalar field present, nearly scale-invariant and Gaussian entropy (isocurvature) perturbations are produced during the ekpyrotic phase. They are squeezed as they exit the horizon and become a stochastic distribution of classical perturbations, while the adiabatic perturbations stay quantum [88]. In a second step, the entropy fluctuations are then converted into curvature perturbations facilitated by a bending in the field space trajectory. Note that in the higher-dimensional theory two universal scalar fields are always present; the radion field, which determines the distance between the two branes, and the volume modulus of the internal manifold called the (Calabi-Yau) dilaton. In the following we briefly review the standard entropic mechanism, which

we then contrast with the new non-minimal version in chapter 4.

The 4-dimensional effective action for two scalar fields,  $\phi$  and  $\chi$ , minimally coupled to gravity and in a potential reads

$$S = \int d^4x \sqrt{-g} \left[ \frac{1}{2}R + \frac{1}{2}g^{\mu\nu}\partial_\mu\phi\partial_\nu\phi + \frac{1}{2}g^{\mu\nu}\partial_\mu\chi\partial_\nu\chi - V(\phi, \chi) \right], \quad (2.143)$$

We assume an exponential potential for both fields during the ekpyrotic phase,

$$V(\phi, \chi) = -V_1 e^{-c_1 \phi} - V_2 e^{-c_2 \chi}, \quad (2.144)$$

where  $V_{1,2}$  are positive constants and we allow  $c_1 = c_1(\phi)$ ,  $c_2 = c_2(\chi)$  to be field-dependent. Via a rotation in field space we can decompose the new fields and their perturbations into the adiabatic variable  $\sigma$  and the entropic direction  $s$ , pointing along the background trajectory in field space and perpendicular to it, respectively [89, 90]. They are depicted in Fig. 2.11 and defined via [6]

$$\dot{\sigma} \equiv \cos \theta \dot{\phi} + \sin \theta \dot{\chi} = \sqrt{\dot{\phi}^2 + \dot{\chi}^2}, \quad \dot{s} \equiv \cos \theta \dot{\chi} - \sin \theta \dot{\phi} = 0, \quad (2.145)$$

with

$$\cos \theta = \frac{\dot{\phi}}{\dot{\sigma}}, \quad \sin \theta = \frac{\dot{\chi}}{\dot{\sigma}}, \quad (2.146)$$

where  $\theta$  is the angle of the background trajectory with the  $\phi$ -direction.

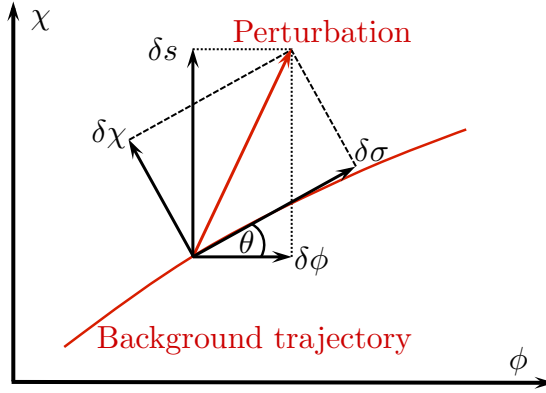


Figure 2.11: The decomposition into the adiabatic direction,  $\sigma$ , and the transverse direction,  $s$ , is shown. Perturbations along the direction of the background trajectory are adiabatic/curvature perturbations, whereas perturbations orthogonal to the trajectory represent entropy/isocurvature perturbations. Based on [6].

The two-field scaling solution becomes

$$a \propto (-t)^{\frac{1}{\epsilon}}, \quad \sigma = -\sqrt{\frac{2}{\epsilon}} \ln \left[ -\sqrt{\epsilon V_0 t} \right], \quad \dot{s} = 0, \quad \theta = \text{const.} \quad (2.147)$$

Notice that it follows from  $s = \text{const}$  along the classical trajectory that entropy perturbations are automatically gauge-invariant [91]. The two-field ekpyrotic potential can be re-expressed in terms of the new coordinate system [20],

$$V = -V_0 e^{-\sqrt{2\epsilon}\sigma} \left[ 1 + \epsilon s^2 + \frac{\kappa_3}{3!} \epsilon^{3/2} s^3 + \frac{\kappa_4}{4!} \epsilon^2 s^4 + \dots \right], \quad (2.148)$$

and is illustrated in Fig. 2.12. In terms of the parameters in the potential,  $\kappa_{3,4}$  are given by

$$\kappa_3 = 2\sqrt{2} \frac{c_1^2 - c_2^2}{|c_1 c_2|}, \quad \kappa_4 = 4 \frac{c_1^6 + c_2^6}{c_1^2 c_2^2 (c_1^2 + c_2^2)}. \quad (2.149)$$

As long as a microphysical derivation of the potential is not available, we use this new, more general, parametrisation of the potential (2.148) and set  $\kappa_{3,4} \sim \mathcal{O}(1)$ . The scaling solution (2.147) describes motion along the ridge of the potential along

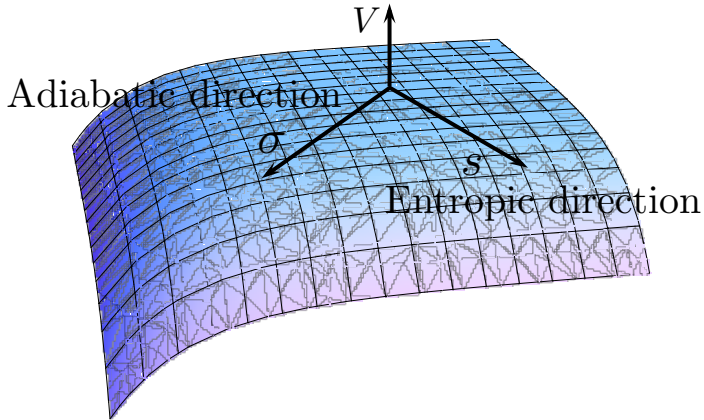


Figure 2.12: After a rotation in field space, the two-field ekpyrotic potential decomposes into the adiabatic direction,  $\sigma$ , and the transverse tachyonic direction,  $s$ . The ekpyrotic scaling solution corresponds to motion along the ridge of the potential. Based on [7].

the adiabatic direction. Due to the tachyonic entropic direction the ekpyrotic background evolution is unstable to small perturbations [28, 92] – they are the entropy perturbations which are later converted into curvature perturbations in the entropic mechanism. However, this seems to imply that the initial conditions problem has

not been solved, as the trajectory must be localised extremely close to the ridge at the beginning of the ekpyrotic phase [93]. The problem is resolved in the framework of the cyclic picture where only the habitable regions make it through the ekpyrotic phase [94]. In this ‘‘phoenix universe’’, regions whose trajectories depart too far from the ridge become highly inhomogeneous remnants and black holes that stop cycling and growing. If the dark-energy dominated phase we experience today lasts long enough, regions sufficiently close to the ridge are vastly amplified and lead to a smooth, flat, expanding space with nearly scale-invariant curvature perturbations, as observed today.

We now show how in the first stage of the entropic mechanism nearly scale-invariant entropy perturbations are produced. For two scalar fields, the adiabatic and entropy perturbations are defined as

$$\delta\sigma \equiv \frac{\dot{\phi}\delta\phi + \dot{\chi}\delta\chi}{\dot{\sigma}} \quad \text{and} \quad \delta s \equiv \frac{\dot{\phi}\delta\chi - \dot{\chi}\delta\phi}{\dot{\sigma}}, \quad (2.150)$$

respectively. While the latter is gauge-invariant, the adiabatic perturbation is not. The gauge-invariant and thus physical quantity important here is the comoving curvature perturbation  $\zeta$  introduced in (2.74). At the linearised level, the equation of motion for the entropy perturbation reads

$$\ddot{\delta s} + 3H\dot{\delta s} + \left( \frac{k^2}{a^2} + 3\dot{\theta}^2 + V_{,ss} \right) \delta s = 0. \quad (2.151)$$

In terms of conformal time and with the rescaled entropy field  $\delta S = a(\tau)\delta s$ , the equation for a straight trajectory ( $\dot{\theta} = 0$ ) becomes

$$\delta S'' + \left( k^2 - \frac{a''}{a} + a^2 V_{,ss} \right) \delta S = 0. \quad (2.152)$$

Allowing for the fast-roll parameter  $\epsilon$  to vary slowly, we can derive the following expressions, valid to sub-leading order in  $\epsilon$  [28]

$$\frac{a''}{a} = a^2 H^2 (2 - \epsilon), \quad (2.153)$$

$$V_{,ss} = H^2 \left( -2\epsilon^2 + 6\epsilon + \frac{5}{2}\epsilon_{,N} \right), \quad (2.154)$$

$$aH = \frac{1 + 1/\epsilon + \epsilon_{,N}/\epsilon^2}{\epsilon\tau}, \quad (2.155)$$

where  $dN = d\ln a$ , and  $N$  denotes the remaining number of e-folds of ekpyrosis.

Thus, we arrive at a form for the equation of motion that can easily be solved in terms of a Hankel function,

$$\delta S'' + \left( k^2 - \frac{2 \left( 1 - \frac{3}{2\epsilon} + \frac{3\epsilon_{,N}}{4\epsilon^2} \right)}{\tau^2} \right) \delta S = 0. \quad (2.156)$$

Together with the boundary condition of approaching the Minkowski vacuum state in the far past, the solution is

$$\delta S = \frac{\sqrt{-k\tau}}{2} H_\nu^{(1)}(-k\tau), \quad \text{with} \quad \nu = \frac{3}{2} \left( 1 - \frac{2}{3\epsilon} + \frac{\epsilon_{,N}}{3\epsilon^2} \right), \quad (2.157)$$

where we have neglected an irrelevant phase. At late times,  $-k\tau \ll 1$ , the entropy perturbation becomes

$$\delta S \approx \frac{1}{\sqrt{2}(-\tau)k^\nu}, \quad (2.158)$$

which can be rewritten in terms of the potential at the end of the ekpyrotic phase as

$$\delta s_{\text{ek-end}} \approx \frac{\sqrt{|\epsilon V_{\text{ek-end}}|}}{\sqrt{2}k^\nu}. \quad (2.159)$$

Following the same steps as in the inflationary case in (2.3.2), we can calculate the deviation from scale-invariance in the spectral index of the entropy perturbations [28],

$$n_s - 1 = 3 - 2\nu = \frac{2}{\epsilon} - \frac{\epsilon_{,N}}{\epsilon^2}. \quad (2.160)$$

In order to obtain a red tilt in the spectrum the second term has to outweigh the gravitational contribution in the first term. As illustrated in Fig. 2.9 the steepness of the potential must decrease such that the ekpyrotic phase can come to an end. We can estimate this effect on the spectral index by rewriting the expression in terms of  $\mathcal{N}$ , which measures the number of e-folds of modes which exit the horizon before the end of the ekpyrotic phase, defined via  $d\mathcal{N} = d\ln(aH)$ . Thus,

$$n_s - 1 = \frac{2}{\epsilon} - \frac{d\ln\epsilon}{d\mathcal{N}}, \quad (2.161)$$

where  $\epsilon(\mathcal{N})$  is directly related to the equation of state during the ekpyrotic phase via (2.135), which decreases from a value much greater than one to order unity in the last  $\mathcal{N}$  e-folds. Parameterising  $\epsilon \approx \mathcal{N}^\alpha$  [95], the spectral tilt becomes red for  $\alpha > 1.14$ , whereas the observed  $n_s \approx 0.97$  can be achieved with  $\alpha \approx 2$  [7].

In the second step the approximately scale-invariant entropy perturbations have to be converted into curvature perturbations. The entropy perturbations of interest have all left the horizon and hence we can focus on the large-scale limit, where spatial gradients can be neglected. We now derive a particularly simple and useful form of the evolution equation for the comoving curvature perturbation on large scales [96, 97, 98]. We will work in comoving gauge and take the background to be described by a flat FLRW metric. On large scales the perturbed metric can be written as (cf. (2.74))

$$ds^2 = -dt^2 + a(t)^2 e^{2\zeta(t, x^i)} dx^i dx_i, \quad (2.162)$$

where  $\zeta$  denotes the comoving curvature perturbation and can be thought of as a local perturbation in the scale factor. In a scalar field model the equation of continuity is given by

$$\dot{\rho} + 3(H + \dot{\zeta})(\rho + p) = 0, \quad (2.163)$$

with the background (denoted by over-bars) satisfying

$$\dot{\bar{\rho}} + 3\bar{H}(\bar{\rho} + \bar{p}) = 0. \quad (2.164)$$

On comoving hypersurfaces the energy density is uniform,  $\rho = \bar{\rho}$  (and hence also  $H = \bar{H}$  because of the Friedmann equation). We then obtain

$$\dot{\zeta} = -\bar{H} \frac{\delta p}{\bar{\rho} + \bar{p} + \delta p}, \quad (2.165)$$

where  $\delta p \equiv p(t, x^i) - \bar{p}(t)$ . Since, by definition,  $\delta\rho = 0$  on these hypersurfaces, we can immediately relate the pressure perturbation to a perturbation in the potential,  $\delta p = -2\delta V|_{\delta\rho=0}$ . Plugging this relation into Eq. (2.165), we obtain a compact expression for the evolution of the comoving curvature perturbation on large scales, writing  $\bar{H} = H$ ,

$$\dot{\zeta} = \frac{2H\delta V}{\dot{\sigma}^2 - 2\delta V}, \quad (2.166)$$

which is valid to all orders in perturbation theory.

The evolution equation for the comoving curvature perturbation at linear order is then given by [6]

$$\dot{\zeta} = -\frac{2H}{\dot{\sigma}} \dot{\theta} \delta s = \sqrt{\frac{2}{\epsilon}} \dot{\theta} \delta s. \quad (2.167)$$

It follows immediately that curvature perturbations are sourced by the entropy per-

turbations as soon as the background trajectory bends,  $\dot{\theta} \neq 0$ . Several possible conversion processes have been studied in the past in connection with the standard entropic mechanism. The first is called *ekpyrotic conversion*; the trajectory can stray sufficiently far from the ridge of the potential and thus turn and fall off the potential as the ekpyrotic phase comes to an end [90, 99]. The second is that the trajectory can undergo a bend during the kinetic phase that follows the ekpyrotic phase [28], hence the name *kinetic conversion*. This latter setting is well-motivated by the embedding of cyclic models into heterotic M-theory, where such a bending of the trajectory automatically occurs in the approach to the bounce [100, 101]. For these two possibilities, Eq. (2.167) allows us to estimate the order of magnitude of the curvature perturbation: approximating  $\epsilon$  and  $\delta s$  as constants over the time of the conversion, and assuming a total bending angle of about 1 radian,  $\Delta\theta \approx 1$ , we obtain

$$\zeta_{final} \approx -\frac{1}{\sqrt{\epsilon_c}} \delta s_{ek-end}, \quad (2.168)$$

where  $\delta s_{ek-end}$  denotes the value of the entropy perturbation at the end of the ekpyrotic phase and  $\epsilon_c$  the value of the fast-roll parameter at the time of conversion. During the kinetic phase, the entropy perturbation satisfies the simplified equation of motion  $\ddot{\delta s} + 3H\dot{\delta s} = 0$  and thus grows logarithmically, so that to a first approximation we can ignore this modest growth. Using (2.159) we obtain

$$\langle \zeta_{final}^2 \rangle \equiv \int \frac{dk}{k} \Delta_\zeta^2 \approx \int \frac{d^3k}{(2\pi)^3 \epsilon_c} (\delta s_{ek-end})^2 \approx \int \frac{dk}{k} \frac{\epsilon V_{ek-end}}{(2\pi)^2} k^{n_s-1}, \quad (2.169)$$

where  $V_{ek-end} = |V(t_{ek-end})|$  denotes the magnitude of the potential at the end of the ekpyrotic phase, i.e. it corresponds to the energy scale of the deepest point in the potential. This implies that the potential has to reach the grand unified scale  $V_{ek-end} \approx (10^{-2} M_{Pl})^4$  in order for the curvature perturbations to have an amplitude in agreement with the observed value of  $\Delta_\zeta^2 \approx 2 \times 10^{-9}$  [9].

There is reason to assume that the curvature perturbations produced during ekpyrotic or kinetic conversion pass through the bounce/big bang transition essentially unchanged. It has been shown (for example in [102, 103]) that it is possible to make predictions for density perturbations which are independent of the details of the bouncing phase. In the next section 2.5 we discuss the bounce in more detail.

A final possibility, of a somewhat different character, is that conversion can occur at the bounce itself via the process of modulated (p)reheating [104]. The idea here is that at the bounce massive matter can be copiously produced, and can then

subsequently decay into ordinary fermions. If the coupling  $h(\delta s)$  of the massive matter fields to the fermions depends on the value of the entropy field, then the decay rate will be modulated by the value of the entropy fluctuations, with the result that the spectrum of entropy fluctuations will be imprinted directly onto the produced matter. As shown in [104], the amplitude of the resulting perturbations is proportional to  $h_{,s}/h$ , and thus all predictions depend on being able to derive the precise form of the coupling function  $h(\delta s)$  in a realistic setting. This conversion model has the property that no bending of the trajectory needs to occur before the bounce.

We summarise the results for the local non-Gaussianity in the curvature perturbation produced during ekpyrotic and kinetic conversion here, and refer the reader to chapter 4 for a detailed derivation of all relevant evolution equations, and in particular section 4.3 where we contrast the predictions of the non-minimal to the standard entropic mechanism.

Assuming that the dominant amount of conversion occurs before the bounce, both ekpyrotic and kinetic conversion result in a distinct observational imprint [20, 7]: In terms of the parameter  $c_1$  in the potential (2.144) we obtain for the *ekpyrotic conversion*,

$$f_{NL} = -\frac{5}{12}c_1^2 < 0, \quad |f_{NL}| \sim \mathcal{O}(10 - 100) \quad \text{and} \quad (2.170)$$

$$g_{NL} = \frac{25}{108}c_1^4 > 0, \quad |g_{NL}| \sim \mathcal{O}(10^3 - 10^4). \quad (2.171)$$

In order for the power spectrum of the perturbations to be in agreement with observations, we require  $c_1 \gtrsim 10$ , which implies  $f_{NL} \lesssim -40$  and  $g_{NL} \gtrsim 2500$ . Contrasting these predictions with the current observational bounds on the bi- and trispectrum parameters measured by PLANCK, (2.113) and (2.114), it becomes clear that this type of conversion mechanism is basically ruled out by observations. Moreover, in the light of the phoenix universe described in the beginning of this subsection, it makes sense to focus on conversion that occurs only once the equation of state has become small towards the end of the ekpyrotic phase, or in fact once the kinetic phase is already underway. In the higher-dimensional brane picture it was shown [105, 101] that an effective potential arises along the  $\chi$  axis in the presence of matter on the boundary branes, which causes the field space trajectory to bend in its vicinity. In this case, *kinetic conversion* predicts the following fitting formulae and resulting

order of magnitude estimates

$$f_{NL} = \frac{3}{2}\kappa_3\sqrt{\epsilon} + 5, \quad |f_{NL}| \sim \mathcal{O}(10) \quad \text{and} \quad (2.172)$$

$$g_{NL} = \left(\frac{5}{3}\kappa_4 + \frac{5}{4}\kappa_3^2 - 40\right)\epsilon, \quad |g_{NL}| \sim \mathcal{O}(10^3), \quad (2.173)$$

where the parametrisation is in terms of the ekpyrotic potential as written in (2.148). For typical values such as  $\kappa_{3,4} \sim \mathcal{O}(1)$  and  $\epsilon \gtrsim 50$ , which we need in order for the power spectrum to be in agreement with observations, the bispectrum parameter is of order a few tens, with the sign being typically determined by the sign of  $\kappa_3$ . To be in agreement with current bounds, we need  $|\kappa_3| \lesssim 1$ . Unless  $|\kappa_4|$  is very large,  $g_{NL}$  is of order a few thousand and negative in sign, which is a rather robust prediction of the kinetic conversion mechanism.

We can compare these to the predictions of simple single-field inflationary models in 2.3.2, where both the bi- and trispectrum parameters approach  $\mathcal{O}(1)$ , which are thus substantially different from typical values for ekpyrosis. Moreover, due to the fact that only non-Gaussianity of the local form is produced distinguishes ekpyrotic models from single-field inflationary models with non-canonical kinetic terms such as DBI inflation, which produces equilateral-type non-Gaussianity [106, 107]. The comparison with multi-field inflationary models on the other hand is more difficult to analyse, as some of those models can allow for a wide range of  $f_{NL}$  and  $g_{NL}$  values.

#### 2.4.3 (No) gravitational waves

A profound difference between the predictions from inflation and ekpyrosis concerns the production of primordial gravitational waves. Tensor modes depend only on the evolution of the scale factor, which grows rapidly during inflation but stays approximately constant during the ekpyrotic phase. Gravitational waves are hence produced in the same manner as density perturbations during de Sitter-like expansion. During the ekpyrotic phase, on the other hand, the background spacetime is almost Minkowski, such that no substantial gravitational waves are generated<sup>12</sup> [109]. The dominant contribution is at second order in perturbation theory and arises from the backreaction of the scalar fluctuations onto the metric [110].

Following the prescription from inflation (2.3.3), we can calculate the gravitational wave spectrum [83, 109]. The only tensor perturbation in the flat FLRW

---

<sup>12</sup>This also explains why the adiabatic perturbations produced during the ekpyrotic phase pick up a blue spectrum [108] and are not amplified into classical fluctuations [88].

metric is given by  $\delta g_{ij} = a^2 h_{ij}$  with  $h_{ii} = 0$  and  $\partial_i h_{ij} = 0$ , and it is automatically gauge-invariant. The second-order action for the canonically normalised tensor fluctuations,  $f_{\mathbf{k}} \equiv \frac{a}{2} h_{\mathbf{k}}$  (dropping the superscript  $\lambda$  for the polarisation states), is then given by Eq. (2.121), and leads to the equation of motion,

$$f_{\mathbf{k}}'' + \left( k^2 - \frac{a''}{a} \right) f_{\mathbf{k}} = 0. \quad (2.174)$$

Imposing Bunch-Davies initial conditions in the far past,

$$\lim_{k\tau \rightarrow -\infty} f_{\mathbf{k}} = \frac{e^{-ik\tau}}{\sqrt{2k}}, \quad (2.175)$$

the solution can be shown to be a Hankel function of the first kind,

$$f_{\mathbf{k}}(\tau) = \frac{\sqrt{-\pi\tau}}{2} H_{\nu}^{(1)}(-k\tau), \quad \nu = \frac{\epsilon - 3}{2(\epsilon - 1)}, \quad (2.176)$$

where we have dropped a physically irrelevant phase. The tensor spectral index, defined in (2.125), can be obtained by expanding the Hankel function for small arguments, yielding

$$n_t = 3 - 2\nu = 3 - \frac{\epsilon - 3}{\epsilon - 1}. \quad (2.177)$$

For large  $\epsilon$  the tensor spectrum in ekpyrotic models approximates  $n_t \approx 2$ , which is tilted strongly to the blue.

Thus, ekpyrotic models are falsifiable w.r.t. primordial gravitational waves: while detecting them with a nearly scale-invariant spectrum would constitute very strong evidence in favour of inflation, it would rule out the ekpyrotic scenario. On the other hand, the currently observed upper bound on the tensor-to-scalar ratio already disfavours some inflationary models. Should primordial gravitational waves remain unobserved even with upcoming CMB polarisation experiments of higher sensitivity, other aspects, like non-Gaussianity, will play an important role in discriminating between the two early universe cosmologies.

## 2.5 The bounce

In order to obtain a complete history from the ekpyrotic phase to the present one must supplement these models with a description of the bounce, i.e. with a description of the reversal from contraction to expansion which is identified with the big bang.

Since the Hubble rate is negative during the contracting phase, while it is positive during the subsequent expanding phase, the bounce must allow the Hubble rate  $H$  to increase. If we describe the dominant energy component in the universe as a perfect fluid with energy density  $\rho$  and pressure  $p$ , then the second Friedmann equation for a flat FLRW universe (2.133) implies

$$\dot{H} = -\frac{1}{2}(\rho + p) > 0. \quad (2.178)$$

There exist only two ways in which this inequality can be fulfilled: either the bounce has to be classically *singular* with the Hubble rate instantaneously jumping from negative to positive values, or the bounce is *non-singular* but the null energy condition (NEC) must be violated, i.e.

$$\rho + p < 0. \quad (2.179)$$

Considerable progress has been made in recent years in tackling the puzzle of the initial big bang singularity by replacing it with a bounce. In this thesis, we focus on bouncing theories that have been developed in the context of ekpyrotic and cyclic theories. For a comprehensive review of these and other classical bouncing cosmologies see [111].

The dynamics of a contracting ekpyrotic phase were introduced in the previous section 2.4 as part of a complete cyclic theory. In the original proposal and its extensions like the phoenix universe, the bounce was modelled as the collision of two branes. From the effective 4-dimensional point of view, at the moment of collision the scale factor goes to zero corresponding to a singularity. However, in the 5-dimensional setup, the scale factors on the branes are actually finite, while the bounce is singular in that the extra dimension separating the two branes momentarily disappears (see e.g. [32]). The bounce may thus have been a much milder, and potentially tractable, event, where quantum and/or higher-dimensional effects are conjectured to resolve the singularity, see e.g. [112, 100]. Other bouncing theories include [113], in which a brief antigravity phase is proposed that allows the evolution of the universe to be traced through a singular bounce unambiguously, and [114], which provides evidence for a semiclassical description of the bounce where the fields might pass around the cosmological singularity along complex classical paths.

During a non-singular bounce, the scale factor reaches a minimum at a non-zero value at an energy scale significantly below the Planck scale so that the evolution can be described classically throughout, see e.g. [99, 115, 32, 116, 117, 21]. How-

ever, a generic consequence of violating the null energy condition is the appearance of ghosts, fields with negative kinetic energy. This implies that the energy of the theory is unbounded from below and that therefore the vacuum is unstable, i.e. the vacuum will inevitably decay quantum mechanically. It is possible to overcome this problem and produce an instability-free bounce by introducing new matter fields. The most studied examples in the literature are provided by the ghost condensate, in which the Lagrangian is taken to be an analytic function of the scalar field and the kinetic term,  $\mathcal{L} = \sqrt{-g} P(\phi, X)$  with  $X \equiv -\frac{1}{2}(\partial\phi)^2$  [118], and Galileons, which contain specific higher-derivative terms like  $\mathcal{L} = \sqrt{-g} g(\phi) X \square \phi$  [119]. Their defining feature is that even though the Lagrangian contains higher-derivative terms the resulting equations of motion have at most two derivatives acting on each field. In chapter 5 we study a non-singular bounce achieved via a ghost condensate in detail as part of the theory of conflation. Recent developments indicate that a non-singular bounce may be allowed: It was demonstrated in [120, 121] that long-wavelength perturbations generated during the contracting phase pass through such non-singular bounces unharmed. It has recently been established that non-singular bounces are viable in supergravity [122], which can be taken as an indication that cosmic bounces are allowed by fundamental physics. Moreover, in [103] the existence of healthy descriptions of non-singular bouncing cosmologies has been explicitly confirmed. The temporary violation of the null energy condition in a spatially flat non-singular bounce, achieved through a phase of ghost condensation, was shown to constitute a sensible, trustworthy effective theory.

## Chapter 3

# Covariant formalism and perturbation theory up to third order

The aim of this chapter is to develop a covariant formalism which allows us to study perturbations in the so called non-minimal entropic mechanism. The model is a new variant on the standard entropic mechanism that produces scale-invariant curvature perturbations during an ekpyrotic phase (see section 2.4.2), and will be introduced in chapter 4. We will start by reviewing the covariant formalism for cosmological perturbation theory, up to second order in perturbations and for a theory comprising two scalar fields with non-trivial field space metric. The goal is to derive the evolution equations for the entropy as well as the curvature perturbation. New results at third order will then be presented in section 3.3.2. Note that this chapter is entirely general, and may be used for applications to any two-field cosmological models with arbitrary field space metrics (i.e. to general two-field non-linear sigma models).

In the present work, we will adopt the  $1 + 3$  covariant formalism developed by Langlois and Vernizzi [123, 124, 125, 126], which was inspired by earlier works of Ellis and Bruni [127, 128] and Hawking [129]. This formalism builds on the insight that in a purely time-dependent background metric (in particular in FLRW space-times) spatial derivatives of scalar quantities are automatically gauge-invariant. The formalism allows one to derive rather compact all-orders evolution equations for cosmological perturbations, which, with suitable care, may then be expanded up to the desired order in perturbation theory.

We study the cosmological fluctuations of a system of two non-minimally coupled

scalar fields, i.e. two scalar fields with a non-trivial field space metric (but minimally coupled to gravity). The action of such systems is of the form

$$S = \int d^4x \sqrt{-g} \left( \frac{1}{2}R - \frac{1}{2}G_{IJ}(\phi^K) \nabla_a \phi^I \nabla^a \phi^J - V(\phi^K) \right), \quad (3.1)$$

where the indices  $I, J, K = 1, 2$  label the two scalar fields (in our later examples we will also write  $\phi^1 = \phi, \phi^2 = \chi$ ). The field space metric and its inverse can be used to lower and raise field space indices, respectively, e.g.  $\phi_I = G_{IJ}\phi^J$ . Such actions were studied by Renaux-Petel and Tasinato [19] up to second order in perturbation theory and, for trivial field space metric  $G_{IJ} = \delta_{IJ}$ , the formalism was extended to third order by Renaux-Petel and Lehners [20]. Considering theories with two scalar fields is conceptually of importance, as two-scalar theories admit both adiabatic/curvature and entropic/isocurvature perturbations. The extension to having more than two fields is then straightforward, as the presence of additional fields simply augments the number of independent entropic perturbations.

### 3.1 The covariant formalism

Let us consider a spacetime, with metric  $g_{ab}$ , where a congruence of cosmological observers is defined by an a priori arbitrary unit timelike vector  $u^a = dx^a/d\tau$  (with  $u_a u^a = -1$ ), where  $\tau$  denotes the proper time. The spatial projection tensor orthogonal to the four-velocity  $u^a$  is then given by

$$h_{ab} \equiv g_{ab} + u_a u_b, \quad (h^a{}_b h^b{}_c = h^a{}_c, \quad h_a{}^b u_b = 0). \quad (3.2)$$

To describe the time evolution, we make use of the Lie derivative w.r.t.  $u^a$ , i.e. the covariant definition of the time derivative. It is defined for a generic covector  $Y_a$  by (see e.g. [130])

$$\dot{Y}_a \equiv \mathcal{L}_u Y_a \equiv u^b \nabla_b Y_a + Y_b \nabla_a u^b, \quad (3.3)$$

and will be denoted by a *dot*<sup>1</sup>, as is customary in works on the covariant formalism. For scalar quantities, the covariant time derivative reduces to

$$\dot{f} = u^b \nabla_b f. \quad (3.4)$$

---

<sup>1</sup>We use the convention to denote a Lie derivative by a dot and a coordinate time derivative by a prime in this chapter only, whereas chapters 2, 4 and 5 employ the standard convention where a dot stands for a coordinate time derivative and a prime for a conformal time derivative.

To describe perturbations in the covariant approach, we project the covariant derivative orthogonally to the four-velocity  $u^a$ ; this spatial projection of the covariant derivative will be denoted by  $D_a$ . For a generic tensor, its definition is

$$D_a T_{b\dots}^{c\dots} \equiv h_a^d h_b^e \dots h_f^c \dots \nabla_d T_{e\dots}^{f\dots}. \quad (3.5)$$

Again, for the case of a scalar, this simplifies,

$$D_a f \equiv h_a^b \nabla_b f = \partial_a f + u_a \dot{f}. \quad (3.6)$$

The covariant derivative of any time-like unit vector field  $u^a$  can be decomposed uniquely as follows

$$\nabla_b u_a = \sigma_{ab} + \omega_{ab} + \frac{1}{3} \Theta h_{ab} - a_a u_b, \quad (3.7)$$

with the (trace-free and symmetric) shear tensor  $\sigma_{ab}$  and the (antisymmetric) vorticity tensor  $\omega_{ab}$ . The volume expansion,  $\Theta$ , is defined by

$$\Theta \equiv \nabla_a u^a, \quad (3.8)$$

where the integrated volume expansion,  $\alpha$ , along  $u^a$ ,

$$\alpha \equiv \frac{1}{3} \int d\tau \Theta \quad (\Theta = 3\dot{\alpha}), \quad (3.9)$$

can be interpreted as the number of e-folds of evolution of the scale factor measured along the world-line of a cosmological observer with four-velocity  $u^a$  since  $\Theta/3$  corresponds to the local Hubble parameter. The acceleration vector is given by

$$a^a \equiv u^b \nabla_b u^a. \quad (3.10)$$

Finally, it is always possible to decompose the total energy-momentum tensor as

$$T_{ab} = (\rho + p) u_a u_b + q_a u_b + u_a q_b + g_{ab} p + \pi_{ab}, \quad (3.11)$$

where  $\rho$ ,  $p$ ,  $q_a$  and  $\pi_{ab}$  are the energy density, pressure, momentum and anisotropic stress tensor, respectively, as measured in the frame defined by  $u^a$ .

## 3.2 Two scalar fields with non-trivial field space metric

The energy momentum tensor derived from the action (3.1) is then

$$T_{ab} = G_{IJ} \nabla_a \phi^I \nabla_b \phi^J + g_{ab} \left( -\frac{1}{2} G_{IJ} \nabla_c \phi^I \nabla^c \phi^J - V \right). \quad (3.12)$$

Comparing to the decomposition in (3.11) one finds for the energy density, pressure, momentum and anisotropic stress, respectively,

$$\rho \equiv T_{ab} u^a u^b = T_{00} u^0 u^0 = \dot{\phi}^I \dot{\phi}_I + \frac{1}{2} G_{IJ} \nabla_c \phi^I \nabla^c \phi^J + V, \quad (3.13)$$

$$p \equiv \frac{1}{3} h^{ac} T_{ab} h_c^b = \frac{1}{3} G_{IJ} D_a \phi^I D^a \phi^J - \frac{1}{2} G_{IJ} \nabla_c \phi^I \nabla^c \phi^J - V, \quad (3.14)$$

$$q_a \equiv -u^b T_{bc} h_a^c = -\dot{\phi}_I D_a \phi^I \approx -u^0 T_{0i}, \quad (3.15)$$

$$\pi_{ab} \equiv h_a^c T_{cd} h_b^d - p h_{ab} = G_{IJ} D_a \phi^I D_b \phi^J - \frac{h_{ab}}{3} G_{IJ} D_c \phi^I D^c \phi^J. \quad (3.16)$$

The equation of motion for the scalar fields is obtained by varying the action w.r.t. the fields themselves,

$$\begin{aligned} 0 &= G_{IJ} \nabla_a \nabla^a \phi^J + \Gamma_{IJK} \nabla_a \phi^K \nabla^a \phi^J - V_{,I} \\ &= \ddot{\phi}^I + \Gamma_{JK}^I \left( \dot{\phi}^J \dot{\phi}^K - D_a \phi^J D^a \phi^K \right) + \Theta \dot{\phi}^I + G^{IJ} V_{,J} - D_a D^a \phi^I - a^b D_b \phi^I, \end{aligned} \quad (3.17)$$

where  $\Gamma_{IJK} = G_{IL} \Gamma_{JK}^L = \frac{1}{2} (G_{IJ,K} + G_{IK,J} - G_{JK,I})$  and the second equality above makes use of Eqs. (3.2, 3.5-3.10).

We introduce the following derivatives of field space vectors in curved coordinates in order to simplify notation. The spacetime derivative, given by

$$\mathcal{D}_a A^I \equiv \nabla_a A^I + \Gamma_{JK}^I \nabla_a \phi^K A^K, \quad (3.18)$$

is used to define a time derivative in field space,

$$\mathcal{D}_u A^I \equiv u^a \mathcal{D}_a A^I = \dot{A}^I + \Gamma_{JK}^I \dot{\phi}^J A^K, \quad (3.19)$$

and a spatially projected derivative in field space,

$$\mathcal{D}_{\perp a} T_{b\dots}^{I c\dots} \equiv h_a^d h_b^e \dots h_f^c \dots \mathcal{D}_d T_{e\dots}^{I f\dots}. \quad (3.20)$$

We can then rewrite the evolution equation (3.17) in a more concise form as

$$\mathcal{D}_u \dot{\phi}^I + \Theta \dot{\phi}^I + G^{IJ} V_{,J} - \mathcal{D}_{\perp a} (D^a \phi^I) - a^a D_a \phi^I = 0. \quad (3.21)$$

In the two-field case it is convenient to introduce a particular basis in field space which consists of an adiabatic and an entropic unit vector. This decomposition was first introduced in [6] for two fields in the linear theory, as presented in subsection 2.4.2. The generalisation to multiple fields is discussed in [131, 132] for the linear case and in [133] for the nonlinear theory. The adiabatic unit vector, denoted by  $e_\sigma^I$ , is defined in the direction of the velocity of the two fields, i.e. *tangent* to the field space trajectory. The entropic unit vector, denoted by  $e_s^I$ , is defined along the direction *orthogonal* to it (w.r.t.  $G_{IJ}$ ), namely

$$e_\sigma^I \equiv \frac{\dot{\phi}^I}{\dot{\sigma}}, \quad G_{IJ} e_s^I e_s^J = 1, \quad G_{IJ} e_s^I e_\sigma^J = 0, \quad (3.22)$$

with

$$\dot{\sigma} \equiv \sqrt{G_{IJ} \dot{\phi}^I \dot{\phi}^J}. \quad (3.23)$$

Note that this is only a short-hand notation, i.e.  $\dot{\sigma}$  is generally *not* the derivative along  $u^a$  of a scalar field  $\sigma$ . Furthermore, we introduce the quantity  $\dot{\theta}$  to express the time evolution of the basis vectors,

$$\mathcal{D}_u e_\sigma^I \equiv \dot{\theta} e_s^I, \quad \mathcal{D}_u e_s^I \equiv -\dot{\theta} e_\sigma^I, \quad (3.24)$$

where  $\mathcal{D}_u e_\alpha^I = \dot{e}_\alpha^I + \Gamma_{JK}^I \dot{\sigma} e_\sigma^J e_\alpha^K$ , ( $\alpha = \sigma, s$ ) is given by the definition in (3.19). Again,  $\dot{\theta}$  is *not* the derivative along  $u^a$  of an angle  $\theta$ , although such an angle can be defined for a trivial field space metric [126].

Making use of the basis (3.22), we can then introduce two linear combinations of the scalar field gradients and thus define two covectors by analogy with the similar definitions in the linear context [131]: the *adiabatic* and *entropic* covectors, denoted by  $\sigma_a$  and  $s_a$ , respectively, and given by

$$\sigma_a \equiv e_{\sigma I} \nabla_a \phi^I, \quad (3.25)$$

$$s_a \equiv e_{s I} \nabla_a \phi^I. \quad (3.26)$$

By definition, the entropic covector  $s_a$  is orthogonal to the four-velocity  $u^a$ , i.e.  $u^a s_a = 0$ . By contrast, the adiabatic covector  $\sigma_a$  contains a longitudinal component:  $u^a \sigma_a =$

$\dot{\sigma}$ . At any location in spacetime, one may think of  $\sigma_i$  as describing perturbations in the total energy density (and thus perturbations in the expansion/contraction history of the universe), and of  $s_i$  as describing perturbations in the relative contributions of the two scalar fields to the total energy density.

A covariant generalisation of the comoving energy density perturbation is given by the covector

$$\epsilon_a \equiv D_a \rho - \frac{\dot{\rho}}{\dot{\sigma}} \sigma_a^\perp, \quad (3.27)$$

where  $\sigma_a^\perp \equiv e_{\sigma I} D_a \phi^I = \sigma_a + \dot{\sigma} u_a$  is the spatially projected version of (3.25). It has been shown in [126] that if the shear is negligible on large scales, so is  $\epsilon_a \approx 0$ .

Then, in our two-field system, the (full, all-orders in perturbation theory) evolution equation of the entropy covector  $s_a$  can be expressed on large scales (i.e. to leading order in spatial gradients) as [19]

$$\ddot{s}_a + \Theta \dot{s}_a + \left( V_{;ss} + 3\dot{\theta}^2 + \dot{\sigma}^2 e_s^I e_s^J e_\sigma^K e_\sigma^L R_{IKJL} \right) s_a \approx -2 \frac{\dot{\theta}}{\dot{\sigma}} \epsilon_a, \quad (3.28)$$

with

$$V_s = e_s^I V_{,I}, \quad V_{;ss} = e_s^I e_s^J \mathcal{D}_I \mathcal{D}_J V \quad \text{and} \quad \mathcal{D}_I \mathcal{D}_J V \equiv V_{,IJ} - \Gamma_{IJ}^K V_{,K}, \quad (3.29)$$

and where  $R^I_{\phantom{I}KLJ} = \partial_J \Gamma^I_{KL} - \partial_L \Gamma^I_{KJ} + \Gamma^I_{JP} \Gamma^P_{KL} - \Gamma^I_{LP} \Gamma^P_{KJ}$  is the Riemann tensor associated with the metric  $G_{IJ}$ . An equality valid only on large scales will be denoted by  $\approx$ .

It is a well-known result that in cosmological models with a single scalar field the curvature perturbation is conserved on large scales [134]. However, when a second field is present, entropic perturbations may arise and these can source the curvature perturbation on large scales [6]. In subsection 2.4.2 we derived a particularly simple and useful form of the evolution equation for the comoving curvature perturbation on large scales (2.166). It reads

$$\zeta' = \frac{2H\delta V}{\bar{\sigma}'^2 - 2\delta V}, \quad (3.30)$$

where a prime denotes a coordinate time derivative. It can be extended to the case of having a non-trivial field space metric by taking the metric into account when expressing  $\delta V$  in terms of the adiabatic and entropic fluctuations at the relevant order.

In the following subsection, we will introduce a coordinate system. The evolution equations for the entropy perturbation (3.28) and the comoving curvature perturbation (3.30) can then be straightforwardly translated into the linearised and second-order perturbation equations, while we derive new results at third order in the following section. For convenience, we have collected various background as well as first- and second-order expressions that will be used in this thesis in appendix B.

### 3.3 Perturbation theory

We introduce coordinates  $x^\mu = (t, x^i)$  to describe an almost-FLRW spacetime, in order to relate the covariant formalism to the more familiar coordinate based approach. We will denote a partial derivative with respect to the cosmic time  $t$  by a prime, i.e.  $' = \partial/\partial t$ , since the dot is already reserved for the Lie derivative (3.3). Fields are expanded without factorial factors:

$$X(t, x^i) = \bar{X}(t) + \delta X^{(1)}(t, x^i) + \delta X^{(2)}(t, x^i) + \delta X^{(3)}(t, x^i). \quad (3.31)$$

Quantities with an over-bar like  $\bar{X}$  are evaluated on the background, first order quantities like  $\delta X^{(1)}$  solve the linearised equations of motion, second order quantities like  $\delta X^{(2)}$  the quadratic equations, and so on. In the following, we drop the superscript  $(1)$  for perturbations at linear order when the meaning is unambiguous. For simplicity we choose  $u^a$  such that  $u_i = 0$ . In appendix B we show how  $u_0$  is then determined in terms of metric quantities.

The gauge transformation of a tensor  $\mathbf{T}$  generated by a vector field  $\xi^a$  is given by the exponential map [135]

$$\mathbf{T} \rightarrow e^{\mathcal{L}_\xi} \mathbf{T}. \quad (3.32)$$

With the perturbative expansion  $\xi = \sum_n \frac{1}{n!} \xi_{(n)}$ , the first and second-order perturbations of a tensor  $\mathbf{T}$  are then found to transform as

$$\delta \mathbf{T}^{(1)} \rightarrow \delta \mathbf{T}^{(1)} + \mathcal{L}_{\xi_{(1)}} \mathbf{T}^{(0)}, \quad \delta \mathbf{T}^{(2)} \rightarrow \delta \mathbf{T}^{(2)} + \mathcal{L}_{\xi_{(1)}} \delta \mathbf{T}^{(1)} + \left( \mathcal{L}_{\xi_{(2)}} + \frac{1}{2} \mathcal{L}_{\xi_{(1)}}^2 \right) \mathbf{T}^{(0)}. \quad (3.33)$$

At third order, the transformation is given by [136]

$$\delta \mathbf{T}^{(3)} \rightarrow \delta \mathbf{T}^{(3)} + \mathcal{L}_{\xi_{(1)}} \delta \mathbf{T}^{(2)} + \left( \mathcal{L}_{\xi_{(2)}} + \frac{1}{2} \mathcal{L}_{\xi_{(1)}}^2 \right) \delta \mathbf{T}^{(1)} + \left( \mathcal{L}_{\xi_{(3)}} + \mathcal{L}_{\xi_{(1)}} \mathcal{L}_{\xi_{(2)}} + \frac{1}{6} \mathcal{L}_{\xi_{(1)}}^3 \right) \mathbf{T}^{(0)}. \quad (3.34)$$

### 3.3.1 Perturbation theory up to second order

We start by presenting the definitions of the adiabatic and entropic perturbations up to second order. By expanding Eqs. (3.25) and (3.26) up to second order, one finds, for  $\sigma_i$  and  $s_i$  respectively,

$$\delta\sigma_i = \partial_i\delta\sigma, \quad \delta\sigma \equiv \bar{e}_{\sigma I}\delta\phi^I, \quad (3.35)$$

$$\delta s_i = \partial_i\delta s, \quad \delta s \equiv \bar{e}_{s I}\delta\phi^I. \quad (3.36)$$

at linear order and

$$\delta\sigma_i^{(2)} \equiv \partial_i\delta\sigma^{(2)} + \frac{\bar{\theta}'}{\bar{\sigma}'}\delta\sigma\partial_i\delta s - \frac{1}{2\bar{\sigma}'}V_i, \quad (3.37)$$

$$\delta s_i^{(2)} \equiv \partial_i\delta s^{(2)} + \frac{\delta\sigma}{\bar{\sigma}'}\partial_i\delta s', \quad (3.38)$$

at second order [19], with

$$\delta\sigma^{(2)} \equiv \bar{e}_{\sigma I}\delta\phi^{I(2)} + \frac{1}{2}\bar{e}_{\sigma I}\bar{\Gamma}_{KL}^I\bar{e}_{\alpha}^K\bar{e}_{\beta}^L\delta\sigma^{\alpha}\delta\sigma^{\beta} + \frac{1}{2\bar{\sigma}'}\delta s\delta s', \quad (3.39)$$

$$\delta s^{(2)} \equiv \bar{e}_{s I}\delta\phi^{I(2)} + \frac{1}{2}\bar{e}_{s I}\bar{\Gamma}_{KL}^I\bar{e}_{\alpha}^K\bar{e}_{\beta}^L\delta\sigma^{\alpha}\delta\sigma^{\beta} - \frac{\delta\sigma}{\bar{\sigma}'}\left(\delta s' + \frac{\bar{\theta}'}{2}\delta\sigma\right), \quad (3.40)$$

where the inverse zweibeine are defined via  $\delta\phi^I = e_{\alpha}^I\delta\sigma^{\alpha}$  and  $\alpha = (\sigma, s)$ . The curved nature of the field space metric manifests itself in the appearance of the terms with Christoffel symbols in  $\delta\sigma^{(2)}$  and  $\delta s^{(2)}$ . It is convenient to introduce the spatial vector

$$V_i \equiv \frac{1}{2}(\delta s\partial_i\delta s' - \delta s'\partial_i\delta s), \quad (3.41)$$

which vanishes when  $\delta s$  and  $\delta s'$  have the same spatial dependence. Since relative spatial gradients are heavily suppressed for super-Hubble modes both in inflationary and in ekpyrotic models,  $\delta s'$  and  $\delta s$  indeed obtain the same spatial dependence, i.e.  $\delta s' = g(t)\delta s$ , to high precision.

Using the gauge transformation relations (3.33), it can easily be verified that the entropic perturbations  $\delta s^{(1),(2)}$  are gauge-invariant.

The adiabatic perturbations, however, are not gauge-invariant, but they have been defined such that setting them to zero is equivalent to going to comoving gauge, on large scales. This can be seen by expanding the momentum density  $q_i$  given by

(3.15), which should vanish in comoving gauge:

$$\delta q_i = -\partial_i (\bar{\sigma}' \delta \sigma) \quad (3.42)$$

at linear order, and

$$\delta q_i^{(2)} = -\partial_i \left[ \bar{\sigma}' \delta \sigma^{(2)} + \frac{1}{2} \frac{\bar{\sigma}''}{\bar{\sigma}'} \delta \sigma^2 + \bar{\theta}' \delta \sigma \delta s \right] - \frac{1}{\bar{\sigma}'} \delta \epsilon \partial_i \delta \sigma + V_i, \quad (3.43)$$

at second order. As already mentioned,  $V_i \approx 0$  on large scales for the models we are interested in, and therefore setting the adiabatic perturbations to zero (as a gauge choice) corresponds to adopting comoving gauge on super-Hubble scales.

The equations of motion of the scalar fields were presented in (3.17), which for the background can be rewritten as

$$\bar{G}_{IJ} \square \bar{\phi}^J + \bar{\Gamma}_{IKL} \partial_\mu \bar{\phi}^K \partial^\mu \bar{\phi}^L - \bar{V}_{,I} = 0. \quad (3.44)$$

Substituting  $\bar{\phi}^{J'} = \bar{\sigma}' \bar{e}_\sigma^J$  and using (3.24), they read

$$\bar{e}_{\sigma I} (\bar{\sigma}'' + 3H\bar{\sigma}') + \bar{e}_{sI} \bar{\sigma}' \bar{\theta}' + \bar{V}_{,I} = 0. \quad (3.45)$$

Multiplying with  $\bar{e}_\sigma^I$  and  $\bar{e}_s^I$ , we obtain the background equations of motion for  $\sigma$  and  $s$ , respectively:

$$\bar{\sigma}'' + 3H\bar{\sigma}' + V_{,\sigma} = 0, \quad (3.46)$$

and

$$\bar{\sigma}' \bar{\theta}' + V_{,s} = 0. \quad (3.47)$$

Expanding the equation of motion for  $s_a$  (3.28) to linear order gives

$$\delta s'' + 3H\delta s' + (\bar{V}_{;ss} + 3\bar{\theta}'^2 + \bar{\sigma}'^2 \bar{e}_s^I \bar{e}_s^J \bar{e}_\sigma^K \bar{e}_\sigma^L \bar{R}_{IKJL}) \delta s = -\frac{2\bar{\theta}'}{\bar{\sigma}'} \delta \epsilon \approx 0, \quad (3.48)$$

where we have used

$$\bar{\Theta} = 3H. \quad (3.49)$$

At second order, we get

$$\begin{aligned} \delta s^{(2)''} + 3H\delta s^{(2)'} + (\bar{V}_{;ss} + 3\bar{\theta}'^2 + \bar{\sigma}'^2 \bar{e}_s^I \bar{e}_s^J \bar{e}_\sigma^K \bar{e}_\sigma^L \bar{R}_{IKJL}) \delta s^{(2)} &\approx -\frac{\bar{\theta}'}{\bar{\sigma}'} \delta s'^2 \\ -\frac{2}{\bar{\sigma}'} \left[ \bar{\theta}'' + \frac{\bar{V}_{,\sigma} \bar{\theta}'}{\bar{\sigma}'} - \frac{3}{2} H \bar{\theta}' \right] \delta s \delta s' + \left[ -\frac{1}{2} \bar{V}_{;sss} + \frac{5\bar{V}_{;ss} \bar{\theta}'}{\bar{\sigma}'} + \frac{9\bar{\theta}'^3}{\bar{\sigma}'} \right. \\ \left. + \bar{e}_s^I \bar{e}_s^J \bar{e}_\sigma^K \bar{e}_\sigma^L \left( \bar{\sigma}' \bar{\theta}' \bar{R}_{IKJL} - \frac{1}{2} \bar{\sigma}'^2 \bar{e}_s^N \mathcal{D}_N \bar{R}_{IKJL} \right) \right] \delta s^2 - \frac{2\bar{\theta}'}{\bar{\sigma}'} \delta \epsilon^{(2)}, \end{aligned} \quad (3.50)$$

where we have used  $V_i \approx 0$  on large scales in the second term on the RHS, and  $\delta \epsilon^{(2)} \approx 0$ . The equation for the entropy perturbation forms a closed system; on large scales, it evolves independently of the adiabatic component.

In comoving gauge, expanding the expression for the curvature perturbation (3.30) up to second order, we have

$$\zeta' = \frac{2H\delta V}{\bar{\sigma}'^2 - 2\delta V} \stackrel{\delta\sigma=0}{\approx} \frac{2H}{\bar{\sigma}'^2} \left[ \delta V^{(1)} + \delta V^{(2)} + \frac{2}{\bar{\sigma}'^2} \left( \delta V^{(1)} \right)^2 \right], \quad (3.51)$$

where the  $\delta\sigma = 0$  statement above the  $\approx$  sign indicates that the equations are valid in comoving gauge. Using Eqs. (B.33)-(B.34), we obtain

$$\zeta^{(1)'} \stackrel{\delta\sigma=0}{\approx} -\frac{2H\bar{\theta}'\delta s}{\bar{\sigma}'} \quad (3.52)$$

at first order, and

$$\zeta^{(2)'} \stackrel{\delta\sigma=0}{\approx} \frac{2H}{\bar{\sigma}'^2} \left[ -\bar{\sigma}' \bar{\theta}' \delta s^{(2)} - \frac{\bar{V}_{,\sigma}}{2\bar{\sigma}'} \delta s \delta s' + \left( \frac{1}{2} \bar{V}_{;ss} + 2\bar{\theta}'^2 \right) \delta s^2 \right] \quad (3.53)$$

at second order. It becomes clear that the curvature perturbation is sourced by the entropy perturbation.

In the next section, we will derive the corresponding third-order equations, which are needed for the study of the primordial trispectra of cosmological perturbations.

### 3.3.2 Perturbation theory at third order

We are now in a position to present our main technical developments: we use the covariant formalism to derive the third-order evolution equations for the entropy and the curvature perturbations for two scalar fields with a non-trivial field space metric. These equations will then allow us to calculate and make predictions for the trispectrum of current ekpyrotic models.

The covariant formalism has the advantage of allowing one to derive simple all-orders evolution equations for the adiabatic and entropic co-vectors. However, given that the general all-orders definitions of the adiabatic and entropic convectors are rather implicit and formal, using the covariant formalism to make actual predictions involves the non-trivial step of identifying the proper definitions of adiabatic and entropic fluctuations up to the desired order in perturbation theory. Once these definitions are at hand, it becomes a straightforward exercise to expand the all-orders equations up to the desired order. Thus our first and main task is to find the appropriate definitions of adiabatic and entropic perturbations at third order. Expanding Eq. (3.26) at third order using Eqs. (B.19) and (B.21), one obtains

$$\begin{aligned}\delta s_i^{(3)} = & \partial_i \delta s^{(3)} + \frac{\delta\sigma}{\bar{\sigma}'} \partial_i \delta s^{(2)'} + \frac{\delta\sigma^{(2)}}{\bar{\sigma}'} \partial_i \delta s' - \frac{\bar{\sigma}''}{2\bar{\sigma}'^3} \delta\sigma^2 \partial_i \delta s' + \frac{\delta\sigma^2}{2\bar{\sigma}'^2} \partial_i \delta s'' \\ & + \frac{1}{2\bar{\sigma}'^2} (\delta s' + 2\bar{\theta}'\delta\sigma) \delta s \partial_i \delta s' - \partial_i \left( \frac{1}{6\bar{\sigma}'^2} \delta s \delta s'^2 \right) \\ & + \frac{1}{6} \bar{e}_s^I \bar{e}_s^J \bar{e}_\sigma^K \bar{e}_\sigma^L \bar{R}_{IKJL} (\delta\sigma^2 \partial_i \delta s - \delta\sigma \delta s \partial_i \delta\sigma) \\ & + \frac{1}{3} \bar{e}_{sI} \left[ -\partial_M \bar{\Gamma}_{KL}^I + \bar{\Gamma}_{KP}^I \bar{\Gamma}_{LM}^P + \bar{\Gamma}_{LP}^I \bar{\Gamma}_{KM}^P \right] \bar{e}_s^L (\bar{e}_\sigma^M \bar{e}_s^K - \bar{e}_\sigma^K \bar{e}_s^M) \partial_i (\delta\sigma \delta s^2)\end{aligned}\tag{3.54}$$

where we have defined

$$\begin{aligned}\delta s^{(3)} \equiv & \bar{e}_{sI} \delta\phi^{(3)I} - \frac{\delta\sigma^{(2)}}{\bar{\sigma}'} (\delta s' + \bar{\theta}'\delta\sigma) - \frac{\delta\sigma}{\bar{\sigma}'} \delta s^{(2)'} - \frac{\delta\sigma^2}{2\bar{\sigma}'^2} \left( \bar{\theta}'^2 \delta s + \delta s'' - \frac{\bar{\sigma}''}{\bar{\sigma}'} \delta s' \right) \\ & - \frac{\delta\sigma^3}{6\bar{\sigma}'} \left( \frac{\bar{\theta}'}{\bar{\sigma}'} \right)' - \frac{\bar{\theta}'}{2\bar{\sigma}'^2} \delta\sigma \delta s \delta s' + \frac{1}{6\bar{\sigma}'^2} \delta s \delta s'^2 \\ & + \bar{e}_{sI} \bar{\Gamma}_{KL}^I (\bar{e}_\sigma^L \delta\sigma + \bar{e}_s^L \delta s) \left[ \bar{e}_\sigma^K \left( \delta\sigma^{(2)} - \frac{1}{2\bar{\sigma}'} \delta s \delta s' \right) + \bar{e}_s^K \left( \delta s^{(2)} + \frac{\delta\sigma}{\bar{\sigma}'} \left( \delta s' + \frac{\bar{\theta}'}{2} \delta\sigma \right) \right) \right] \\ & - \frac{1}{6} \left( -\partial_M \bar{\Gamma}_{KL}^I + \bar{\Gamma}_{KP}^I \bar{\Gamma}_{LM}^P + \bar{\Gamma}_{LP}^I \bar{\Gamma}_{KM}^P \right) \bar{e}_{sI} \times \\ & \times \left[ (\bar{e}_\sigma^M \delta\sigma + \bar{e}_s^M \delta s) (\bar{e}_\sigma^L \delta\sigma + \bar{e}_s^L \delta s) (\bar{e}_\sigma^K \delta\sigma + \bar{e}_s^K \delta s) \right. \\ & \left. + \delta\sigma \delta s (\bar{e}_\sigma^L \delta\sigma + 2\bar{e}_s^L \delta s) (\bar{e}_\sigma^M \bar{e}_s^K - \bar{e}_\sigma^K \bar{e}_s^M) \right].\end{aligned}\tag{3.55}$$

Using the transformation of the third-order perturbations of a tensor, given by (3.34), one can show that the entropy perturbation as defined in (3.55) is gauge-invariant. Note that, compared to the earlier work [20], we have added the gauge-invariant term  $\frac{1}{6\bar{\sigma}'^2} \delta s \delta s'^2$  to the definition of  $\delta s^{(3)}$  (and correspondingly subtracted its derivative from  $\delta s_i^{(3)}$ ). This improved definition is motivated by our considerations of ekpyrotic models in section 4.1, as we will further discuss there. Moreover, in appendix A we

will present additional arguments that the term we are adding to the definition of the entropic perturbation is the only sensible one<sup>2</sup>. Apart from this small modification, the present definition now also includes terms due to the curvature of field space.

On large scales, our new definition leads to an extremely simple relationship between the covector  $\delta s_i^{(3)}$  and the entropic perturbation  $\delta s^{(3)}$ : in comoving gauge we have

$$\begin{aligned}\delta s_i^{(3)} &\stackrel{\delta\sigma=0}{\approx} \partial_i \delta s^{(3)} + \frac{1}{2\bar{\sigma}'^2} \delta s \delta s' \partial_i \delta s' - \frac{1}{6\bar{\sigma}'^2} \partial_i (\delta s \delta s'^2) \\ &= \partial_i \delta s^{(3)} + \frac{1}{3\bar{\sigma}'^2} \delta s' V_i \\ &\approx \partial_i \delta s^{(3)}\end{aligned}\tag{3.56}$$

with

$$\begin{aligned}\delta s^{(3)} &\stackrel{\delta\sigma=0}{\equiv} \bar{e}_{sI} \delta \phi^{(3)I} + \frac{1}{6\bar{\sigma}'^2} \delta s \delta s'^2 + \bar{e}_{sI} \bar{\Gamma}_{KL}^I \bar{e}_s^L \delta s \left[ \bar{e}_s^K \delta s^{(2)} - \frac{1}{2\bar{\sigma}'} \bar{e}_\sigma^K \delta s \delta s' \right] \\ &\quad + \frac{1}{6} \bar{e}_{sI} \bar{e}_s^J \bar{e}_s^K \bar{e}_s^L \left[ \partial_J \bar{\Gamma}_{KL}^I - 2\bar{\Gamma}_{JP}^I \bar{\Gamma}_{KL}^P \right] \delta s^3,\end{aligned}\tag{3.57}$$

where we have simplified the last term due to the symmetry in the vielbeine.

The adiabatic perturbation  $\delta\sigma$  is not a gauge-invariant variable, so there is more freedom in choosing a definition. Expanding Eq. (3.25) using Eqs. (B.13) and (B.15), we obtain

$$\begin{aligned}\delta\sigma_i^{(3)} &= \partial_i \delta\sigma^{(3)} - \frac{1}{\bar{\sigma}'} V_i^{(3)} - \frac{\bar{\theta}'}{3\bar{\sigma}'^2} \delta s V_i + \frac{\bar{\theta}'}{\bar{\sigma}'} \left( \delta\sigma \partial_i \delta s^{(2)} + \delta\sigma^{(2)} \partial_i \delta s \right) + \frac{\delta\sigma}{\bar{\sigma}'^2} (\delta s' + \bar{\theta}' \delta\sigma) \partial_i \delta s' \\ &\quad + \frac{1}{2\bar{\sigma}'^2} (\delta s' + \bar{\theta}' \delta\sigma)^2 \partial_i \delta\sigma + \left[ \left( \frac{\bar{\theta}'}{\bar{\sigma}'} \right)' \frac{\delta\sigma}{2} - \frac{1}{\bar{\sigma}'^2} (\bar{V}_{ss} + 2\bar{\theta}'^2) \delta s + \frac{\bar{V}_{,\sigma}}{\bar{\sigma}'^2} \delta s' \right] \delta\sigma \partial_i \delta s \\ &\quad + (\bar{e}_\sigma^K \bar{e}_s^L + \bar{e}_s^K \bar{e}_\sigma^L) \bar{e}_\sigma^J \delta\sigma \delta s \partial_i (\bar{e}_\sigma^I \delta\sigma + \bar{e}_s^I \delta s) \left[ \frac{1}{2} (\bar{G}_{IP,J} - \bar{G}_{IJ,P}) \bar{\Gamma}_{KL}^P \right. \\ &\quad \left. - \bar{G}_{JP,L} \bar{\Gamma}_{IK}^P + \frac{1}{4} (\bar{G}_{KL,IJ} - \bar{G}_{IK,LJ} - \bar{G}_{IL,KJ} + 2\bar{G}_{IJ,KL}) \right],\end{aligned}\tag{3.58}$$

---

<sup>2</sup>This new definition does not change the results of [20], as our new definition differs from the old one by a gauge-invariant term.

with

$$\begin{aligned}
\delta\sigma^{(3)} \equiv & \bar{e}_{\sigma I} \delta\phi^{(3)I} + \frac{1}{2\bar{\sigma}'} \left( \delta s' \delta s^{(2)} + \delta s \delta s^{(2)'} \right) + \frac{\bar{\theta}'}{6\bar{\sigma}'^2} \delta s^2 \delta s' \\
& + \bar{e}_{\sigma I} \bar{\Gamma}_{KL}^I \left( \bar{e}_{\sigma}^L \delta\sigma + \bar{e}_s^L \delta s \right) \left[ \bar{e}_{\sigma}^K \left( \delta\sigma^{(2)} - \frac{1}{2\bar{\sigma}'} \delta s \delta s' \right) \right. \\
& \left. + \bar{e}_s^K \left( \delta s^{(2)} + \frac{\delta\sigma}{\bar{\sigma}'} \left( \delta s' + \frac{\bar{\theta}'}{2} \delta\sigma \right) \right) \right] + \frac{1}{2} \bar{e}_s^I \bar{e}_s^J \bar{e}_{\sigma}^K \bar{e}_{\sigma}^L \bar{R}_{IKJL} \delta\sigma \delta s^2 \\
& + \frac{1}{6} \bar{e}_{\sigma I} \left( \bar{e}_{\sigma}^J \bar{e}_{\sigma}^K \bar{e}_{\sigma}^L \delta\sigma^3 + \bar{e}_s^J \bar{e}_s^K \bar{e}_s^L \delta s^3 \right) \left[ \partial_J \bar{\Gamma}_{KL}^I - 2 \bar{\Gamma}_{JP}^I \bar{\Gamma}_{KL}^P \right].
\end{aligned} \tag{3.59}$$

We have defined the natural generalisation of the third-order non-local term  $V_i$  as

$$V_i^{(3)} = \frac{1}{2} \left( \delta s^{(2)} \partial_i \delta s' + \delta s \partial_i \delta s^{(2)'} - \delta s^{(2)'} \partial_i \delta s - \delta s' \partial_i \delta s^{(2)} \right), \tag{3.60}$$

which again vanishes when the total entropy perturbation  $\delta s = \delta s^{(1)} + \delta s^{(2)}$  factorises into its time and spatial dependence, i.e.  $\delta s' = g(t)\delta s$ . We can neglect it as such differences in spatial gradients are heavily suppressed on large scales in both inflationary and ekpyrotic models. For  $\delta\sigma = \delta\sigma^{(2)} = 0$  the adiabatic perturbation at third order reduces to

$$\begin{aligned}
\delta\sigma^{(3)} \stackrel{\delta\sigma=0}{\approx} & \bar{e}_{\sigma I} \delta\phi^{(3)I} + \frac{1}{2\bar{\sigma}'} \left( \delta s' \delta s^{(2)} + \delta s \delta s^{(2)'} \right) + \frac{\bar{\theta}'}{6\bar{\sigma}'^2} \delta s^2 \delta s' \\
& + \bar{e}_{\sigma I} \bar{\Gamma}_{KL}^I \bar{e}_s^L \delta s \left[ \bar{e}_s^K \delta s^{(2)} - \frac{1}{2\bar{\sigma}'} \bar{e}_{\sigma}^K \delta s \delta s' \right] \\
& + \frac{1}{6} \bar{e}_{\sigma I} \bar{e}_s^J \bar{e}_s^K \bar{e}_s^L \delta s^3 \left[ \partial_J \bar{\Gamma}_{KL}^I - 2 \bar{\Gamma}_{JP}^I \bar{\Gamma}_{KL}^P \right].
\end{aligned} \tag{3.61}$$

One may check that this is a useful definition of the adiabatic perturbation by expanding the momentum density (3.15) to third order and verifying that it vanishes on large scales,  $\delta q_i^{(3)} \stackrel{\delta\sigma=0}{\approx} 0$ , in comoving gauge  $\delta\sigma = \delta\sigma^{(2)} = \delta\sigma^{(3)} = 0$ .

Now that we have the definitions of the adiabatic and entropic fluctuations, we can obtain their equations of motion. To this end, we expand the equation of motion

for  $s_a$  (3.28) to third order, with the result

$$\begin{aligned}
0 \approx & \delta s^{(3)''} + 3H\delta s^{(3)'} + (\bar{V}_{;ss} + 3\bar{\theta}'^2 + \bar{\sigma}'^2 \bar{e}_s^I \bar{e}_s^J \bar{e}_\sigma^K \bar{e}_\sigma^L \bar{R}_{IKJL}) \delta s^{(3)} + 2\frac{\bar{\theta}'}{\bar{\sigma}'} \delta s' \delta s^{(2)'} \\
& + \left( \frac{2}{\bar{\sigma}'} \bar{\theta}'' + \frac{2}{\bar{\sigma}'^2} \bar{V}_{;\sigma} \bar{\theta}' - \frac{3}{\bar{\sigma}'} H \bar{\theta}' \right) (\delta s \delta s^{(2)})' \\
& + \left( \bar{V}_{;sss} - \frac{10}{\bar{\sigma}'} \bar{V}_{;ss} \bar{\theta}' - \frac{18}{\bar{\sigma}'} \bar{\theta}'^3 + \bar{e}_s^I \bar{e}_s^J \bar{e}_\sigma^K \bar{e}_\sigma^L (-2\bar{\sigma}' \bar{\theta}' \bar{R}_{IKJL} + \bar{\sigma}'^2 \bar{e}_s^N \mathcal{D}_N \bar{R}_{IKJL}) \right) \delta s \delta s^{(2)} \\
& + \frac{\bar{V}_{,\sigma}}{3\bar{\sigma}'^3} \delta s'^3 + \frac{1}{\bar{\sigma}'^2} \left[ \frac{2}{3} \bar{V}_{;\sigma\sigma} + \frac{2\bar{V}_{,\sigma}^2}{\bar{\sigma}'^2} + \frac{1}{\bar{\sigma}'} H \bar{V}_{,\sigma} - \bar{V}_{;ss} - \frac{8}{3} \bar{\theta}'^2 - \bar{\sigma}'^2 \bar{e}_s^I \bar{e}_s^J \bar{e}_\sigma^K \bar{e}_\sigma^L \bar{R}_{IKJL} \right] \delta s \delta s'^2 \\
& + \left[ -\frac{22}{3\bar{\sigma}'^2} \bar{\theta}' \bar{\theta}'' - \frac{7}{6\bar{\sigma}'} \bar{V}_{;ss\sigma} - \frac{11}{3\bar{\sigma}'^3} \bar{V}_{;ss} \bar{V}_{,\sigma} - \frac{13}{3\bar{\sigma}'^3} \bar{V}_{,\sigma} \bar{\theta}'^2 - \frac{1}{\bar{\sigma}'^2} H \bar{V}_{;ss} + \frac{18}{\bar{\sigma}'^2} H \bar{\theta}'^2 \right. \\
& \quad \left. - \frac{4\bar{V}_{,\sigma}}{3\bar{\sigma}'} \bar{e}_s^I \bar{e}_s^J \bar{e}_\sigma^K \bar{e}_\sigma^L \bar{R}_{IKJL} - \frac{\bar{\sigma}'}{6} \bar{e}_s^I \bar{e}_s^J \bar{e}_\sigma^K \bar{e}_\sigma^L \bar{e}_\sigma^M \mathcal{D}_M \bar{R}_{IKJL} \right] \delta s^2 \delta s' \\
& + \left[ \frac{1}{6} \bar{V}_{;ssss} - \frac{7}{3\bar{\sigma}'} \bar{V}_{;sss} \bar{\theta}' + \frac{5}{3\bar{\sigma}'^2} \bar{V}_{;ss}^2 + \frac{19}{\bar{\sigma}'^2} \bar{V}_{;ss} \bar{\theta}'^2 + \frac{24}{\bar{\sigma}'^2} \bar{\theta}'^4 \right. \\
& \quad \left. + \frac{1}{3} \bar{e}_s^I \bar{e}_s^J \bar{e}_\sigma^K \bar{e}_\sigma^L \left( \bar{R}_{IKJL} (\bar{V}_{;ss} + \bar{\theta}'^2) - 2\bar{\sigma}' \bar{\theta}' \bar{e}_s^N \mathcal{D}_N \bar{R}_{IKJL} \right. \right. \\
& \quad \left. \left. + \bar{\sigma}'^2 \bar{e}_s^N \bar{e}_s^Q \left( \frac{1}{2} \mathcal{D}_Q \mathcal{D}_N \bar{R}_{IKJL} - \bar{R}_{IKJL} \bar{R}_{NLQ}^P + \bar{R}_{IKJL} \bar{R}_{NPQ}^P \right) \right) \right] \delta s^3, \tag{3.62}
\end{aligned}$$

where we have used  $V_i \approx 0$  and  $V_i^{(3)} \approx 0$  on large scales. The equation of motion is fully covariant, as it should be. Notice that upon the introduction of the extra term in the definition of  $\delta s^{(3)}$  in (3.55) compared to [20] the numerical factors of some of the terms have changed – see appendix A for the equivalent equation of motion without the extra term. Moreover, the non-trivial field space metric manifests itself in the appearance of terms with Riemann tensors and their covariant derivatives. Just as was the case at lower orders, the large-scale equation for the entropy perturbation is closed at third order.

On large scales, the evolution of the curvature perturbation at third order is given

by expanding (3.30) and using (B.33)-(B.35), leading to

$$\begin{aligned}
\zeta^{(3)'} &\stackrel{\delta\sigma=0}{\approx} \frac{2H}{\bar{\sigma}'^2} \left[ \delta V^{(3)} + \frac{4}{\bar{\sigma}'^2} \delta V^{(1)} \delta V^{(2)} + \frac{4}{\bar{\sigma}'^4} \left( \delta V^{(1)} \right)^3 \right] \\
&= \frac{2H}{\bar{\sigma}'^2} \left[ -\bar{\sigma}' \bar{\theta}' \delta s^{(3)} - \frac{\bar{V}_{,\sigma}}{2\bar{\sigma}'} \left( \delta s \delta s^{(2)} \right)' + \left( \bar{V}_{;ss} + 4\bar{\theta}'^2 \right) \delta s \delta s^{(2)} + \frac{\bar{\theta}'}{6\bar{\sigma}'} \delta s \delta s'^2 \right. \\
&\quad \left. + \left( \frac{11}{6} \frac{\bar{\theta}' \bar{V}_{,\sigma}}{\bar{\sigma}'^2} - \frac{1}{2\bar{\sigma}'} \bar{V}_{;s\sigma} \right) \delta s^2 \delta s' + \left( \frac{1}{6} \bar{V}_{;sss} - 2 \frac{\bar{\theta}' \bar{V}_{;ss}}{\bar{\sigma}'} - 4 \frac{\bar{\theta}'^3}{\bar{\sigma}'} \right) \delta s^3 \right]. \tag{3.63}
\end{aligned}$$

It is the third-order counterpart of Eqs. (3.52) and (3.53) and shows how the adiabatic/curvature perturbations are sourced by entropic perturbations. As is apparent from the first line, once the potential  $V$  becomes irrelevant,  $\zeta$  is conserved on large scales. This is for instance the case in the approach to the bounce in ekpyrotic models.

## Chapter 4

# The non-minimally coupled ekpyrotic model

The evolution equations derived in the previous section (3.3) can be applied to any inflationary or ekpyrotic model described by two scalar fields with a non-trivial field space metric and a potential. In this chapter we are interested in the “non-minimal entropic mechanism”, which is a mechanism for generating ekpyrotic density perturbations. It was first proposed by Qiu, Gao and Saridakis [21] as well as by Li [22], and further developed and generalised in [24, 23]. The model contains two scalar fields:  $\phi$  is assumed to have an ordinary kinetic term and a steep negative potential – thus  $\phi$  drives the ekpyrotic contracting phase. A second scalar,  $\chi$ , is non-minimally coupled to  $\phi$  such that in the ekpyrotic background it obtains nearly scale-invariant perturbations. Compared to the standard entropic mechanism described in subsection 2.4.2, the model has the advantage that it does not require an unstable potential to generate nearly scale-invariant perturbations. In fact, in this model the potential, depicted in Fig. 4.1, need not depend on the second scalar  $\chi$  at all during the ekpyrotic phase. The entropic mechanism consists of a two-stage process: first nearly scale-invariant, Gaussian entropy perturbations are produced during the ekpyrotic phase, which are then converted into curvature perturbations in the subsequent kinetic phase by a bending in the field space trajectory. We will assume that the conversion process also occurs during the contracting phase of the universe. To complete the model, one may then consider both a prescription for initial conditions [137, 138, 29, 139] and a non-singular bounce into the current expanding phase of the universe as outlined in section 2.5.

As just described, we will consider the case where the second scalar field  $\chi$  is

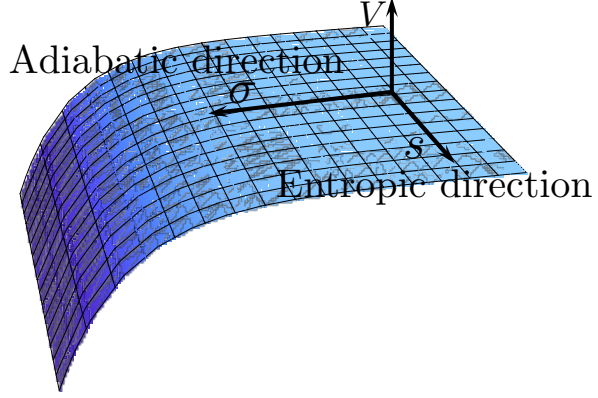


Figure 4.1: After a rotation in field space, the two-field ekpyrotic potential can be viewed as composed of an ekpyrotic direction ( $\sigma$ ) and a transverse direction ( $s$ ). The ekpyrotic scaling solution corresponds to motion along the adiabatic direction. Perturbations along the direction of the trajectory are adiabatic/curvature perturbations, while perturbations transverse to the trajectory are entropy/isocurvature perturbations.

coupled to the first scalar  $\phi$  by a function  $\Omega(\phi)^2$ , i.e. the field space metric and its inverse are given by

$$G_{IJ} = \begin{pmatrix} 1 & 0 \\ 0 & \Omega(\phi)^2 \end{pmatrix}, \quad \text{and} \quad G^{IJ} = \begin{pmatrix} 1 & 0 \\ 0 & \Omega(\phi)^{-2} \end{pmatrix}. \quad (4.1)$$

In an FLRW universe, the background equations of motion derived from the action (3.1) are then

$$\ddot{\phi} + 3H\dot{\phi} + \bar{V}_{,\phi} - \Omega\Omega_{,\phi}\dot{\chi}^2 = 0, \quad (4.2)$$

$$\ddot{\chi} + \left(3H + 2\Omega^{-1}\Omega_{,\phi}\dot{\phi}\right)\dot{\chi} + \Omega^{-2}\bar{V}_{,\chi} = 0, \quad (4.3)$$

$$H^2 = \frac{1}{6} \left( \dot{\phi}^2 + \Omega^2 \dot{\chi}^2 + 2\bar{V} \right), \quad (4.4)$$

where, unlike in the previous chapter, a dot denotes a derivative w.r.t. physical time.

In order to obtain the spectrum as well as the non-Gaussianity parameters, we solve for the entropy and curvature perturbations, first analytically during the ekpyrotic phase in the next section, and then numerically for the conversion phase in section 4.2. Simplifications brought about by our choice of field space metric in (4.1) are detailed in appendix C.

## 4.1 The ekpyrotic phase

During the ekpyrotic phase we will consider potentials that are of exponential form,

$$V(\phi) = -V_0 e^{-c\phi}, \quad (4.5)$$

where in the general analysis the parameter  $c$  is a constant, but in deriving the spectrum of the perturbations in the following subsection we allow it to slowly vary with time. Moreover, in this context we consider a specific example for the field-dependent function in the field space metric,  $\Omega$ , namely

$$\Omega(\phi)^2 = e^{-b\phi}, \quad (4.6)$$

where we take  $b$  to be constant. In the following, we solve the equations of motion for the entropy and curvature perturbations order by order in perturbation theory.

### 4.1.1 The background solution

During the ekpyrotic phase, the potential is a function of  $\phi$  alone,  $V = V(\phi)$ , and hence  $V_{,\chi} = 0$ . From the background equation of motion for  $\chi$  (4.3) it is immediately clear that  $\chi$  being constant is a solution. Coordinates can be chosen such that

$$\chi = 0 \quad (4.7)$$

corresponds to the background. The remaining background equations (4.2, 4.4) then simply reduce to those for a single scalar in an ekpyrotic potential (4.5), and they admit the scaling solution [83]

$$a(t) \propto (-t)^{1/\epsilon}, \quad \phi = \sqrt{\frac{2}{\epsilon}} \ln \left[ - \left( \frac{V_0 \epsilon^2}{(\epsilon - 3)} \right)^{\frac{1}{2}} t \right], \quad \epsilon = \frac{c^2}{2}, \quad (4.8)$$

where  $t$  is negative and runs from large negative towards small negative values. The fast-roll parameter  $\epsilon \equiv \dot{\phi}^2/(2H^2)$  is directly related to the equation of state  $w = 2\epsilon/3 - 1$  and for a successful ekpyrotic phase where the universe becomes flat and anisotropies are suppressed we require  $w > 1$  or  $\epsilon > 3$  (i.e.  $c^2 > 6$ ). Compared to the scaling solution for the standard ekpyrotic case given in Eq. (2.134), we have not simplified the solution for large  $\epsilon \gg 1$ , but left the solution exact. Note that it was shown in [23] that for any ekpyrotic equation of state it is possible to

choose the potential and the kinetic coupling such that nearly scale-invariant entropy perturbations are produced.

The relative energy density in curvature scales as  $1/(aH)^2$ , and a standard analysis (cf. the flatness problem in 2.2.2) then shows that in order to solve the flatness problem  $aH$  has to grow by about 70 or more e-folds in magnitude over the course of the ekpyrotic phase. Thus we require

$$\frac{aH|_{ek-end}}{aH|_{ek-beg}} \equiv e^N \gtrsim e^{70}, \quad (4.9)$$

where  $N$  denotes the number of e-folds of ekpyrosis. Using Eq. (4.2), we obtain

$$\sqrt{\frac{\epsilon}{2}} \left( \frac{1-\epsilon}{\epsilon} \right) (\phi_{ek-end} - \phi_{ek-beg}) \equiv \frac{\epsilon-1}{\sqrt{2\epsilon}} \Delta\phi \gtrsim 70, \quad (4.10)$$

and therefore the flatness problem is solved if the ekpyrotic phase takes place over a field range  $\Delta\phi \gtrsim 70\sqrt{2\epsilon}/(\epsilon-1)$ . It is over this field range that the potential must take the form expressed in Eq. (4.5). As is intuitively clear, the steeper the potential, the shorter the required field range.

#### 4.1.2 Linear perturbations

We want to calculate the spectrum produced by the linear entropy perturbations during the ekpyrotic phase. The non-minimal coupling between the two scalar fields  $\phi$  and  $\chi$  in the kinetic term for  $\chi$  is given by (4.6). The idea is that when  $b \approx c$  (where  $c$  is the constant appearing in the exponent of the potential (4.5)), the ekpyrotic scalar  $\phi$  effectively provides a de Sitter-like background for the entropy field  $\chi$  and thus (nearly) scale-invariant entropy perturbations can be generated<sup>1</sup>, but crucially without classical instabilities.

In terms of  $\delta s$ , we then obtain the simple evolution equation from (3.48) together with the potential (4.5) and non-minimal coupling (4.6) (first derived in [143]):

$$\ddot{\delta s} + 3H\dot{\delta s} + \left[ \frac{k^2}{a^2} - \frac{b^2}{4} \dot{\phi}^2 - \frac{b}{2} \bar{V}_{,\phi} \right] \delta s = 0. \quad (4.11)$$

We can solve this equation by switching to conformal time, defined via  $dt = ad\tau$ ,

---

<sup>1</sup>This is reminiscent of the pseudo-conformal mechanism [140, 141] and of Galilean genesis [142].

and defining the canonically normalized entropy perturbation  $v_s \equiv a\delta s$ , leading to

$$v_s'' + \left[ k^2 - \frac{a''}{a} - \frac{b^2}{4} \phi'^2 - \frac{b}{2} a^2 V_{,\phi} \right] v_s = 0, \quad (4.12)$$

where a prime denotes a derivative w.r.t. conformal time. To proceed, we must evaluate all the terms enclosed by the square brackets above. In the ekpyrotic scaling solution the scale factor evolves as  $a(\tau) \propto (-\tau)^{1/(\epsilon-1)}$ , so that

$$\frac{a''}{a} = -\frac{(\epsilon-2)}{(\epsilon-1)^2 \tau^2}. \quad (4.13)$$

Using the definition of the fast-roll parameter  $\epsilon$ , we also obtain

$$\phi' = \sqrt{2\epsilon} \mathcal{H} = \frac{\sqrt{2\epsilon}}{(\epsilon-1)\tau}, \quad (4.14)$$

where  $\mathcal{H} = a'/a$ , while the Friedmann equation in conformal time can be used to calculate the potential

$$a^2 V = -a^2 V_0 e^{-c\phi} = 3\mathcal{H}^2 - \frac{1}{2} \phi'^2 = -\frac{(\epsilon-3)}{(\epsilon-1)^2 \tau^2}, \quad (4.15)$$

and one can use this expression to evaluate  $a^2 V_{,\phi} = -\sqrt{2\epsilon} a^2 V$ . We now have all the ingredients necessary to solve the entropy perturbation equation, which reduces to

$$v_s'' + \left[ k^2 - \frac{1}{(\epsilon-1)^2 \tau^2} \left( -\epsilon + 2 + \frac{b}{c} (\epsilon^2 - 3\epsilon) + \frac{b^2}{c^2} \epsilon^2 \right) \right] v_s = 0, \quad (4.16)$$

where  $\epsilon = c^2/2$ . In the above expression, we have intentionally written out factors of  $c$  in two places – this is because it will be convenient to define a parameter  $\Delta$ , which quantifies the difference in the coefficients  $b$  and  $c$  and in terms of which the final result is most easily expressed,

$$\frac{b}{c} \equiv 1 + \Delta. \quad (4.17)$$

Then the equation above can be solved in terms of Hankel functions. Imposing the usual boundary condition that in the far past ( $-k\tau \gg 1$ ) the mode function is that of a fluctuation in Minkowski space,

$$\lim_{\tau \rightarrow -\infty} v_s = \frac{1}{\sqrt{2k}} e^{-ik\tau}, \quad (4.18)$$

we obtain (up to a phase that is irrelevant here)

$$v_s = \sqrt{\frac{\pi}{4}} \sqrt{-\tau} H_\nu^{(1)}(-k\tau), \quad (4.19)$$

where  $H_\nu^{(1)}$  denotes a Hankel function of the first kind with index  $\nu$ , where

$$\nu^2 = \frac{9}{4} \left( 1 + \frac{2}{3} \frac{\Delta\epsilon}{(\epsilon-1)} \right)^2 \quad \rightarrow \quad \nu = \frac{3}{2} + \frac{\Delta\epsilon}{(\epsilon-1)}. \quad (4.20)$$

Remarkably, the expression for  $\nu^2$  combines into a perfect square and thus we can write out the index of the Hankel function without having to make an approximation. (Note that there also exists a second branch where one takes the negative root  $\nu = -\frac{3}{2} - \frac{\Delta\epsilon}{(\epsilon-1)}$ . However, this branch turns out to correspond to an unstable solution, and hence we will not consider it further.) At late times, the entropy perturbations then have the following wavenumber and time dependence

$$v_s \propto k^{-\nu} (-\tau)^{1/2-\nu} \quad (|k\tau| \ll 1). \quad (4.21)$$

The spectral index of the entropy perturbations is found to be

$$n_s = 4 - 2\nu = 1 - 2\Delta \frac{\epsilon}{(\epsilon-1)}. \quad (4.22)$$

Note that when the two exponents  $b$  and  $c$  in the potential and non-minimal coupling are equal, we obtain an exactly scale-invariant spectrum,  $n_s = 1$ . However, when  $b$  and  $c$  differ slightly, we obtain deviations from scale-invariance. Since we have  $\epsilon > 3$ , we can see that the deviation from scale-invariance is always between  $-3\Delta$  and  $-2\Delta$ . Thus, if  $b$  is larger than  $c$  by about two percent, we obtain the central value  $n_s = 0.96$  reported by the PLANCK team [9]. If we imagine that  $b$  and  $c$  start out being equal, then it is in fact not implausible that  $c$  should decrease somewhat over time: in order to have a successful model of the early universe, at some point the ekpyrotic phase must come to an end, which is most easily achieved if  $c$  is diminished during the ekpyrotic phase.

Motivated by these arguments, we are led to extend the above analysis to allow for  $c$  to be a slowly-varying function of time. Up to this point, we have not made any approximations. Here, however, we find that we can only obtain useful and simple expressions in the limit that  $\epsilon \gg 1$ . Expressing the change in  $c$  in terms of scale-factor “time”  $N = \ln a$ , with  $dN = Hdt$ , we can derive the relations (see also

[28])

$$\mathcal{H} \approx (\epsilon\tau)^{-1} \left( 1 + \frac{1}{\epsilon} + \frac{\epsilon_{,N}}{\epsilon^2} \right), \quad -\frac{a''}{a} = \mathcal{H}^2(\epsilon-2) \approx \tau^{-2} \left( \frac{1}{\epsilon} - \frac{4}{\epsilon^3} + \frac{2\epsilon_{,N}}{\epsilon^3} \right), \quad (4.23)$$

and

$$\phi' = \sqrt{2\epsilon} \mathcal{H} \approx \tau^{-1} \sqrt{\frac{2}{\epsilon}} \left( 1 + \frac{1}{\epsilon} + \frac{\epsilon_{,N}}{\epsilon^2} \right), \quad a^2 V_{,\phi} = \tau^{-2} \frac{1}{\sqrt{2\epsilon}} \left( 2 - \frac{2}{\epsilon} + 3 \frac{\epsilon_{,N}}{\epsilon^2} \right). \quad (4.24)$$

Using these, and repeating the same steps as above, the spectral index can be approximated by

$$n_s - 1 = -2\Delta - \frac{7}{3} \frac{\epsilon_{,N}}{\epsilon^2} \quad (\epsilon \gg 1). \quad (4.25)$$

Note that  $N$  decreases during the ekpyrotic phase since the universe is contracting, and hence decreasing  $\epsilon$  corresponds to  $\epsilon_{,N} > 0$ . Thus a decreasing  $\epsilon$  or  $c$ , required in order for the ekpyrotic phase to come to an end, leads to a red tilt in the spectrum of the entropy perturbations.

#### 4.1.3 Higher-order perturbations

We will now turn our attention to the higher-order perturbations, where we include results at linear order for a general non-minimal coupling term  $\Omega(\phi)^2$  for completeness. During the ekpyrotic phase, the curvature perturbations have a blue spectrum [108] and moreover they are not amplified [144, 88], such that we do not need to discuss them. The entropic perturbations are of more interest. In the constant  $\chi$  background the entropic direction in field space is precisely the  $\chi$  direction.

The specification of comoving gauge,  $\delta\sigma^{(1)} = \delta\sigma^{(2)} = 0$ , translates directly to

$$\delta\phi^{(1)}|_{\text{ekp}} = 0 \quad (4.26)$$

at linear order from (3.35), and

$$\delta\phi^{(2)}|_{\text{ekp}} = \frac{1}{2\dot{\sigma}} \left( \delta s \dot{\delta s} - \Omega^{-1} \Omega_{,\phi} \dot{\phi} \delta s^2 \right) = -\frac{1}{2} \Omega^2 \dot{\phi}^{-1} \delta\chi \dot{\delta\chi} \quad (4.27)$$

at second order from (3.39). With the definitions of the entropy perturbation at linear and quadratic order from Eqs. (3.36) and (3.40),

$$\delta s|_{\text{ekp}} = -\Omega(\phi) \delta\chi, \quad (4.28)$$

and

$$\delta s^{(2)}|_{\text{ekp}} = -\Omega(\phi)\delta\chi^{(2)}, \quad (4.29)$$

the evolution equations for the entropy perturbation simplify significantly: at linear order, starting from (3.48) we obtain

$$\ddot{\delta s} + 3H\dot{\delta s} + \left[\Omega^{-1}\Omega_{,\phi}\bar{V}_{,\phi} - \Omega^{-1}\Omega_{,\phi\phi}\dot{\phi}^2\right]\delta s \approx 0, \quad (4.30)$$

which rewritten in terms of  $\delta\chi$  and making use of the background equation for  $\phi$  (4.2) becomes

$$\ddot{\delta\chi} + \left(3H + 2\Omega^{-1}\Omega_{,\phi}\dot{\phi}\right)\dot{\delta\chi} \approx 0. \quad (4.31)$$

It is immediately clear that  $\dot{\delta\chi} = 0$  is a solution during the ekpyrotic phase<sup>2</sup>. This further simplifies our definitions; the second-order perturbation in the first scalar field (4.27) vanishes,

$$\delta\phi^{(2)}|_{\text{ekp}} = 0. \quad (4.32)$$

It is straightforward then to show that during the ekpyrotic phase the equation of motion for the entropy perturbation at second order, given by (3.50), takes the same form as the first-order one, namely

$$\ddot{\delta s}^{(2)} + 3H\dot{\delta s}^{(2)} + \left[\Omega^{-1}\Omega_{,\phi}\bar{V}_{,\phi} - \Omega^{-1}\Omega_{,\phi\phi}\dot{\phi}^2\right]\delta s^{(2)} \approx 0. \quad (4.33)$$

No source term arises for the second-order entropy perturbation  $\delta s^{(2)}$ , and we have the trivial solution

$$\delta s^{(2)}|_{\text{ekp}} = 0, \quad (4.34)$$

generating no intrinsic non-Gaussianity for the entropy perturbations. By contrast, the entropy perturbations develop significant local non-Gaussian corrections in the standard entropic mechanism already during the ekpyrotic phase, due to the  $\chi$ -dependence of the potential [97, 145, 146, 147, 20, 98, 7].

Having solved for the entropy perturbation, we can use Eqs. (3.52) and (3.53) to obtain the evolution equation for the curvature perturbation at linear and quadratic order, respectively, as

$$\dot{\zeta}^{(1)}|_{\text{ekp}} \approx 0, \quad (4.35)$$

---

<sup>2</sup>The solution at linear order is non-zero ( $\delta\chi^{(1)} = \text{constant}$ ) due to the quantization and associated amplification of the perturbations.

noting that  $\dot{\theta}|_{\text{ekp}} = 0$ , and

$$\zeta^{(2)}|_{\text{ekp}} \approx \frac{H\bar{V}_{,\phi}}{\dot{\sigma}^2} \left[ \dot{\sigma}^{-1} \delta s \dot{\delta s} + \Omega^{-1} \Omega_{,\phi} \delta s^2 \right] = -\frac{H\bar{V}_{,\phi}}{\dot{\phi}^3} \Omega^2 \delta \chi \dot{\delta \chi} = 0, \quad (4.36)$$

where the last equality follows from (4.31). Thus, during the ekpyrotic phase, no second-order curvature perturbation is generated,  $f_{NL \text{ integrated}} = 0$ . This becomes clear once one realises that the linearised solution, given by  $\delta \chi = \text{constant}$ , behaves analogously to the background.

For the explicit parametrisation of the potential in terms of  $c$  in (4.5) and the non-minimal coupling in terms of  $b$  in (4.6), we argued that a natural extension is to allow the equation of state (or fast-roll) parameter  $\epsilon$  to be a slowly varying function of time. In that case the time-dependence of the entropic mode functions is slightly modified, leading to a small source term for the second-order curvature perturbation during the ekpyrotic phase, with

$$\begin{aligned} \zeta^{(2)\prime} &= -\frac{\mathcal{H}}{\bar{\sigma}^{\prime 2}} a^2 \bar{V}_{,\sigma} \delta s^{(1)} \left[ \frac{\delta s^{(1)\prime}}{\bar{\sigma}'} - \frac{b}{2} \delta s^{(1)} \right] \\ &= -\frac{1}{12} \frac{v_s^2}{a^2} \frac{1}{(-\tau)} \frac{\epsilon_{,N}}{\epsilon^2}. \end{aligned} \quad (4.37)$$

If we approximate the time dependence of the fluctuation modes  $v_s/a \propto 1/\tau$  then we can easily perform the integral, obtaining

$$\zeta_{ek}^{(2)} = -\frac{1}{24} (\delta s_{ek-end})^2 \frac{\epsilon_{,N}}{\epsilon^2}. \quad (4.38)$$

We can see that the coefficient of  $(\delta s_{ek-end})^2$  is tiny, of  $\mathcal{O}(10^{-3})$  at most for realistic cases. Thus, the non-minimal entropic mechanism generates almost perfectly Gaussian entropy perturbations over the course of the ekpyrotic phase.

We can now apply our new results from the previous chapter to extend this discussion to third order. During the ekpyrotic phase and with the field space metric given in (4.1), the equation of motion (3.62) at third order simplifies to

$$\ddot{\delta s}^{(3)} + 3H\dot{\delta s}^{(3)} + \left[ \Omega^{-1} \Omega_{,\phi} \bar{V}_{,\phi} - \Omega^{-1} \Omega_{,\phi\phi} \dot{\phi}^2 \right] \delta s^{(3)} \approx 0 \quad (4.39)$$

allowing the solution

$$\delta s^{(3)}|_{\text{ekp}} = -\Omega \delta \chi^{(3)} = 0. \quad (4.40)$$

As at second order, no intrinsic non-Gaussianity for the entropy perturbations is generated at third order for this class of models. Note that if we had not added the gauge-invariant term  $\frac{1}{6\dot{\sigma}^2}\delta s\dot{\delta s}^2$  to the definition of the third-order entropy perturbation in (3.55), then  $\delta s^{(3)}$  would have been non-zero. This would not have changed any results for physically measurable quantities, but it is clear that our present definition of the third-order entropy perturbation is preferable to the older definition of [20], both on physical and aesthetic grounds.

The curvature perturbation at third order can be calculated by noting that during the ekpyrotic phase,  $\bar{V}_{,\chi} = \dot{\theta} = 0$ , and hence

$$\delta V|_{\text{ekp}} = \bar{V}_{,\phi}\delta\phi + \bar{V}_{,\phi}\delta\phi^{(2)} + \frac{1}{2}\bar{V}_{,\phi\phi}\delta\phi^2 + \bar{V}_{,\phi}\delta\phi^{(3)} + \bar{V}_{,\phi\phi}\delta\phi\delta\phi^{(2)} + \frac{1}{6}\bar{V}_{,\phi\phi\phi}\delta\phi^3 + \mathcal{O}(4), \quad (4.41)$$

which simplifies to

$$\delta V|_{\text{ekp}} \stackrel{\delta\sigma=0}{\approx} \bar{V}_{,\phi}\delta\phi^{(3)} + \mathcal{O}(4), \quad (4.42)$$

in comoving gauge. From Eq. (3.61), we have that during the ekpyrotic phase (in comoving gauge on large scales)

$$\delta\sigma^{(3)}|_{\text{ekp}} \stackrel{\delta\sigma=0}{\approx} -\delta\phi^{(3)} = 0. \quad (4.43)$$

Thus there is no source for the curvature perturbation during the ekpyrotic phase,

$$\zeta^{(3)}|_{\text{ekp}} = \frac{2H}{\dot{\sigma}^2}\delta V^{(3)} \stackrel{\delta\sigma=0}{\approx} \frac{2H}{\dot{\sigma}^2}\bar{V}_{,\phi}\delta\phi^{(3)} = 0, \quad (4.44)$$

and at third order also the comoving curvature perturbation remains zero during the ekpyrotic phase, i.e. we have  $g_{NL \text{ integrated}} = 0$ .

In summary, we find that the ekpyrotic phase produces no local non-Gaussianity at all – at least up to third order in perturbation theory – neither for the entropy nor the curvature fluctuations. As we will now see, the conversion process of entropy into curvature fluctuations will change this result appreciably.

## 4.2 The conversion phase

What we observe in the cosmic background radiation are not entropy perturbations, but rather the temperature fluctuations stemming directly from curvature perturbations. Thus, if we want our model to be viable, we must ensure that the entropy perturbations discussed so far can be converted into curvature fluctuations. It is im-

portant to keep in mind that during the ekpyrotic phase and at the linearised level, quantum curvature perturbations are not amplified into classical perturbations, unlike the entropic modes discussed above [144, 88]. Hence, at the end of the ekpyrotic phase, the entropy perturbations are the only classical perturbations there are. The equation governing the evolution of the comoving curvature perturbation on large scales is derived in subsection 2.4.2. At the linearised level, it is given by (2.167),

$$\dot{\zeta} = \frac{2H\bar{V}_{,s}}{\dot{\sigma}^2} \delta s = -\sqrt{\frac{2}{\epsilon}} \dot{\theta} \delta s. \quad (4.45)$$

Note that in comoving gauge the perturbations in the first scalar field are gauged away,  $\delta\phi = -\delta\sigma = 0$ , and the curvature perturbation corresponds to a local rescaling of the scale factor – see Eq. (3.30). Thus  $\zeta$  can be thought of as a perturbation parallel to the background trajectory. As Eq. (4.45) shows, the entropy perturbations  $\delta s$  act as a source for the curvature perturbations when  $V_{,s} \neq 0$ , i.e. when there is a transverse force on the background trajectory. This equation clearly illustrates that whenever the background trajectory bends, curvature perturbations are generated. Since there is no  $k$ -dependence in Eq. (4.45), the spectrum of the resulting curvature perturbations will be identical to that of the entropy perturbations that source them, and thus the spectral index of the curvature perturbations will be given by Eq. (4.22) (or, when  $\epsilon$  evolves and with  $\epsilon \gg 1$ , by Eq. (4.25)).

Following the logic in subsection 2.4.2 we can estimate the amplitude of the curvature perturbations produced during ekpyrotic or kinetic conversion. We obtain a power spectrum

$$P_\zeta = \frac{k^3}{(2\pi)^2} \langle \zeta_{final}^2 \rangle \approx \frac{k^3}{(2\pi)^2 \epsilon_c} (\delta s_{ek-end})^2 \approx \frac{(\epsilon - 1)^2}{\epsilon_c(\epsilon - 3)} \frac{V_{ek-end}}{(2\pi)^2}, \quad (4.46)$$

where  $V_{ek-end} = |V(t_{ek-end})|$  again denotes the magnitude of the potential at the end of the ekpyrotic phase, which corresponds to the energy scale of the deepest point in the potential. Unless the fast-roll parameter  $\epsilon$  during the ekpyrotic phase is very close to 3, this implies that (just as for the standard entropic mechanism) the potential has to reach the grand unified scale  $V_{ek-end} \approx (10^{-2} M_{Pl})^4$  in order for the curvature perturbations to have an amplitude in agreement with the observed value of about  $2 \times 10^{-9}$  [9]. When  $\epsilon$  is close to 3, which for the non-minimal entropic mechanism becomes a real possibility since the departure from scale-invariance of the spectral index is not related to the magnitude of  $\epsilon$ , the energy scale of the potential minimum can be lower.

In the following, we will solve the equations of motion numerically, focussing on the kinetic conversion process: After the ekpyrotic phase has come to an end, the conversion from entropy to curvature perturbations during the subsequent kinetic phase is achieved by a bending in the field space trajectory. This bending occurs naturally in the heterotic M-theory embedding of the ekpyrotic/cyclic model [83, 100, 105, 101], though other origins of such a bending may of course also be envisaged. The bending of the scalar field space trajectory can be modelled by having a repulsive potential (given a specific realisation of the cyclic model in heterotic M-theory, this repulsive potential can in principle be calculated [101]). Here, in order to be general, we consider four different representative forms for the repulsive potential, namely

$$V_{1,2} = v [x^{-2} + r x^{-6}], \quad v [(\sinh x)^{-2} + r (\sinh x)^{-4}], \quad (4.47)$$

with  $r = 0, 1$  and where the dependence of the potential on  $x = -\frac{\phi}{2} + \frac{\sqrt{3}\chi}{2}$  expresses the fact that the repulsive potential forms an angle (here chosen to be  $\pi/6$ ) with respect to the background trajectory. The different potentials as well as a typical reflected field space trajectory are shown in Fig. 4.2.

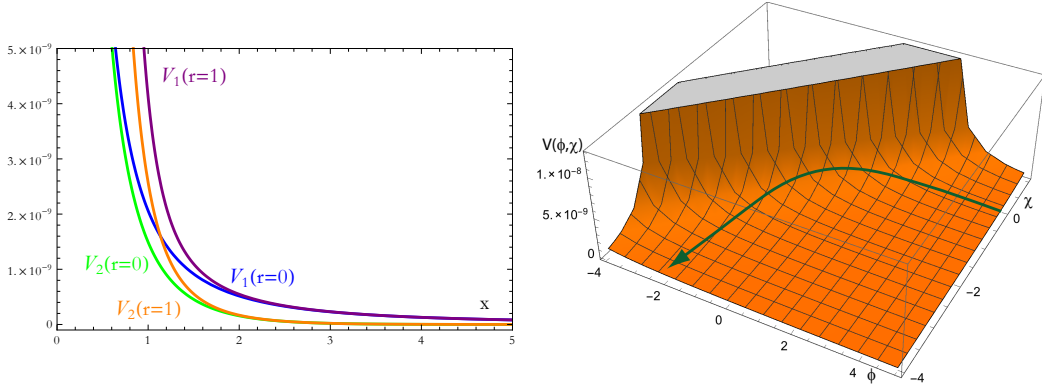


Figure 4.2: *Left:* The repulsive potentials ( $V_{1,2}$  with  $r = 0, 1$ ) given in Eq. (4.47). *Right:* The field space trajectory in the repulsive potential  $V_1(r = 0)$ .

One of the important parameters is the duration of the conversion process. We measure it by the number of e-folds  $N$  of the evolution of  $|aH|$  during conversion. That is, one e-fold of conversion corresponds to  $\dot{a}(t_{\text{conv-end}}) = e \cdot \dot{a}(t_{\text{conv-beg}})$ . In our numerical studies we determine  $N$  by determining the number of e-folds during which 90 percent of the total bending takes place, i.e. we require  $\int_{t_{\text{conv-beg}}}^{t_{\text{conv-end}}} \dot{\theta} dt / \int_{t_{\text{kin-beg}}}^{t_{\text{kin-end}}} \dot{\theta} dt = 0.9$ . Conversions lasting about one e-fold correspond to what we call smooth conversions, while shorter conversions are sharper. We find that the results depend very

significantly on the smoothness of conversion.

In the non-minimal entropic mechanism the local bispectrum produced during the conversion process is small when the conversion is efficient (which corresponds to the conversion being smooth [147]). However, it is rather non-trivial to obtain such an efficient conversion process. This becomes clear when we analyse the equation of motion for  $\chi$  given in (4.3), where the potential is now the repulsive potential modelling the conversion. Even small changes along the background trajectory (along  $\sigma \sim \phi$ ) lead to an enormous factor  $\Omega^{-2} \sim e^\phi$  multiplying the now non-zero  $\chi$ -derivative of the potential. This causes the background trajectory to be sharply deflected, leading to an extremely inefficient conversion. So whenever the scalar curvature, given by

$$R = -2 \frac{\Omega_{,\phi\phi}}{\Omega}, \quad (4.48)$$

is significant, the conversion is highly inefficient. This has the consequence of leading to a small amplitude for the curvature perturbations, and large non-Gaussianities in clear contradiction with observations. What this means is that the field space metric, taken to be  $\Omega = e^{-b\phi/2}$  during the ekpyrotic phase, has to become flatter again during the conversion process. Thus, in the same way as the potential turns off after the end of the ekpyrotic phase, the field space metric must progressively return to being trivial.

#### 4.2.1 Linearly decaying field space metric

Motivated by the previous discussion, we want to analyse cases where the field space metric returns to being trivial during the conversion process, after the end of the ekpyrotic phase. We will first concentrate on the case where the Ricci scalar of the field space decays linearly with time. This can be modelled by a kinetic coupling function of the form

$$\Omega = 1 - b \cdot I_0(d \cdot e^{c\phi/2}), \quad (4.49)$$

where  $I_0$  is a modified Bessel function of the first kind. This has the nice property that the scalar curvature (4.48) has a constant slope  $\dot{R}$  and decays linearly, as seen in the rightmost panel of Fig. 4.3. We have plotted  $\Omega$  in the central panel in the region of the conversion, and the leftmost panel of the same figure shows the bending of the trajectory for a typical smooth conversion lasting one e-fold.

Fig. 4.4 shows plots of the local non-linearity parameters  $f_{NL}$  (parametrising the local bispectrum) and  $g_{NL}$  (parametrising the local trispectrum) for different dura-

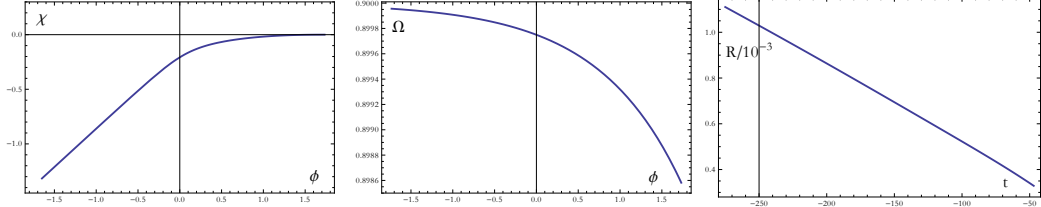


Figure 4.3: The evolution of the fields (left), the field space metric and the scalar (Ricci) curvature (right) during one e-fold of conversion (from  $t = -275$  to  $t = -47$ ), plotted for the specific case with  $V_2(r = 1) = v \left[ (\sinh x)^{-2} + (\sinh x)^{-4} \right]$ , and  $\Omega(c = 1, b = d = \frac{1}{10}) = 1 - \frac{1}{10} I_0 \left( \frac{1}{10} e^{\phi/2} \right)$ , giving  $f_{\text{NL}} = -1.3$  and  $g_{\text{NL}} = -544$ .

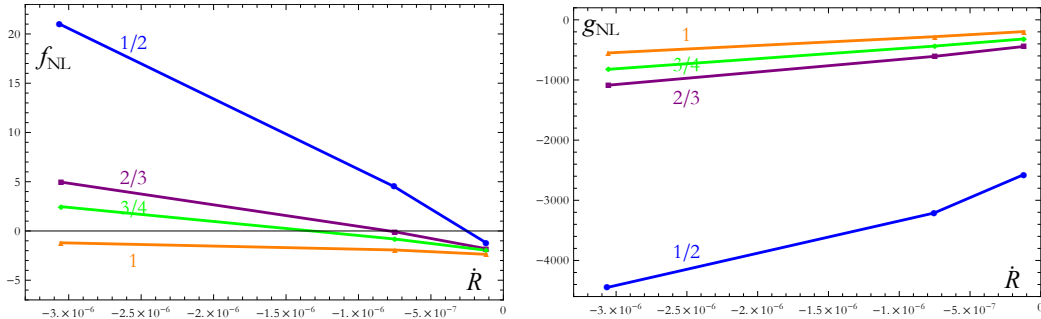


Figure 4.4: Non-Gaussianity plotted against different slopes of the scalar curvature ( $\dot{R}$ ) for different durations of the conversion ( $N = 1/2, 2/3, 3/4, 1$ ) for the repulsive potential  $V_2$  with  $r = 1$ . The slope  $\dot{R}$  is varied by choosing different values for  $d = 1/10, 1/20, 1/50$ . Note that the magnitudes of  $f_{\text{NL}}$  and  $g_{\text{NL}}$  are significantly reduced for smoother conversion processes.

tions of conversion and as a function of the slope  $\dot{R}$ . (The non-linearity parameters of the comoving curvature perturbation are defined in Eqs. (2.111) and (2.112).) There are two obvious trends: the smoother, and thus the longer and more efficient, the conversion process is, the smaller the non-Gaussianity. And the closer the field space metric is to trivial, again the smaller in magnitude are the non-linearity parameters  $f_{NL}$  and  $g_{NL}$ . Note that for smoother conversions, the dependence on the slope  $\dot{R}$  is much weaker, and hence, to some extent, the predictions converge for smooth conversions. Referring back to our previous discussion, it is easy to see by extrapolation that large and rapidly varying field space curvatures very quickly lead to values of the non-Gaussianity parameters that are much larger than allowed for by current observational bounds. On the other hand, for smooth conversions and small and slowly changing field space curvatures the local bispectrum parameter  $f_{NL}$  is of magnitude  $|f_{NL}| \lesssim 5$  while the trispectrum parameter is always negative and of magnitude  $|g_{NL}| \sim \mathcal{O}(10^2) - \mathcal{O}(10^3)$ . These values are confirmed by an analysis of the effect of changing the functional form of the repulsive potential (while specialising to smooth conversions lasting one e-fold), as shown in Fig. 4.5. Note that the two potentials  $V_1$  and  $V_2$  with  $r = 0$ , colour coded in blue and green, respectively, give nearly identical predictions.

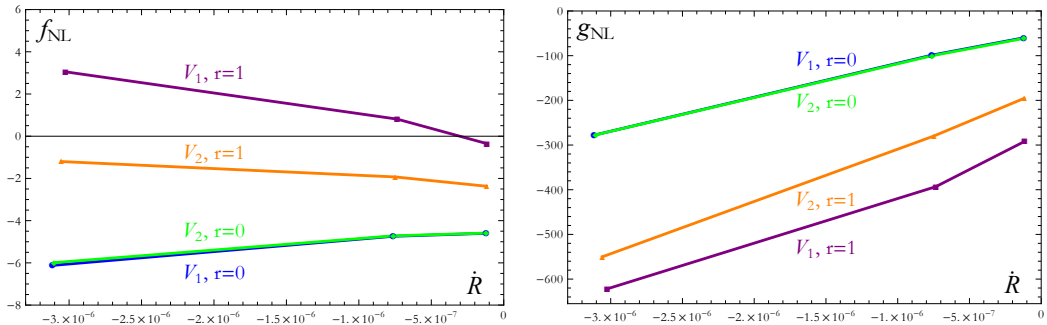


Figure 4.5: Non-Gaussianity plotted against different slopes of the scalar curvature ( $\dot{R}$ ) for different potentials ( $V_{1,2}$  with  $r = 0, 1$ ) for a conversion duration of one e-fold. The two  $r = 0$  lines happen to be virtually coincident. Note that the values for  $f_{NL}$  are clustered around zero, while the values for  $g_{NL}$  are always appreciably negative. This is a characteristic feature of current ekpyrotic models.

#### 4.2.2 Asymptotically flat field space metric

In order to check the robustness of our results, we will now consider a different functional form of the metric, namely we will consider the case where a trivial metric

is approached exponentially fast (in field space),

$$\Omega = 1 - be^{d\phi/2}, \quad (4.50)$$

where  $b$  and  $d$  are free parameters. We have plotted  $\Omega$  in the central panel of Fig. 4.6 in the region of the conversion. The corresponding field space trajectory and curvature scalar are shown in the left and right panels, respectively.

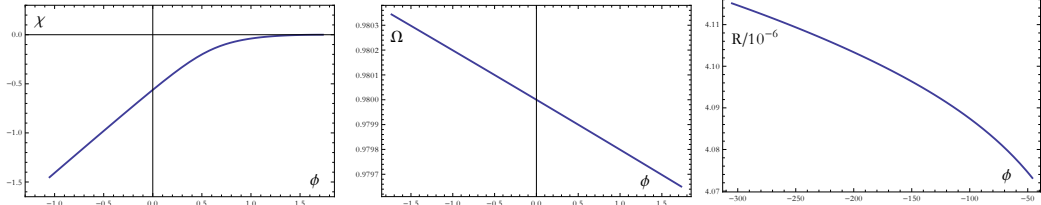


Figure 4.6: The evolution of the fields, the field space metric and the scalar curvature during one e-fold of conversion (from  $t = -304$  to  $t = -46$ ), plotted for the specific case with  $V_2(r = 1) = v \left[ (\sinh x)^{-2} + (\sinh x)^{-4} \right]$ , and  $\Omega (b = d = \frac{1}{50}) = 1 - \frac{1}{50} e^{\phi/100}$ , giving  $f_{NL} = 1.0$  and  $g_{NL} = -235$ .

Once again, we can verify the importance of the efficiency of conversion – see Fig. 4.7. We have plotted the results as a function of  $b = d$ : for  $b \neq d$  we found similar results (though typically slightly less variation in the non-linearity parameters). As the figure demonstrates, an efficient/smooth conversion is crucial, in the sense that in this case the typical values of the bispectrum are of  $\mathcal{O}(1)$ . Note that for less efficient conversions the spread in values is much larger, and hence no generic predictions can be made. For the trispectrum, the situation is analogous, with efficient conversions drastically reducing the range of possible values of  $g_{NL}$ .

We can also determine the effect of changing the functional form of the repulsive potential in scalar field space. The results are shown in Fig. 4.8, where for all cases we have assumed one e-fold of conversion. As can be seen from the figure, for such smooth conversions the expected values for the bispectrum are in the range  $|f_{NL}| \lesssim 5$ , while those for the trispectrum are  $|g_{NL}| \sim \mathcal{O}(10^2) - \mathcal{O}(10^3)$  and negative in sign, exactly as for the case of a linearly changing scalar field curvature.

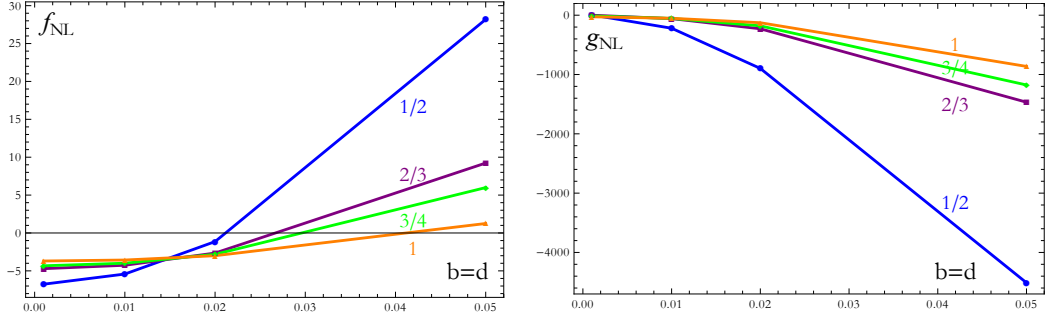


Figure 4.7: Non-Gaussianity plotted against different field space metrics ( $\Omega = 1 - be^{d\phi/2}$  with  $b = d$ ) for different durations of the conversion ( $N = 1/2, 2/3, 3/4, 1$ ) for the potential  $V_2$  with  $r = 0$ . Note that as in the case with a linearly decaying field space curvature, the magnitudes of  $f_{NL}$  and  $g_{NL}$  are significantly reduced for smoother conversion processes.

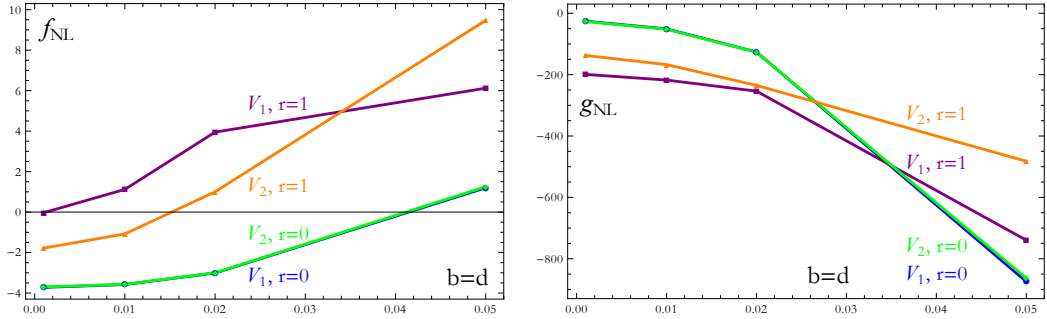


Figure 4.8: Non-Gaussianity plotted against different field space metrics ( $\Omega = 1 - be^{d\phi/2}$  with  $b = d$ ) for different potentials ( $V_{1,2}$  with  $r = 0, 1$ ) for a conversion duration of one e-fold.

### 4.3 Comparison to the minimally coupled entropic mechanism

It may be interesting to compare these results to those obtained via the older, minimally coupled entropic mechanism [87, 148, 28, 89, 90] as introduced in subsection 2.4.2. In that case, the kinetic terms of the scalar fields are canonical, but one assumes a potential that is unstable in the entropic direction. During the ekpyrotic phase, the potential is usefully written as (2.148),

$$V_{\text{min. entropic mech., ek}} = -V_0 e^{-\sqrt{2\epsilon}\sigma} \left[ 1 + \epsilon s^2 + \frac{\kappa_3}{3!} \epsilon^{3/2} s^3 + \frac{\kappa_4}{4!} \epsilon^2 s^4 + \dots \right], \quad (4.51)$$

where  $\kappa_3$  and  $\kappa_4$  are important for the bispectrum and trispectrum, respectively. In these models, and in contrast to the non-minimal entropic mechanism, a substantial part of the total non-Gaussianity can arise during the ekpyrotic phase. This can be seen by solving the equation of motion (3.62) for the entropy perturbation during the ekpyrotic phase. Expanding to leading order in  $1/\epsilon$ , for large  $\epsilon$ , we have as the initial conditions for the start of the conversion phase

$$\delta s = \delta s_L + \frac{\kappa_3 \sqrt{\epsilon}}{8} \delta s_L^2 + \epsilon \left( \frac{\kappa_4}{60} + \frac{\kappa_3^2}{80} - \frac{19}{60} \right) \delta s_L^3. \quad (4.52)$$

Notice the different numerical factor in the term proportional to  $\epsilon$  compared to [20] due to the change in the definition of the third-order entropy perturbation. As is clear from this expression, there is typically already a significant non-Gaussian component to the entropy perturbation prior to the phase of conversion. What is more, some of this conversion already occurs during the ekpyrotic phase, where the comoving curvature obeys the evolution equation (with  $\zeta = \zeta^{(1)} + \zeta^{(2)} + \zeta^{(3)}$ )

$$\zeta' = \frac{2H}{\bar{\sigma}'^2} \left[ -\frac{\bar{V}_{,\sigma}}{\bar{\sigma}'} \delta s \delta s' + \bar{V}_{;ss} \delta s^2 + \frac{1}{3} \bar{V}_{;sss} \delta s^3 \right], \quad (4.53)$$

Using Eqs. (2.111) and (2.112), this leads to

$$f_{NL \text{ integrated}} = \frac{5}{12} \frac{[\delta s_L(t_{\text{ek-end}})]^2}{|\zeta_L(t_{\text{conv-end}})|^2}, \quad (4.54)$$

$$g_{NL \text{ integrated}} = \frac{275}{1296} \kappa_3 \sqrt{\epsilon} \frac{[\delta s_L(t_{\text{ek-end}})]^3}{|\zeta_L(t_{\text{conv-end}})|^3}. \quad (4.55)$$

In order to calculate the contribution from the additional conversion process due to the subsequent bending of the scalar field trajectory, we have solved and integrated the equations of motion (3.62) and (3.63) numerically, using the expression (4.52) as the initial condition for the entropy perturbation.

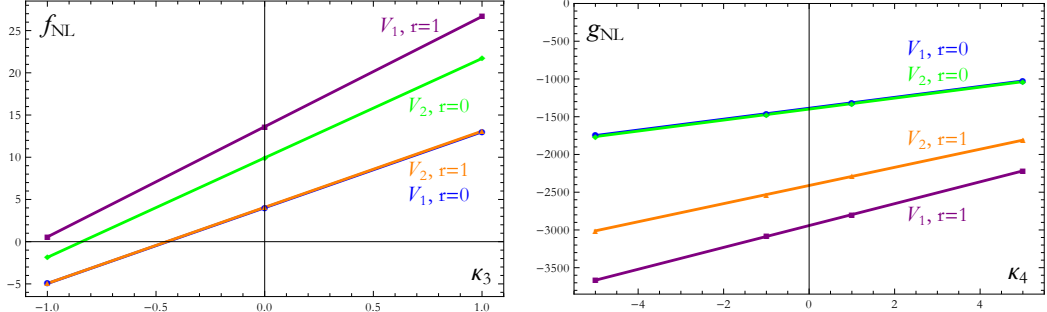


Figure 4.9: Non-Gaussianity plotted against different potentials ( $V_{1,2}$  with  $r = 0, 1$ ) for a conversion duration of one e-fold for the minimal entropic mechanism.

The minimal case was analysed in [20] in some detail. There it was shown that the range of predicted values for the non-Gaussianity parameters narrows drastically as the conversion process becomes smoother, just as we have found here. Specialising to conversions lasting one e-fold, we have reproduced the results of [20]: Fig. 4.9 shows the expected values of  $f_{NL}$  as a function of  $\kappa_3$  and those of  $g_{NL}$  as a function of  $\kappa_4$  (this time assuming  $\kappa_3 = 0$ ). As already discussed in [31], one can obtain a bispectrum in agreement with observations by assuming that the potential is (nearly) symmetric, which corresponds to  $|\kappa_3| \lesssim 1$ . In this case, the trispectrum remains negative and of  $\mathcal{O}(10^3)$ . Thus we see that if we restrict to symmetric potentials, the minimally coupled entropic mechanism leads to similar predictions for the non-Gaussianity parameters  $f_{NL}$  and  $g_{NL}$  as the non-minimally coupled model considered in the present paper, though  $g_{NL}$  is typically up to an order of magnitude larger in the minimally coupled case due to the significant intrinsic contribution represented by the very last ( $\kappa_{3,4}$ -independent, but  $\epsilon$ -dependent) term in (4.52).

#### 4.4 Gravitational waves

Just as in the standard ekpyrotic phase, the universe contracts very slowly,  $a(t) \propto (\tau)^{1/\epsilon}$  with  $\epsilon > 3$ . Thus, the background spacetime is to a first approximation similar to Minkowski spacetime, and consequently gravitational waves are not amplified. This provides a heuristic way to understand the result that no significant primordial

gravitational waves are produced by an ekpyrotic phase [109].

In fact, the dominant contribution to the primordial gravitational wave background in ekpyrotic models tends to arise at second order in perturbation theory, where the scalar curvature perturbations act as a source for the gravitational field. However, as this is a second-order effect, it also leads to the conclusion that detecting primordial gravitational waves stemming from ekpyrotic models is unlikely [110]. Hence, a detection of primordial gravitational waves of a significant amplitude would falsify all current ekpyrotic models.

## Chapter 5

# Conflation – a new type of accelerated expansion

In this chapter we will present a new cosmological model that combines features of both inflation and ekpyrosis. This is in the same spirit as the recently proposed “anamorphic” universe of Ijjas and Steinhardt [149], the distinction being that we are combining different elements of these models. We will work in the framework of scalar-tensor theories of gravity. By making use of a field redefinition (more precisely a conformal transformation of the metric), we transform an ekpyrotic contracting model into a phase of accelerated expansion. Moreover, we are specifically interested in the situation where matter degrees of freedom couple to the new (Jordan frame) metric, so that observers made of this matter will measure the universe to be expanding. Conflation is reminiscent of inflation in the sense that the background expands in an accelerated fashion. This immediately implies that the homogeneous spatial curvature and anisotropies are diluted, thus providing a solution to the flatness problem. However, other features of the model are inherited from the ekpyrotic starting point of our construction: for instance, the model assumes a negative potential. This might have implications for supergravity and string theory, where negative potentials arise very naturally and where it is in fact hard to construct reliable standard inflationary models with positive potentials [77]. Also, conflation does not amplify adiabatic curvature perturbations (or tensor perturbations). Hence eternal inflation, which relies on the amplification of large, but rare, quantum fluctuations, does not occur. This has the important consequence that the multiverse problem is avoided. As we will show, one can however obtain nearly scale-invariant curvature perturbations by considering an entropic mechanism analogous to the one used in ekpyrotic

models in the previous chapters. This allows the construction of specific examples of a conflationary phase in agreement with current cosmological observations.

For related studies starting from an inflationary phase and transforming that one into other frames, see [150, 151, 152, 153]. In the language of the anamorphic universe [149], we are looking at the situation where  $\Theta_m > 0$  and  $\Theta_{Pl} < 0$ , while Ijjas and Steinhardt consider  $\Theta_m < 0$  and  $\Theta_{Pl} > 0$  (note that inflation corresponds to  $\Theta_m > 0$  and  $\Theta_{Pl} > 0$  and ekpyrosis to  $\Theta_m < 0$  and  $\Theta_{Pl} < 0$ ).

## 5.1 Conflation

Our starting point is an ekpyrotic phase constructed in the standard Einstein frame where the scalar field is minimally coupled to gravity. We refer the reader to subsection 2.4.1 for a detailed analysis of the background solution, and will only repeat the most important results here for convenience.

We model the ekpyrotic phase with a scalar field in a steep and negative potential,  $V(\phi) = -V_0 e^{-c\phi}$ , with action

$$S = \int d^4x \sqrt{-g} \left[ \frac{R}{2} - \frac{1}{2} g^{\mu\nu} \partial_\mu \phi \partial_\nu \phi - V(\phi) \right]. \quad (5.1)$$

In a flat FLRW universe, the equation of motion for the scalar field admits the (attractor) scaling solution (4.8), [83]

$$a(t) = a_0 \left( \frac{t}{t_0} \right)^{1/\epsilon}, \quad \phi = \sqrt{\frac{2}{\epsilon}} \ln \left( \frac{t}{t_0} \right), \quad \text{where } t_0 = -\sqrt{\frac{\epsilon-3}{V_0 \epsilon^2}} \quad \text{and } c = \sqrt{2\epsilon}. \quad (5.2)$$

The coordinate time  $t$  is negative and runs from large negative values to small negative values, and for a successful ekpyrotic phase we need  $\epsilon > 3$  ( $w > 1$ ).

In the following we perform a conformal transformation to the so-called Jordan frame, where the scalar field is now non-minimally coupled to gravity.

### 5.1.1 Jordan frame action

A general transformation to Jordan frame is obtained by redefining the metric using a positive field-dependent function  $F(\phi)$ , with

$$g_{\mu\nu} = F(\phi) g_{J\mu\nu}. \quad (5.3)$$

The corresponding action is given by

$$S_J = \int d^4x \sqrt{-g_J} \left[ F(\Phi) \frac{R_J}{2} - \frac{1}{2} k g_J^{\mu\nu} \partial_\mu \Phi \partial_\nu \Phi - V_J(\Phi) + \mathcal{L}_m(\psi, g_{J\mu\nu}) \right], \quad (5.4)$$

where we have included the possibility of the kinetic term being of the “wrong” sign by keeping the prefactor  $k$  unspecified for now. Note that we have added a matter Lagrangian to the model, where we assume that the matter couples to the Jordan frame metric, with the consequence that the Jordan frame metric may be regarded as the physical metric. The Jordan frame scalar field  $\Phi$  is defined via

$$\frac{d\Phi}{d\phi} = \sqrt{\frac{F}{k} \left( 1 - \frac{3}{2} \frac{F_{,\phi}^2}{F^2} \right)} \quad (5.5)$$

and the potential becomes

$$V_J(\Phi) = F(\phi)^2 V(\phi). \quad (5.6)$$

From the metric transformation (5.3), we can immediately deduce the transformation of the scale factor,

$$a = \sqrt{F} a_J. \quad (5.7)$$

The transformation of the 00-component of the metric is absorbed into the coordinate time interval,

$$dt = \sqrt{F} dt_J, \quad (5.8)$$

such that the line element transforms as  $ds^2 = F(\phi) ds_J^2$ . Moreover, by differentiating the scale factor w.r.t  $dt$ , we can determine the Hubble parameter

$$H \equiv \frac{a_{,t}}{a} = \frac{1}{\sqrt{F}} \left( H_J + \frac{F_{,tJ}}{2F} \right), \quad (5.9)$$

where the Hubble parameter in Jordan frame is given by  $H_J \equiv \frac{a_{J,tJ}}{a_J}$ .

### 5.1.2 A specific transformation

We will now specialise to the following ansatz

$$F(\phi) = \xi \Phi^2 = e^{c\gamma\phi}, \quad (5.10)$$

which is inspired by the dilaton coupling in string theory, see for example [154], and has been used for instance in [152, 153]. This type of non-minimal coupling is also

known as induced gravity [155]; see e.g. [156, 157, 158] for related studies. Plugging in the solution for  $\phi$  from (5.2), we can now integrate  $dt$  to find the relationship between the times in the two frames, yielding

$$\frac{t_J}{t_{J,0}} = \left( \frac{t}{t_0} \right)^{1-\gamma}, \quad (5.11)$$

where

$$t_{J,0} = \frac{t_0}{1-\gamma}. \quad (5.12)$$

Using this result, we can calculate the scale factor in the Jordan frame from (5.7)

$$a_J = a_0 \left( \frac{t}{t_0} \right)^{\frac{1-\epsilon\gamma}{\epsilon}} = a_0 \left( \frac{t_J}{t_{J,0}} \right)^{\frac{1-\epsilon\gamma}{\epsilon(1-\gamma)}}. \quad (5.13)$$

In order to obtain accelerated expansion, the  $t_J$ -exponent has to be larger than 1,

$$\frac{1-\epsilon\gamma}{\epsilon(1-\gamma)} > 1. \quad (5.14)$$

Moreover, an ekpyrotic phase in the Einstein frame has  $\epsilon > 3$ . From (5.14), we see that for  $\gamma < 1$  the denominator is positive and hence we would need  $\epsilon < 1$ , which cannot be satisfied for our case. We conclude that to realise a phase of accelerated expansion in Jordan frame (from an ekpyrotic phase in Einstein frame), we need

$$\boxed{\gamma > 1}. \quad (5.15)$$

Another constraint is obtained from the relationship between the fields, given by the transformation in (5.5) and the ansatz we have chosen for  $F$  in (5.10). Substituting the latter into the first and integrating, we get

$$\Phi = \frac{1}{\sqrt{\xi}} e^{\frac{c\gamma\phi}{2}}, \quad (5.16)$$

where the parameter  $\xi$  is now determined in terms of  $c = \sqrt{2\epsilon}$ ,  $\gamma$  and  $k$  and given by

$$\xi = \frac{c^2\gamma^2 k}{4 - 6c^2\gamma^2}, \quad (5.17)$$

or alternatively,

$$\epsilon = \frac{2\xi}{\gamma^2(6\xi + k)}. \quad (5.18)$$

The parameter  $\xi$  has to be positive for the gravity term in the Jordan frame action to be positive. A negative  $\xi$  would lead to tensor ghosts. Thus we need

$$\xi > 0 \iff k < 0 \quad (5.19)$$

since  $\gamma > 1$  and  $\epsilon > 3$ . Hence we see that we need the kinetic term for the scalar field to have the opposite of the usual sign, and we set

$$k = -1. \quad (5.20)$$

Note that this “wrong” sign does not lead to ghosts, as there are additional contributions from the scalar-tensor coupling to the fluctuations of  $\Phi$ , and these additional contributions render the total fluctuation positive (as we will show more explicitly in section 5.2). With the above choice of  $k$  we then also obtain a bound on the parameter  $\xi^1$ ,

$$\xi > \frac{1}{6}. \quad (5.21)$$

The Jordan frame potential can be reexpressed in terms of  $\Phi$  as

$$V_J(\Phi) = F^2(\phi)V(\phi) = -V_0 e^{(2\gamma-1)\phi} = -V_{J,0}\Phi^{4-2/\gamma}, \quad (5.22)$$

where we have defined  $V_{J,0} \equiv V_0\xi^{2-1/\gamma}$ . The negative exponential of the ekpyrotic phase is transformed into a *negative* power-law potential. We thus see that it is possible to obtain a phase of accelerated expansion in the presence of a negative potential in Jordan frame, starting from ekpyrosis in Einstein frame together with the conditions  $\gamma > 1$ ,  $k = -1$ , and  $\xi > 1/6$ . We will refer to this new phase of accelerated expansion as the conflationary phase.

### 5.1.3 Equations of motion in Jordan frame

Varying the action (5.4) w.r.t. the Jordan frame metric and scalar field, we obtain the Friedmann equations and the equation of motion for the scalar field  $\Phi$ :

$$3H_J^2 F + 3H_J F_{,t_J} = \frac{1}{2}k\Phi_{,t_J}^2 + V_J, \quad (5.23)$$

$$2FH_{J,t_J} + k\Phi_{,t_J}^2 - H_J F_{,t_J} + F_{,t_J t_J} = 0, \quad (5.24)$$

$$\Phi_{,t_J t_J} + 3H_J\Phi_{,t_J} - \frac{3F_{,\Phi}}{k}(H_{J,t_J} + 2H_J^2) + \frac{V_{J,\Phi}}{k} = 0. \quad (5.25)$$

---

<sup>1</sup>In the language of Brans-Dicke scalar-tensor gravity, this condition translates to  $\omega_{\text{BD}} > -3/2$ .

The first Friedmann equation (5.23) can be solved for the Hubble parameter,

$$H_J = -\frac{F_{,t_J}}{2F} \pm \sqrt{\frac{F_{,t_J}^2}{4F^2} + \frac{k}{6F}\Phi_{,t_J}^2 + \frac{1}{3F}V_J}. \quad (5.26)$$

$H_J$  will give two positive solutions as the square root is always less than  $-\frac{F_{,t_J}}{2F} > 0$ , since  $k, V_J < 0$ . To determine the solution that corresponds to contraction in Einstein frame, we note that the Hubble parameter in Einstein frame given in (5.9) has to be negative. Hence, we have to pick out the solution for  $H_J$  which satisfies

$$H_J < -\frac{F_{,t_J}}{2F}. \quad (5.27)$$

This is exactly the first term in front of the square root in the expression for  $H_J$  in (5.26). Hence, the square root has to be subtracted off the first term:

$$H_J = -\frac{F_{,t_J}}{2F} - \sqrt{\frac{F_{,t_J}^2}{4F^2} + \frac{k}{6F}\Phi_{,t_J}^2 + \frac{1}{3F}V_J}. \quad (5.28)$$

We can rewrite  $\Phi$  as a function of Jordan frame time,  $t_J$ , using Eqs. (5.2) and (5.11),

$$\Phi(t_J) = \frac{1}{\sqrt{\xi}} \left( \frac{t_J}{t_{J,0}} \right)^{\frac{\gamma}{1-\gamma}}. \quad (5.29)$$

We can then determine the quantity  $V_J/\Phi_{,t_J}^2$  using Eq. (5.22), obtaining

$$\frac{V_J}{\Phi_{,t_J}^2} = \frac{\epsilon - 3}{\epsilon(2 - 6\epsilon\gamma^2)}. \quad (5.30)$$

This combination is (non-trivially) time-independent, and hence once it is satisfied for the initial conditions of a particular solution it will hold at any time. This equation will be useful in setting the initial conditions for specific numerical examples, as will be done in the next section.

#### 5.1.4 Initial conditions and evolution with a shifted potential

In this subsection we verify that our construction does indeed lead to accelerated expansion in Jordan frame. We choose the parameters  $\epsilon = 10$  and  $\gamma = 2$ , leading to a negative  $\Phi^3$  potential in Jordan frame – see Fig. 5.1. For an initial field value of  $\Phi(t_{beg}) = 10$  and  $V_{J,0} = 10^{-10}$ , we require an initial field velocity (using Eqs. (5.22)

and (5.30)) of  $|\Phi_{,t_J}| \approx 5.83 \cdot 10^{-3}$ . Furthermore we set  $a_J(t_{beg}) = 1$ . Numerical solutions for the scale factor and scalar field are shown in Fig. 5.2, where the blue curves indeed reproduce the conflationary transform of the ekpyrotic scaling solution.

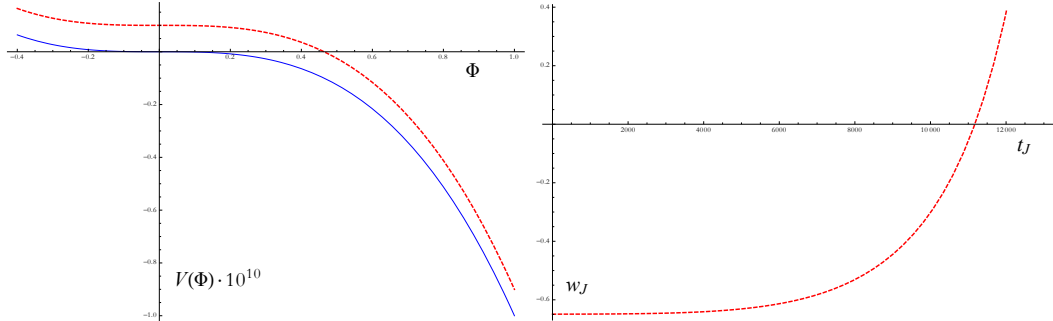


Figure 5.1: *Left:* The original Jordan frame potential  $V_J$  is shown in blue, the shifted potential  $U_J$  in dashed red. *Right:* The equation of state in Jordan frame, for the shifted potential.

Note that it follows from Eqs. (5.13) and (5.29) – similarly to inflationary models – that there is a spacetime singularity at  $t_J = 0$ ,  $a_J = 0$ ,  $\Phi = \infty$ , which should be resolved in a more complete theory. Either the effective description might break down at that time, or we might never reach such times in a more complete (cyclic) embedding of the theory. We leave such considerations for future work.

Eventually, the conflationary phase has to come to an end. As a first attempt at a graceful exit we shift the potential in Jordan frame by a small amount  $V_1$  (it will turn out that this simple modification is too naive and we will improve on it in the next subsection),

$$U_J(\Phi) = V_J(\Phi) + V_1. \quad (5.31)$$

The shifted potential, with  $V_1 = \frac{V_{J,0}}{10}$ , is plotted in Fig. 5.1. The corresponding evolution of the scalar field  $\Phi$  and the scale factor in Jordan frame are now shown as the red dashed curves in Fig. 5.2, while the equation of state is plotted in the right-hand panel of Fig. 5.1. The conflationary phase lasts until  $t_J \approx 10000$  when the equation of state grows larger than  $w_J = -1/3$ , and accelerated expansion ends. The scalar field continues on to about  $\Phi \approx 0.4$  and then rolls back down the potential. Meanwhile, the scale factor reaches a maximum value and starts re-contracting. This re-contraction in Jordan frame is unavoidable: from Eq. (5.28), bearing in mind that  $F_{,t_J} < 0$ , it becomes clear that whenever  $\rho_J = \frac{k}{2}\Phi_{,t_J}^2 + V_J = 0$  we have  $H_J = 0$  resulting in a re-contraction in Jordan frame. Given that we start out with both a negative kinetic term ( $k = -1$ ) and a negative potential, but then want to reach

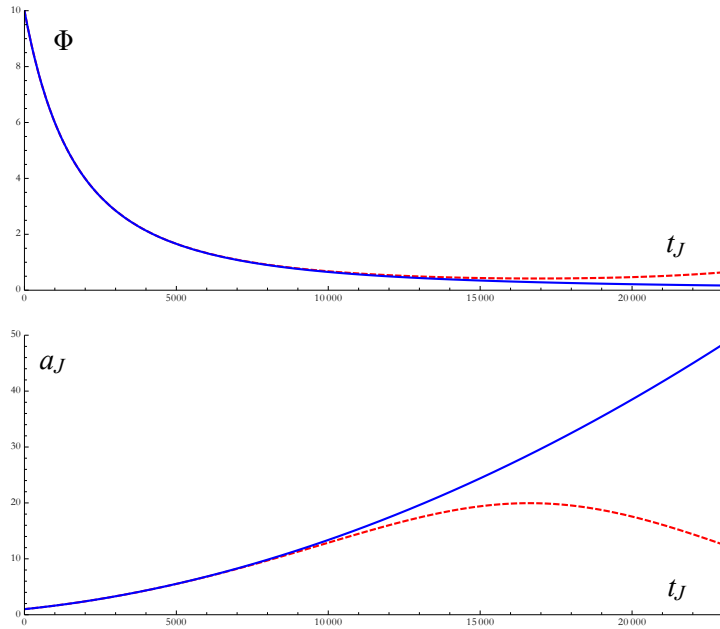


Figure 5.2: Scalar field and scale factor in Jordan frame: the blue curves show the transformed ekpyrotic scaling solution and the red dashed curves correspond to the field evolutions in the shifted potential.

positive potential values, means that we will necessarily pass through  $\rho_J = 0$  as the scalar field slows down. It is clear that a shift in the Jordan frame potential is not sufficient for a graceful exit – more elaborate dynamics are needed to avoid collapse. One might imagine that the scalar field could stabilise at a positive value of the potential. It could then either stay there and act as dark energy, or decay such that reheating would take place. Once the scalar field stabilises, the Einstein and Jordan frame descriptions become essentially equivalent<sup>2</sup>. However, this means that the scale factor will only revert to expansion if a bounce also occurs in Einstein frame. This motivates us to extend the present model by including dynamics that can cause a smooth bounce to occur after the ekpyrotic phase.

### 5.1.5 Transforming an Einstein frame bounce

In ekpyrotic models, after the ekpyrotic contracting phase has come to an end the universe must bounce into an expanding hot big bang phase. Many ideas for bounces have been put forward, see e.g. [99, 115, 159, 116, 117, 160, 112, 113] – here we will

---

<sup>2</sup>When the scalar field is constant, the two frames are equivalent. However, when the scalar field is perturbed, then fluctuations in the Jordan frame will still feel the direct coupling to gravity.

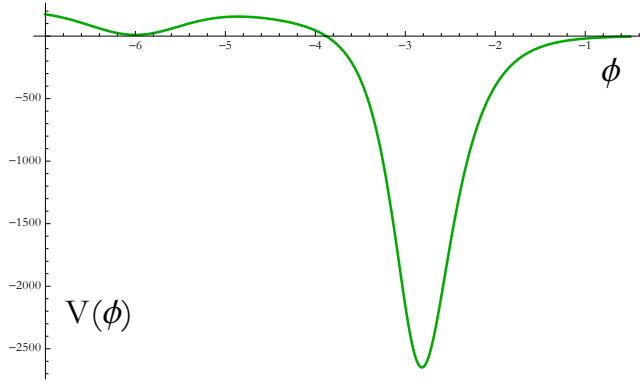


Figure 5.3: The Einstein frame scalar potential used in the bounce model (5.32).

focus on a non-singular bounce achieved via a ghost condensate [122, 139]. This model has the advantage of being technically fairly simple, and, importantly, it is part of a class of models for which it has been demonstrated that long-wavelength perturbations are conserved through the bounce [120, 121]. Moreover, it was shown in [103] (where the scale at which quantum corrections occur was calculated) that such models constitute healthy effective field theories. The action we will consider takes the form

$$S = \int d^4x \sqrt{-g} \left[ \frac{R}{2} + P(X, \phi) \right], \quad (5.32)$$

with

$$P(X, \phi) = K(\phi)X + Q(\phi)X^2 - V(\phi), \quad (5.33)$$

and where  $X \equiv -\frac{1}{2}g^{\mu\nu}\partial_\mu\phi\partial_\nu\phi$  denotes the ordinary kinetic term. The shape of the functions  $K(\phi)$  and  $Q(\phi)$  can be chosen in various ways. The important feature is that at a certain time (here at  $\phi = -4$ ) the higher derivative term is briefly turned on while the sign of the kinetic term changes. Moreover, we add a local minimum to the potential, as shown in Fig. 5.3: after the bounce the scalar field rolls into a dip in the potential where it stabilises and reheating can occur. For specificity we will use the functions [139]

$$K(\phi) = 1 - \frac{2}{\left(1 + \frac{1}{2}(\phi + 4)^2\right)^2}, \quad (5.34)$$

$$Q(\phi) = \frac{V_0}{\left(1 + \frac{1}{2}(\phi + 4)^2\right)^2}, \quad (5.35)$$

$$V(\phi) = -\frac{1}{e^{3\phi} + e^{-4(\phi+5)}} + 100 \left[ (1 - \tanh(\phi + 4)) \left(1 - 0.95e^{-2(\phi+6)^2}\right) \right] \quad (5.36)$$

where compared to [139] the theory has been rescaled via  $g_{\mu\nu} \rightarrow V_0^{1/2} g_{\mu\nu}$  which implies  $K \rightarrow K$ ,  $Q \rightarrow V_0 Q$  and  $V \rightarrow V_0^{-1} V$ . The equations of motion obtained by varying the action (5.32) read

$$\nabla_\mu (P_{,X} \nabla^\mu \phi) - P_{,\phi} = 0, \quad (5.37)$$

$$3H^2 = \rho, \quad (5.38)$$

$$\dot{H} = -\frac{1}{2}(\rho + p), \quad (5.39)$$

where the pressure and energy density are given by  $p = P$  and  $\rho = 2XP_{,X} - P$ . Note that  $\dot{H} = -XP_{,X}$ , which shows that the Hubble rate can increase (as is necessary for a bounce) when the ordinary kinetic term switches sign. The purpose of the  $X^2$  term in the action is twofold: it allows the coefficient of the ordinary kinetic term to pass through zero, and it contributes to the fluctuations around the bounce solution in such a way as to avoid ghosts. The Einstein frame bounce solution is shown in Fig. 5.4, where we have chosen the initial conditions  $\phi_0 = 0$ ,  $\dot{\phi}_0 = -2.4555$ ,  $a_0 = 100$  and have set  $V_0 = 10^{-6}$  and  $c = 3$ . The scalar field first rolls down the potential during the ekpyrotic phase. A bounce then occurs near  $\phi = -4$  due to the sign change of the kinetic term. After this, the universe starts expanding, the potential becomes positive and the scalar field rolls into the dip where it oscillates with decaying amplitude – see Fig. 5.4.

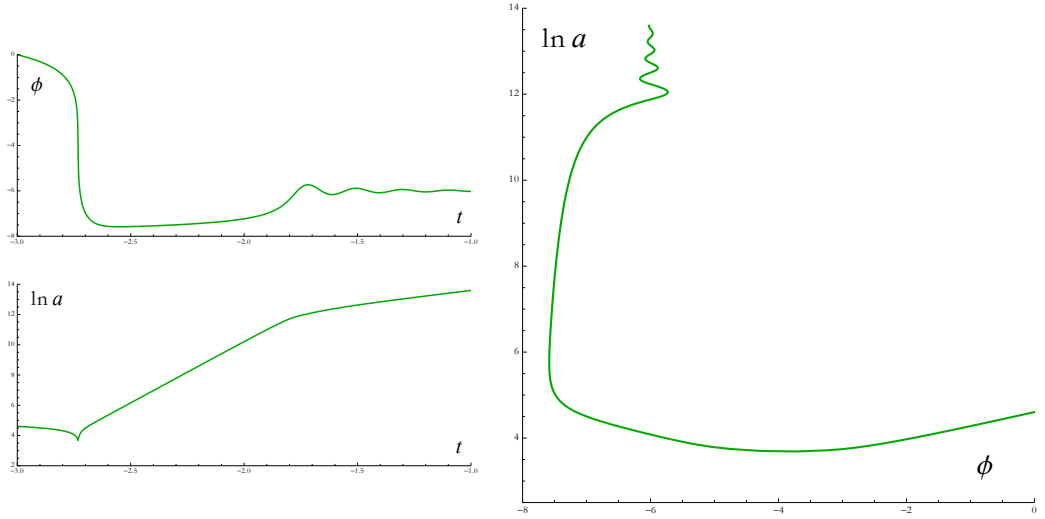


Figure 5.4: *Left:* Scalar field and scale factor for the bounce solution in Einstein frame. *Right:* Parametric plot of the scalar field and scale factor in Einstein frame. This plot nicely illustrates the smoothness of the bounce.

In the following we want to transform this bouncing solution into Jordan frame, in order to see how such a bounce translates into a graceful exit for the conflationary phase. The Ricci scalar transforms under our conformal transformation (5.3) as [130]

$$R = \frac{1}{F} \left( R_J - 6\Box_J \ln \sqrt{F} - 6g_J^{\mu\nu} \partial_\mu \left( \ln \sqrt{F} \right) \partial_\nu \left( \ln \sqrt{F} \right) \right), \quad (5.40)$$

where the second term contributes as a total derivative in the action. Note that the kinetic term transforms as

$$X \equiv -\frac{1}{2}g^{\mu\nu} \partial_\mu \phi \partial_\nu \phi = -\frac{1}{2F}g_J^{\mu\nu} \partial_\mu \phi \partial_\nu \phi = -\frac{1}{2F} \left( \frac{\partial \phi}{\partial \Phi} \right)^2 g_J^{\mu\nu} \partial_\mu \Phi \partial_\nu \Phi \equiv \frac{1}{F} \left( \frac{\partial \phi}{\partial \Phi} \right)^2 X_J. \quad (5.41)$$

Plugging everything into Eq. (5.32) yields the action in Jordan frame

$$S_J = \int d^4x \sqrt{-g_J} \left[ F(\Phi) \frac{R_J}{2} + P_J(X_J, \Phi) \right], \quad (5.42)$$

where we have defined the new functions in Jordan frame as

$$P_J \equiv K_J X_J + Q_J X_J^2 - V_J, \quad (5.43)$$

$$K_J \equiv F \left( K - \frac{3}{2} \frac{F_{,\phi}^2}{F^2} \right) \left( \frac{\partial \phi}{\partial \Phi} \right)^2 = 4\xi \left( \frac{K}{c^2 \gamma^2} - \frac{3}{2} \right), \quad (5.44)$$

$$Q_J \equiv Q \left( \frac{\partial \phi}{\partial \Phi} \right)^4 = \frac{16}{c^4 \gamma^4 \Phi^4} Q, \quad (5.45)$$

$$V_J \equiv F^2 V = \xi^2 \Phi^2 V, \quad (5.46)$$

and we have used

$$\frac{\partial \phi}{\partial \Phi} = \frac{2}{c \gamma \Phi} \quad \text{and} \quad F(\Phi) = \xi \Phi^2. \quad (5.47)$$

Thus the equations of motions in Jordan frame are given by

$$\nabla_\mu (P_{J,X} \nabla^\mu \Phi) = P_{J,\Phi} + \frac{1}{2} R_J F_{,\Phi}, \quad (5.48)$$

$$3F H_J^2 + 3H_J F_{,t_J} = \rho_J, \quad (5.49)$$

$$\rho_J + p_J + 2F H_{J,t_J} - H_J F_{,t_J} + F_{,t_J t_J} = 0, \quad (5.50)$$

with the effective energy density  $\rho_J = 2X_J P_{J,X} - P_J$  and effective pressure  $p_J = P_J$ .

The conflationary solution is shown in Fig. 5.5. The scalar field  $\Phi$  rolls up the approximately  $-\Phi^3$  potential with decreasing velocity. It starts out at  $\Phi_0 = 2.4267$

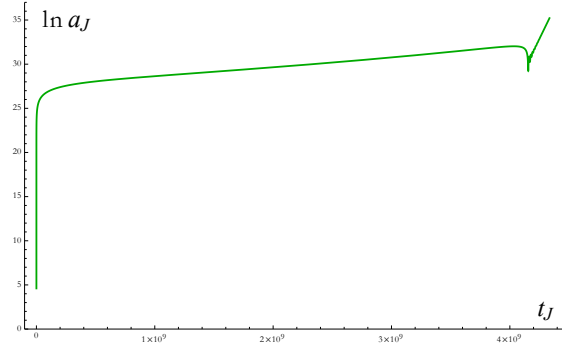


Figure 5.5: Full evolution of the scale factor for the transformed solution in Jordan frame. The conflationary phase lasts while the scalar field rolls up the potential towards  $\Phi \sim 10^{-9}$ . During this period the scale factor increases by many orders of magnitude. During the exit of the conflationary phase the scale factor and scalar field undergo non-trivial evolution which is hard to see in the present figure and is shown in detail in Fig. 5.6

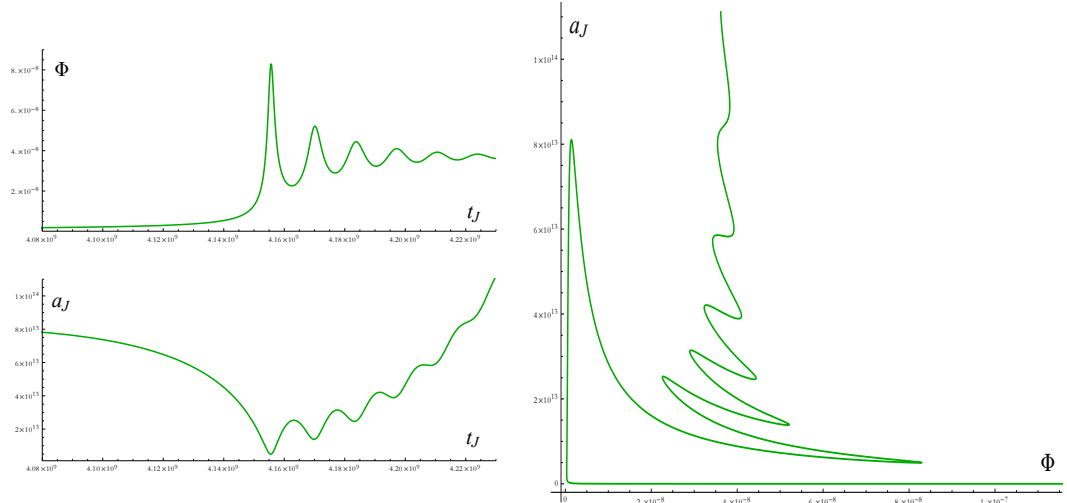


Figure 5.6: *Left:* Scalar field and scale factor for the transformed solution in Jordan frame towards the end of the evolution. *Right:* Parametric plot of the scalar field and scale factor in Jordan frame. Note that initially the scalar field decreases in value very rapidly. Later on, as the scalar field stabilises, the scale factor goes through oscillations, but eventually increases monotonically.

and very quickly decreases to a field value  $\Phi \sim 10^{-9}$  where it stays for a long time. By this time, the bounce in Einstein frame has already taken place, but interestingly it leads to nothing dramatic in Jordan frame: the universe simply keeps expanding and the scalar field keeps decreasing. The more interesting dynamics in Jordan frame occur later, see Fig. 5.6. As we have already discussed, the universe re-contracts for  $\rho_J = 0$ . The potential energy increases to positive values (in this model accelerated expansion ends as the potential becomes positive!) and the kinetic term decreases leading to a re-contraction at  $t_J \approx 4.05 \cdot 10^9$ . The re-contraction  $H_J < 0$  leads to an increased scalar field velocity, allowing the scalar field to roll over the potential barrier and into the dip, where it starts oscillating around the minimum, eventually settling at the bottom. The Hubble rate  $H_J$  changes sign each time the energy density passes through zero, so that the scale factor oscillates together with the scalar field. Once the scalar field is settled, continuous expansion occurs. Note that these oscillations of the scale factor do not correspond to a violation of the null energy condition – they are simply due to the coupling between the scalar field and gravity in Jordan frame. It would be interesting to see whether reheating might speed up the settling down of the scalar field – we leave such an analysis for future work.

## 5.2 Perturbations

It is known that under a conformal transformation of the metric perturbations are unaffected. Thus we know what kind of cosmological perturbations our model leads to: during the ekpyrotic phase, both adiabatic scalar fluctuations and tensor perturbations have a blue spectrum and are not amplified. However, with the inclusion of a second scalar field, nearly scale-invariant entropy perturbations can be generated first, which can then be converted into adiabatic scalar curvature fluctuations at the end of the ekpyrotic phase. Translated into the inflationary framework of the Jordan frame, these results are nevertheless surprising: they imply that we have a phase of accelerated expansion during which adiabatic perturbations as well as tensor fluctuations have a spectrum very far from scale-invariance, and moreover they are not amplified. It is thus instructive to calculate these perturbations explicitly in this frame, which is what we will do next. In the following subsection, we will also describe the entropic mechanism from the point of view of the Jordan frame. Throughout this section, we will use the notation that a prime denotes a derivative w.r.t. conformal time  $\tau$ , which is equal in both frames as  $dt/a = dt_J/a_J$ .

### 5.2.1 Perturbations for a single field

As was calculated for instance in [152], the quadratic action for the comoving curvature perturbation  $\zeta_J$  in Jordan frame is given by

$$S_J^{(2)} = \frac{1}{2} \int d^4x \frac{a_J^2 \Phi'^2}{(\mathcal{H}_J + \frac{\Phi'}{\Phi})^2} (6\xi - 1) \left( \zeta_J'^2 - (\partial_i \zeta_J)^2 \right), \quad (5.51)$$

where we have assumed  $F(\Phi) = \xi \Phi^2$ . The absence of ghost fluctuations can thus be seen to translate into the requirement

$$\xi > \frac{1}{6}, \quad (5.52)$$

which is the same condition on  $\xi$  that we discovered before in Eq. (5.21). We can define

$$z_J^2 = \frac{a_J^2 \Phi'^2}{(\mathcal{H}_J + \frac{\Phi'}{\Phi})^2} (6\xi - 1), \quad (5.53)$$

so that for the canonically normalised Mukhanov-Sasaki variable  $v_J = z_J \zeta_J$  we obtain the mode equation in standard form, namely

$$v_{Jk}'' + \left( k^2 - \frac{z_J''}{z_J} \right) v_{Jk} = 0. \quad (5.54)$$

Note however that  $z_J$  does *not* have the usual form  $\sim a_J \Phi' / \mathcal{H}_J$ , but has an extra contribution from the scalar field in the denominator. This contribution is crucial, as it implies that the usual intuition gained from studying inflationary models in Einstein frame is not applicable here. For the conflationary transform of the ekpyrotic scaling solution we have

$$a_J(t_J) = a_0 \left( \frac{t_J}{t_{J,0}} \right)^{\frac{1-\epsilon\gamma}{\epsilon(1-\gamma)}}, \quad \Phi(t_J) = \frac{1}{\sqrt{\xi}} \left( \frac{t_J}{t_{J,0}} \right)^{\frac{\gamma}{1-\gamma}}, \quad (5.55)$$

while the relationship between physical time and conformal time is given by

$$t_J \sim (-\tau)^{\frac{\epsilon(1-\gamma)}{\epsilon-1}}. \quad (5.56)$$

These relations imply that  $z_J(\tau) \sim (-\tau)^{1/(\epsilon-1)}$ , which leads to

$$\frac{z_J''}{z_J} = \frac{2-\epsilon}{(\epsilon-1)^2} \frac{1}{\tau^2}. \quad (5.57)$$

Imposing Bunch-Davies boundary conditions in the far past selects the solution (given here up to a phase)

$$v_{Jk} = \sqrt{-\frac{\pi}{4}\tau} H_{\nu}^{(1)}(-k\tau), \quad (5.58)$$

where  $H_{\nu}^{(1)}$  is a Hankel function of the first kind with index  $\nu = \frac{1}{2} - \frac{1}{\epsilon-1}$ . This leads to a scalar spectral index

$$n_{\zeta} - 1 \equiv 3 - 2\nu = 3 - \left| \frac{\epsilon - 3}{\epsilon - 1} \right|, \quad (5.59)$$

where  $\epsilon$  corresponds to the Einstein frame slow-roll/fast-roll parameter. Here  $\epsilon > 3$  and thus the (blue) spectrum is always between  $3 < n_{\zeta} < 4$ , i.e. the spectrum is identical to that of the adiabatic perturbation during an ekpyrotic phase, as expected [108].

The calculation of the (transverse, traceless) tensor perturbations  $\gamma_{Jij}$  proceeds in an analogous fashion. Their quadratic action is given by

$$S_J = -\frac{1}{8} \int d^4x F(\Phi) \sqrt{g_J} g_J^{\mu\nu} \partial_{\mu} \gamma_{Jij} \partial_{\nu} \gamma_{Jij}. \quad (5.60)$$

Writing the canonically normalised perturbations as  $h \epsilon_{ij} \equiv z_T \gamma_{Jij}$ , where  $\epsilon_{ij}$  is a polarisation tensor and  $z_T^2 = F(\Phi) a_J^2$ , the mode equation in Fourier space again takes the usual form

$$h_k'' + \left( k^2 - \frac{z_T''}{z_T} \right) h_k = 0, \quad (5.61)$$

except that here  $z_T$  is not just given by the scale factor but involves the scalar field too. In fact  $z_T \propto \Phi a_J \propto (-\tau)^{1/(\epsilon-1)}$  and thus  $z_T \propto z_J$ . The spectral index comes out as

$$n_T \equiv 3 - \left| \frac{\epsilon - 3}{\epsilon - 1} \right|, \quad (5.62)$$

which is the same blue spectrum as that obtained during an ekpyrotic phase, as expected.

These simple calculations have an important consequence. In the limit where  $|k\tau| \ll 1$ , which corresponds to the late-time/large-scale limit, the adiabatic scalar and tensor mode functions behave as [144, 88]

$$v_{Jk}, h_k \propto \frac{\pi}{2^{2\nu} \Gamma(\nu) \Gamma(\nu + 1)} (-k\tau)^{1 - \frac{1}{\epsilon-1}} - i(-k\tau)^{\frac{1}{\epsilon-1}}. \quad (5.63)$$

Given that  $\epsilon > 3$ , this implies that as  $(-k\tau) \rightarrow 0$  neither the scalar nor the tensor perturbations are amplified. In other words, the perturbations remain quantum and do not become squeezed in contrast with standard models of inflation where  $\epsilon < 1$  and the second term on the right hand side in Eq. (5.63) is massively amplified. Thus we have found an example of a model in which the spacetime is rendered smooth via accelerated expansion, but without the amplification of perturbations and thus also without the possibility for the run-away behaviour of eternal inflation. Note that eternal inflation happens because rare, but large quantum fluctuations change the background evolution by prolonging the smoothing phase in certain regions, with these regions becoming dominant due to the high expansion rate. In the absence of these amplified quantum fluctuations, the background evolution will be essentially unaffected and will proceed as in the purely classical theory. This property certainly deserves further consideration in the future.

### 5.2.2 Non-minimal entropic mechanism in Jordan frame

In order to obtain a nearly scale-invariant spectrum for the scalar perturbations, a second field has to be introduced. There are two possibilities that have been studied extensively in the ekpyrotic literature and which have been discussed in this thesis: either one introduces an unstable direction in the potential (see subsection 2.4.2) [87, 148, 28, 89], or one allows for a non-minimal kinetic coupling between the two scalars (as introduced in chapter 4) [22, 21, 24, 23, 161]. In both cases nearly scale-invariant entropy perturbations can be generated during the ekpyrotic phase, and these can then be converted to adiabatic curvature perturbations subsequently. Here we will discuss the case of non-minimal coupling, and show that it carries over into the context of conflation.

In Einstein frame, one starts with an action of the form [22, 21]

$$S = \int d^4x \sqrt{-g} \left[ \frac{1}{2}R - \frac{1}{2}g^{\mu\nu}\partial_\mu\phi\partial_\nu\phi - \frac{1}{2}g^{\mu\nu}e^{-b\phi}\partial_\mu\chi\partial_\nu\chi + V_0e^{-c\phi} \right]. \quad (5.64)$$

In the ekpyrotic background, the second scalar  $\chi$  is constant. One can then see from the scaling solution (5.2) that when  $b = c$  the non-minimal coupling mimics an exact de Sitter background  $e^{-b\phi} \propto 1/t^2$  for the fluctuations  $\delta\chi$  (which correspond to gauge-invariant entropy perturbations), which are then amplified and acquire a scale-invariant spectrum. When  $b$  and  $c$  differ slightly, a small tilt of the spectrum can be generated.

Transforming the action (5.64) to Jordan frame, we obtain

$$S_J = \int d^4x \sqrt{-g_J} \left[ \xi \Phi^2 \frac{R_J}{2} + \frac{1}{2} g_J^{\mu\nu} \partial_\mu \Phi \partial_\nu \Phi - \frac{1}{2} g_J^{\mu\nu} \xi^{\frac{\gamma c - b}{\gamma c}} \Phi^{\frac{2\gamma c - 2b}{\gamma c}} \partial_\mu \chi \partial_\nu \chi + V_{J,0} \Phi^{4 - \frac{2}{\gamma}} \right]. \quad (5.65)$$

The background equations of motion read

$$\square \Phi + \frac{\gamma c - b}{\gamma c} \xi^{\frac{\gamma c - b}{\gamma c}} \Phi^{\frac{\gamma c - 2b}{\gamma c}} g_J^{\mu\nu} \partial_\mu \chi \partial_\nu \chi - \frac{1}{2} F(\Phi)_{,\Phi} R_J + V(\phi)_{J,\Phi} = 0, \quad (5.66)$$

$$\square \chi - \frac{2\gamma c - 2b}{\gamma c} \frac{\Phi'}{\Phi} \chi' - 2a_J^2 \xi^{\frac{b - \gamma c}{\gamma c}} \Phi^{\frac{2b - 2\gamma c}{\gamma c}} V(\Phi)_{J,\chi} = 0. \quad (5.67)$$

Since the potential is again independent of  $\chi$ , we still have the background solution  $\chi = \text{constant}$ . To first order, the equation of motion for the (gauge-invariant) entropy perturbation  $\delta\chi$  is given by

$$\delta\chi'' + \left( 2 \frac{a_J'}{a_J} + n \frac{\Phi'}{\Phi} \right) \delta\chi' + k^2 \delta\chi = 0, \quad (5.68)$$

with  $n = \frac{2\gamma c - 2b}{\gamma c}$ . We introduce the canonically normalised variable  $v_{Js}$ ,

$$v_{Js} = a_J \Phi^{\frac{n}{2}} \delta\chi, \quad (5.69)$$

whose Fourier modes (dropping the subscript  $k$ ) satisfy the mode equation

$$v_{Js}'' + \left[ k^2 + \frac{n}{2} \frac{\Phi'^2}{\Phi^2} - \frac{n^2}{4} \frac{\Phi'^2}{\Phi^2} + \frac{a_J''}{a_J} (3n\xi - 1) - a_J^2 \frac{n}{2} \frac{V_{J,\Phi}}{\Phi} \right] v_{Js} = 0. \quad (5.70)$$

Here we have made use of the background equation for  $\Phi$ . Plugging in our inflationary background, and using the notation  $\Delta = \frac{b}{c} - 1$  so that  $n = 2\frac{\gamma - \Delta - 1}{\gamma}$ , we obtain

$$v_{Js}'' + \left( k^2 - \frac{1}{(\epsilon - 1)^2 \tau^2} [2 - (4 + 3\Delta)\epsilon + (2 + 3\Delta + \Delta^2)\epsilon^2] \right) v_{Js} = 0 \quad (5.71)$$

This equation can be solved as usual by  $\sqrt{-\tau}$  multiplied by a Hankel function of the first kind with index

$$\nu = \frac{3}{2} + \frac{\Delta\epsilon}{\epsilon - 1}, \quad (5.72)$$

which translates into a spectral index

$$n_s - 1 = 3 - 2\nu = -2\Delta \frac{\epsilon}{(\epsilon - 1)}. \quad (5.73)$$

The spectrum is independent of  $\gamma$ , and in fact it coincides precisely with the spectral index obtained in Einstein frame (4.22). Thus, even for this two-field extension, the predictions for perturbations are unchanged by the field redefinition from Einstein to Jordan frame. As discussed in the previous chapter, for models of this type there is no need for an unstable potential, as considered in earlier ekpyrotic models. Also, given that the action does not contain terms in  $\chi$  of order higher than quadratic, the ekpyrotic phase does not produce non-Gaussianities. However, the subsequent process of converting the entropy fluctuations into curvature fluctuations (which we assume to occur via a turn in the scalar field trajectory after the end of the inflationary phase) induces a small contribution  $|f_{NL}^{local}| \lesssim 5$ , and potentially observable negative  $|g_{NL}^{local}| \approx \mathcal{O}(10^2) - \mathcal{O}(10^3)$ , as long as the non-minimal field space metric progressively returns to trivial, in agreement with observational bounds (see (6.1)) [9, 10]. It would be interesting to study this and perhaps new conversion mechanisms in more detail from the point of view of the Jordan frame.

# Chapter 6

## Conclusions

In this thesis, we have studied two alternatives to the theory of inflation: non-minimal ekpyrosis and conflation. The standard  $\Lambda$ CDM model of cosmology describes the universe extremely well, starting from a time shortly after the big bang, when the universe consisted of a hot and dense quark-gluon plasma, to the present day. Yet, it cannot dynamically explain the initial conditions emerging from the big bang. The early universe revealed by the precise data from the PLANCK satellite is surprisingly simple: at the background level the universe is approximately flat, homogeneous and isotropic, supplemented with small nearly scale-invariant and Gaussian density perturbations. Extrapolating backwards in time, the background properties imply that the big bang cannot have simply occurred at a single point, but several causally disconnected regions must have started out with the same initial conditions independently. Moreover, their spatial flatness must have been very close to zero to lead to the nearly flat universe we observe today. The goal of any theory of the early universe should be to explain these special initial conditions dynamically.

In section 2.3 we introduced the theory of inflation describing a phase of accelerated expansion, which can solve the horizon and flatness problem by smoothing out inhomogeneities, anisotropies and the curvature of space. Furthermore, by stretching quantum perturbations they become squeezed into a stochastic distribution of classical density perturbations as they exit the horizon. In this way, inflation provides a paradigm for the generation of primordial density fluctuations seeding the structure of our universe. A range of different inflationary models has been constructed, some of which fit the observational data well, whereas other models that were theoretically favoured have had to be, or are on the verge of being, abandoned. The plateau-like single-field inflationary models, that seem to be the best fit to the data, come at

the price of several conceptual challenges. Two of the most important ones are the issue of initial conditions and the measure problem arising from the eternal nature of these inflationary models.

The non-minimal entropic mechanism that we discussed in chapter 4 is technically more involved than these single-field plateau models of inflation, as it requires two scalar fields, with a specific coupling between the scalars. Moreover, it becomes necessary to include a description of a bounce phase that links the ekpyrotic phase to the currently expanding phase of our universe. Due to the non-trivial nature of the field space metric, we have adopted the covariant formalism to derive exact evolution equations for non-linear perturbations in chapter 3. We then expanded the equations of motion for the entropy fluctuation (3.62) and the comoving curvature perturbation (3.63) up to third order in perturbation theory, from which the non-linearity parameters for the observed density perturbations can be deduced. In these ekpyrotic models, the primordial curvature perturbations are generated via the non-minimal entropic mechanism in a two-stage process: nearly scale-invariant entropy perturbations are first generated due to the non-minimal kinetic coupling between two scalar fields. Subsequently, these perturbations are converted into curvature perturbations by a bending in the field space trajectory. Solving the equations of motion analytically during the ekpyrotic phase we find vanishing bi- and trispectra for the entropy perturbations. However, this property is significantly modified during the conversion process to curvature perturbations. We find that the efficiency of the conversion process is crucial: inefficient conversions would lead to curvature perturbations with a small amplitude and very large and wildly varying non-Gaussianities. On the other hand, for efficient conversions the results converge and lead to the following predictions (which we compare to the current observational bounds [10]):

Non-minimal entropic mechanism	Observational bounds
$ f_{NL}^{\text{local}}  \lesssim 5$	$f_{NL}^{\text{local}} = 0.8 \pm 5.0 \quad (1\sigma)$ (6.1)
$g_{NL}^{\text{local}} \sim \mathcal{O}(-10^2)$ or $\mathcal{O}(-10^3)$	$g_{NL}^{\text{local}} = (9.0 \pm 7.7) \times 10^4 \quad (1\sigma)$ (6.2)
$\alpha_s \sim \mathcal{O}(-10^{-3})$	$\alpha_s = 0.003 \pm 0.007 \quad (1\sigma)$ (6.3)

Here, for completeness, we have added the prediction for the running of the spectral index  $\alpha_s \equiv \frac{dn_s}{d \ln k}$  that is expected in these models [162]. Note the highly interesting prediction that all three observables should actually be observable in the near future. Also, an important feature is that  $f_{NL}$  may be small, but  $g_{NL}$  is typically not

simultaneously close to zero as well, and in fact there is a clear correlation between all observables, as both the running and the trispectrum parameter are expected to be negative and significant. As in all currently known ekpyrotic models, no large-amplitude primordial gravitational waves are produced [109, 110]. Detecting these would in fact be the best way to falsify the model. Thus the present model has the potential to be refuted or supported by observations with significant levels of confidence. Moreover, one of the main benefits compared to single-field slow-roll models of inflation is that the measure problem is essentially absent, since the smoothing phase proceeds almost entirely at a very small Hubble rate [163, 164].

Contrasting with the standard entropic mechanism, in which the entropy perturbations are produced due to an instability in the potential instead of a non-trivial field space metric, we note that:

- The initial conditions problem is markedly improved in the non-minimal ekpyrotic model, since the potential is stable everywhere.
- Nearly scale-invariant curvature perturbations with the observed amplitude and spectral index can naturally be produced. Moreover, the spectrum does not depend on the value of the equation of state parameter  $\epsilon$  – thus even low values  $\epsilon \gtrsim 3$  are allowed. (This is the equivalent to having an inflationary model where  $\epsilon$  can be almost 1.)
- The entropy perturbations generated during the ekpyrotic phase have an exactly vanishing bi- and trispectrum.

In this thesis we have focused on the production of perturbations during the ekpyrotic phase. Moreover, a subsequent conversion phase is necessary in order to obtain density perturbations matching those observed in the CMB. The main questions for future research concern the embedding of these phases into a more complete, potentially cyclic model.

It would be interesting to investigate how the conversion process may best fit together with the bounce dynamics. In particular, considering the issue of model building, we learned that the kinetic coupling between the two scalar fields has to return to the trivial case after the ekpyrotic phase, in much the same way as the potential has to turn off. One may wonder whether such a feature could arise in a plausible manner from the point of view of a more fundamental theory. A more complete answer to this question will of course have to await further developments

in fundamental physics, and especially in quantum gravity, but we would like to exhibit one example where such a feature is indeed seen. This comes from considering supergravity coupled to scalar fields with higher-derivative kinetic terms [165, 166]. In this class of models, the higher-derivative terms add corrections to both the ordinary kinetic terms and the potential of the theory, even when the higher-derivative terms are not significant dynamically. More precisely, in these theories the dominant contribution is of the form

$$(\partial A)^2(\partial A^*)^2 - 2e^{K/3}FF^* \partial A \cdot \partial A^* + e^{2K/3}(FF^*)^2, \quad (6.4)$$

where  $A$  is a complex scalar field (or may be thought of as two real scalars, just as in ekpyrotic theories), while  $F$  is a complex auxiliary field and  $K$  is the Kähler potential, which is just a function of  $A$  and  $A^*$ . The value of the auxiliary field depends on the superpotential – crucially,  $F$  is small when the superpotential is small. Now keeping in mind that the expression above is a correction term to the usual kinetic terms, we see that when the superpotential becomes unimportant, the potential in the theory turns off but so does the correction to the kinetic term  $FF^* \partial A \cdot \partial A^*$ . This is exactly what would be required for the conversion process in the class of models we have analysed in the present work. It would certainly be interesting to see whether a more complete embedding in supergravity could be realised.

Moreover, the efficiency of the conversion process is crucial. On the one hand, as the conversions become smoother, the predicted range of values for the non-linearity parameters narrows considerably, which allows us to make rather definite predictions. On the other hand, the question remains whether the effective conversion potential can be shown to lead to an efficient conversion process due to some more fundamental physical principle.

In the phoenix universe, the unstable potential produces entropy perturbations transverse to the background trajectory. When the fluctuations become too large, the field is kicked off the sides of the potential, implying that large portions of the universe are converted into inhomogeneous remnants and black holes, which are not able to pass through the cycles. In this way, regions of the universe are selected that follow the classical trajectory for long enough to pass through the bounce. Most importantly, the amplitude of primordial density fluctuations for these regions must satisfy  $Q_\zeta \lesssim 10^{-4.5}$  [167]. However appealing this result might be, the model produces large amounts of non-Gaussianities that stem from the entropic mechanism. In the non-minimal version, the resulting bispectrum for an efficient conversion is

much closer to the observed bound. Due to the stable ekpyrotic potential, naively, a phoenix type universe seems impossible. It would be interesting to investigate how a non-minimal ekpyrotic phase could be embedded into a full cyclic theory. One could also study a more general setting, in which an unstable potential is combined with a non-trivial field space metric.

In chapter 5 we have introduced the idea of conflation, which corresponds to a phase of accelerated expansion in a scalar-tensor theory of gravity. This new type of cosmology is closely related to anamorphic cosmology [149], in that it also combines elements from inflation and ekpyrosis – in fact, our model may be seen as being complementary to anamorphic models. In the conflationary model, the universe is rendered smooth by a phase of accelerated expansion, like in inflation. However, the potential is negative, and adiabatic scalar and tensor fluctuations are not amplified, just as for ekpyrosis.

Several features deserve more discussion and further study in the future: the first is that, as just mentioned, the conflationary phase described here does not amplify adiabatic fluctuations and consequently does not lead to eternal inflation and a multiverse. This remains true in the presence of a second scalar field, which generates cosmological perturbations via an entropic mechanism, since the entropy perturbations that are generated have no impact on the background dynamics. In other words, even a large entropy perturbation is harmless, as it does not cause the conflationary phase to last longer, or proceed at a higher Hubble rate, in that region. This provides a new way of avoiding a multiverse and the associated problems with predictivity, and may be viewed as the most important insight of chapter 5. The second point is that it would be interesting to study the question of initial conditions required for this type of cosmological model, and contrast it with the requirements for standard, positive potential, inflationary models. A third avenue for further study would be to see how cyclic models in Einstein frame are transformed. Finally, it will be very interesting to see if a conflationary model can arise in supergravity or string theory, with for instance the dilaton playing the role of the scalar field being coupled non-minimally to gravity. Being able to use negative potentials while obtaining a background with accelerated expansion opens up new possibilities not considered so far in early universe cosmology.

As discussed in the introduction, the surface of last scattering prohibits direct access to the very early universe. On the other hand, the precisely measured properties and statistics of the tiny fluctuations imprinted on the CMB put remarkably

tight constraints on early universe model-building. This thesis represents important steps in understanding the early universe and in particular alternatives to inflation, making use of this information. In the near future, it might become possible to detect primordial gravitational waves via a B-mode polarisation signal in the CMB. The detection (or absence) of primordial gravitational waves will help in discriminating between different early universe theories. In this light, it remains as important as ever to understand the predictions of cosmological models of the early universe.

## Appendix A

# A new definition of the entropy perturbation $\delta s^{(3)}$

In this appendix, we show how we are led to defining  $\delta s^{(3)}$  as given in Eq. (3.55) in chapter 3. Expanding the equation of motion for  $s_a$  (3.28) to third order without the extra term, i.e. with  $\delta s^{(3)}|_{\text{old}} = \delta s^{(3)} - \frac{1}{6\bar{\sigma}^2} \delta s \delta s'^2$ , we obtain

$$\begin{aligned}
0 \approx & \delta s^{(3)}|_{\text{old}}'' + 3H\delta s^{(3)}|_{\text{old}}' + (\bar{V}_{;ss} + 3\bar{\theta}'^2 + \bar{\sigma}'^2 \bar{e}_s^I \bar{e}_s^J \bar{e}_\sigma^K \bar{e}_\sigma^L \bar{R}_{IKJL}) \delta s^{(3)}|_{\text{old}} + 2\frac{\bar{\theta}'}{\bar{\sigma}'} \delta s' \delta s^{(2)'} \\
& + \left( \frac{2}{\bar{\sigma}'} \bar{\theta}'' + \frac{2}{\bar{\sigma}'^2} \bar{V}_{;\sigma} \bar{\theta}' - \frac{3}{\bar{\sigma}'} H \bar{\theta}' \right) \left( \delta s \delta s^{(2)} \right)' \\
& + \left( \bar{V}_{;sss} - \frac{10}{\bar{\sigma}'} \bar{V}_{;ss} \bar{\theta}' - \frac{18}{\bar{\sigma}'} \bar{\theta}'^3 + \bar{e}_s^I \bar{e}_s^J \bar{e}_\sigma^K \bar{e}_\sigma^L (-2\bar{\sigma}' \bar{\theta}' \bar{R}_{IKJL} + \bar{\sigma}'^2 \bar{e}_s^N \mathcal{D}_N \bar{R}_{IKJL}) \right) \delta s \delta s^{(2)} \\
& + \frac{\bar{V}_{;\sigma}}{\bar{\sigma}'^3} \delta s'^3 + \frac{1}{\bar{\sigma}'^2} \left[ \bar{V}_{;\sigma\sigma} + \frac{3\bar{V}_{;\sigma}^2}{\bar{\sigma}'^2} + \frac{3}{\bar{\sigma}'} H \bar{V}_{;\sigma} - 2\bar{V}_{;ss} - 6\bar{\theta}'^2 - \bar{e}_s^I \bar{e}_s^J \bar{e}_\sigma^K \bar{e}_\sigma^L \bar{R}_{IKJL} \right] \delta s \delta s'^2 \\
& + \left[ -\frac{10}{\bar{\sigma}'} \bar{\theta}' \bar{\theta}'' - \frac{3}{2\bar{\sigma}'} \bar{V}_{;ss\sigma} - \frac{5}{\bar{\sigma}'^3} \bar{V}_{;ss} \bar{V}_{;\sigma} - \frac{7}{\bar{\sigma}'^3} \bar{V}_{;\sigma} \bar{\theta}'^2 - \frac{3}{\bar{\sigma}'^2} H \bar{V}_{;ss} + \frac{14}{\bar{\sigma}'^2} H \bar{\theta}'^2 \right. \\
& \quad \left. - 2\frac{\bar{V}_{;\sigma}}{\bar{\sigma}'} \bar{e}_s^I \bar{e}_s^J \bar{e}_\sigma^K \bar{e}_\sigma^L \bar{R}_{IKJL} - \frac{\bar{\sigma}'}{2} \bar{e}_s^I \bar{e}_s^J \bar{e}_\sigma^K \bar{e}_\sigma^L \bar{e}_\sigma^M \mathcal{D}_M \bar{R}_{IKJL} \right] \delta s^2 \delta s' \\
& + \left[ \frac{1}{6} \bar{V}_{;ssss} - \frac{7}{3\bar{\sigma}'} \bar{V}_{;sss} \bar{\theta}' + \frac{2}{\bar{\sigma}'^2} \bar{V}_{;ss}^2 + \frac{21}{\bar{\sigma}'^2} \bar{V}_{;ss} \bar{\theta}'^2 + \frac{27}{\bar{\sigma}'^2} \bar{\theta}'^4 + \frac{\bar{\sigma}'^2}{3} (\bar{e}_s^I \bar{e}_s^J \bar{e}_\sigma^K \bar{e}_\sigma^L \bar{R}_{IKJL})^2 \right. \\
& \quad \left. + \frac{1}{3} \bar{e}_s^I \bar{e}_s^J \bar{e}_\sigma^K \bar{e}_\sigma^L \left( \bar{R}_{IKJL} (3\bar{V}_{;ss} + 7\bar{\theta}'^2) - 2\bar{\sigma}' \bar{\theta}' \bar{e}_s^N \mathcal{D}_N \bar{R}_{IKJL} \right. \right. \\
& \quad \left. \left. + \bar{\sigma}'^2 \bar{e}_s^N \bar{e}_s^Q \left( \frac{1}{2} \mathcal{D}_Q \mathcal{D}_N \bar{R}_{IKJL} - \bar{R}_{IKJL} \bar{R}_{NLQ}^P + \bar{R}_{IKJL} \bar{R}_{NPQ}^P \right) \right) \right] \delta s^3, \tag{A.1}
\end{aligned}$$

where we have used  $V_i \approx 0$  and  $V_i^{(3)} \approx 0$  on large scales. Note that a prime denotes a derivative w.r.t. coordinate time. This equation reduces to the one derived in [20] for a trivial field space metric. During the non-minimally coupled ekpyrotic phase the equation of motion for  $\delta s^{(3)}$  simplifies to

$$0 \approx \delta s^{(3)}|_{\text{old}}'' + 3H\delta s^{(3)}|_{\text{old}}' + [\Omega^{-1}\Omega_{,\phi}\bar{V}_{,\phi} - \Omega^{-1}\Omega_{,\phi\phi}\bar{\phi}'^2] \delta s^{(3)}|_{\text{old}} + \bar{\phi}'^2 \left[ \frac{2}{3}\Omega^{-3}\Omega_{,\phi}^2\Omega_{,\phi\phi} + \frac{2}{3}\Omega^{-2}\Omega_{,\phi\phi}^2 + \frac{1}{3}\Omega^{-2}\Omega_{,\phi}\Omega_{,\phi\phi\phi} - \frac{1}{3\bar{\phi}'^2}\Omega^{-2}\Omega_{,\phi}\Omega_{,\phi\phi}\bar{V}_{,\phi} \right] \delta s^3, \quad (\text{A.2})$$

where we used  $\delta s^{(2)} = 0$  as well as  $\delta s' = -\bar{\sigma}'\Omega^{-1}\Omega_{,\phi}\delta s$ . However, the third-order entropy perturbation, given by

$$\delta s^{(3)}|_{\text{old,ekp}} = -\Omega\delta\chi^{(3)} - \frac{1}{6}\Omega^{-2}\Omega_{,\phi}^2\delta s^3, \quad (\text{A.3})$$

contains a  $\delta s^3$ -term acting as a source in the equation of motion, while  $\delta\chi^{(3)} = 0$  trivially solves the equation of motion (A.2). It is certainly more natural to define the entropic perturbation in such a way that during the non-minimal ekpyrotic phase the solution is given by  $\delta s^{(3)} = \delta\chi^{(3)} = 0$ . This motivates us to add a gauge-invariant term to the definition of  $\delta s^{(3)}$  that reduces to  $+\frac{1}{6}\Omega^{-2}\Omega_{,\phi}^2\delta s^3$  during the ekpyrotic phase. The choice is not unique however, and the terms that can be added are

$$T = A\delta s'^3 + B\delta s\delta s'^2 + C\delta s^2\delta s' + D\delta s^3, \quad (\text{A.4})$$

where we leave  $A, B, C, D$  arbitrary for now. During the ekpyrotic phase,  $\delta s' = -\bar{\sigma}'\Omega^{-1}\Omega_{,\phi}\delta s$ , and hence we need

$$T = \frac{1}{6}\Omega^{-2}\Omega_{,\phi}^2\delta s^3 = [-A\bar{\sigma}'^3\Omega^{-3}\Omega_{,\phi}^3 + B\bar{\sigma}'^2\Omega^{-2}\Omega_{,\phi}^2 - C\bar{\sigma}'\Omega^{-1}\Omega_{,\phi} + D] \delta s^3. \quad (\text{A.5})$$

It is immediately clear that we can set  $A = 0$ . The derivative of the term  $T$  added to the definition of  $\delta s^{(3)}$  has to be subtracted from  $\delta s_i^{(3)}$ , giving the following contri-

bution to the entropic equation of motion at third order:

$$\begin{aligned}
& - [T'' + 3HT' + (\bar{V}_{;ss} + 3\bar{\theta}'^2 + \bar{\sigma}'^2 \bar{e}_s^I \bar{e}_s^J \bar{e}_\sigma^K \bar{e}_\sigma^L \bar{R}_{IKJL}) T] \\
& = \delta s^3 \left[ -D'' + 2 [D + C' - B (\bar{V}_{;ss} + 3\bar{\theta}'^2 + \bar{\sigma}'^2 \bar{e}_s^I \bar{e}_s^J \bar{e}_\sigma^K \bar{e}_\sigma^L \bar{R}_{IKJL})] \right. \\
& \quad \left. (\bar{V}_{;ss} + 3\bar{\theta}'^2 + \bar{\sigma}'^2 \bar{e}_s^I \bar{e}_s^J \bar{e}_\sigma^K \bar{e}_\sigma^L \bar{R}_{IKJL}) - 3HD' + C \left[ \bar{\sigma}' \bar{V}_{;ss\sigma} - 6H\bar{\theta}'^2 - 4 \frac{\bar{\theta}'^2}{\bar{\sigma}'} \bar{V}_{,\sigma} + 8\bar{\theta}'\bar{\theta}'' \right. \right. \\
& \quad \left. \left. - 2\bar{\sigma}' (3H\bar{\sigma}' + \bar{V}_{,\sigma}) \bar{e}_s^I \bar{e}_s^J \bar{e}_\sigma^K \bar{e}_\sigma^L \bar{R}_{IKJL} + \bar{\sigma}'^3 \bar{e}_s^I \bar{e}_s^J \bar{e}_\sigma^K \bar{e}_\sigma^L \bar{e}_\sigma^M \mathcal{D}_M \bar{R}_{IKJL} \right] \right] \\
& + \delta s^2 \delta s' \left[ -6D' - C'' + 3H'C + 3HC' + (6C + 4B' - 12HB) \right. \\
& \quad \left. (\bar{V}_{;ss} + 3\bar{\theta}'^2 + \bar{\sigma}'^2 \bar{e}_s^I \bar{e}_s^J \bar{e}_\sigma^K \bar{e}_\sigma^L \bar{R}_{IKJL}) + 2B \left[ \bar{\sigma}' \bar{V}_{;ss\sigma} - 6H\bar{\theta}'^2 - 4 \frac{\bar{\theta}'^2}{\bar{\sigma}'} \bar{V}_{,\sigma} + 8\bar{\theta}'\bar{\theta}'' \right. \right. \\
& \quad \left. \left. - 2\bar{\sigma}' (3H\bar{\sigma}' + \bar{V}_{,\sigma}) \bar{e}_s^I \bar{e}_s^J \bar{e}_\sigma^K \bar{e}_\sigma^L \bar{R}_{IKJL} + \bar{\sigma}'^3 \bar{e}_s^I \bar{e}_s^J \bar{e}_\sigma^K \bar{e}_\sigma^L \bar{e}_\sigma^M \mathcal{D}_M \bar{R}_{IKJL} \right] \right] \\
& + \delta s \delta s'^2 \left[ -6D - 4C' + 3H(4C - 6HB) - B'' + 6H'B + 9HB' \right. \\
& \quad \left. + 6B (\bar{V}_{;ss} + 3\bar{\theta}'^2 + \bar{\sigma}'^2 \bar{e}_s^I \bar{e}_s^J \bar{e}_\sigma^K \bar{e}_\sigma^L \bar{R}_{IKJL}) \right] \\
& + \delta s'^3 \left[ -2C - 2B' + 12HB \right]. \tag{A.6}
\end{aligned}$$

In order to satisfy Eq. (A.5) during the ekpyrotic phase  $C$  would have to contain one Christoffel symbol, and  $D$  the product of two  $\bar{\Gamma}$ 's. As can be seen from the previous equation, this is problematic as the terms that would be added to the equation of motion are not covariant. Take the simple example of  $C \sim \bar{\Gamma}$ : there are no terms in the equation of motion that can be combined with the new term  $\sim \bar{\Gamma} \delta s'^3$  to make it covariant. Similarly for  $D \neq 0$ . We are forced to choose  $B = \frac{1}{6\bar{\sigma}'^2}$  with  $C = D = 0$ .

## Appendix B

# Useful formulae for the covariant formalism

**Metric:** On large scales where spatial gradients can be neglected, the metric can be written as

$$ds^2 = -(1 + 2A) dt^2 + a(t)^2 (1 - 2\psi) \delta_{ij} dx^i dx_j, \quad (\text{B.1})$$

where  $A = A^{(1)} + A^{(2)} + A^{(3)}$ , and  $\psi = \psi^{(1)} + \psi^{(2)} + \psi^{(3)}$  up to third order.

Thus, the 00-component of the inverse metric is given by

$$g^{00} = -1 + 2A^{(1)} + 2A^{(2)} - 4 \left( A^{(1)} \right)^2 + 2A^{(3)} - 8A^{(1)}A^{(2)} + 8 \left( A^{(1)} \right)^3 = -u^0 u^0, \quad (\text{B.2})$$

from which we can deduce

$$u^0 = 1 - A^{(1)} - A^{(2)} + \frac{3}{2} \left( A^{(1)} \right)^2 - A^{(3)} + 3A^{(1)}A^{(2)} - \frac{5}{2} \left( A^{(1)} \right)^3. \quad (\text{B.3})$$

Moreover, for simplicity we choose  $u^a$  such that  $u_i = 0$ , and on large scales we can show that  $u^i \approx 0$ .

**Scalar field perturbations:** Rewriting the perturbation in the scalar fields in terms of adiabatic and entropic fields we have

$$\delta\phi^J = \bar{e}_\sigma^J \delta\sigma + \bar{e}_s^J \delta s, \quad (\text{B.4})$$

$$\delta\phi^{J'} = \bar{e}_\sigma^J \delta\sigma' + \bar{e}_s^J \delta s' + \bar{\theta}' (\bar{e}_s^J \delta\sigma - \bar{e}_\sigma^J \delta s) - \bar{\sigma}' \bar{\Gamma}_{LK}^J \bar{e}_\sigma^L (\bar{e}_\sigma^K \delta\sigma + \bar{e}_s^K \delta s), \quad (\text{B.5})$$

at linear order and

$$\begin{aligned}\delta\phi^{(2)J} &= \bar{e}_\sigma^J \left[ \delta\sigma^{(2)} - \frac{1}{2\bar{\sigma}'} \delta s \delta s' \right] + \bar{e}_s^J \left[ \delta s^{(2)} + \frac{\delta\sigma}{\bar{\sigma}'} \left( \delta s' + \frac{\bar{\theta}'}{2} \delta\sigma \right) \right] \\ &\quad - \frac{1}{2} \bar{\Gamma}_{LK}^J (\bar{e}_\sigma^L \delta\sigma + \bar{e}_s^L \delta s) (\bar{e}_\sigma^K \delta\sigma + \bar{e}_s^K \delta s),\end{aligned}\tag{B.6}$$

$$\begin{aligned}\delta\phi^{(2)J'} &= \bar{e}_\sigma^J \left[ \delta\sigma^{(2)} - \frac{1}{2\bar{\sigma}'} \delta s \delta s' \right]' + \bar{e}_s^J \left[ \delta s^{(2)} + \frac{\delta\sigma}{\bar{\sigma}'} \left( \delta s' + \frac{\bar{\theta}'}{2} \delta\sigma \right) \right]' \\ &\quad + \bar{\theta}' \left[ \bar{e}_s^J \left( \delta\sigma^{(2)} - \frac{1}{2\bar{\sigma}'} \delta s \delta s' \right) - \bar{e}_\sigma^J \left( \delta s^{(2)} + \frac{\delta\sigma}{\bar{\sigma}'} \left( \delta s' + \frac{\bar{\theta}'}{2} \delta\sigma \right) \right) \right] \\ &\quad - \bar{\sigma}' \bar{\Gamma}_{MN}^J \bar{e}_\sigma^M \left[ \bar{e}_\sigma^N \left( \delta\sigma^{(2)} - \frac{1}{2\bar{\sigma}'} \delta s \delta s' \right) + \bar{e}_s^N \left( \delta s^{(2)} + \frac{\delta\sigma}{\bar{\sigma}'} \left( \delta s' + \frac{\bar{\theta}'}{2} \delta\sigma \right) \right) \right] \\ &\quad - \bar{\Gamma}_{LK}^J (\bar{e}_\sigma^L \delta\sigma + \bar{e}_s^L \delta s) [\bar{e}_\sigma^K (\delta\sigma' - \bar{\theta}' \delta s) + \bar{e}_s^K (\delta s' + \bar{\theta}' \delta\sigma)] \\ &\quad + \bar{\sigma}' \bar{e}_\sigma^M (\bar{e}_\sigma^L \delta\sigma + \bar{e}_s^L \delta s) (\bar{e}_\sigma^K \delta\sigma + \bar{e}_s^K \delta s) \left[ -\frac{1}{2} \partial_M \bar{\Gamma}_{LK}^J + \bar{\Gamma}_{LN}^J \bar{\Gamma}_{MK}^N \right]\end{aligned}\tag{B.7}$$

at second order. The perturbation in the scalar field at third order in *comoving gauge* is given by<sup>1</sup>

$$\begin{aligned}\delta\phi^{(3)J} &\approx \bar{e}_s^J \left[ \delta s^{(3)} - \frac{1}{6\bar{\sigma}'^2} \delta s \delta s'^2 \right] - \bar{e}_\sigma^J \left[ \frac{1}{2\bar{\sigma}'} \left( \delta s \delta s^{(2)'} + \delta s' \delta s^{(2)} \right) + \frac{\bar{\theta}'}{6\bar{\sigma}'^2} \delta s^2 \delta s' \right] \\ &\quad - \bar{\Gamma}_{KL}^J \bar{e}_s^L \delta s \left[ \bar{e}_s^K \delta s^{(2)} - \bar{e}_\sigma^K \frac{1}{2\bar{\sigma}'} \delta s \delta s' \right] - \frac{1}{6} \bar{e}_s^K \bar{e}_s^L \bar{e}_s^I [\partial_I \bar{\Gamma}_{KL}^J - 2\bar{\Gamma}_{IP}^J \bar{\Gamma}_{KL}^P] \delta s^3.\end{aligned}\tag{B.8}$$

**Field space metric:** Explicitely, we have (using Eqs. (B.4) and (B.6))

$$\delta G_{IJ} = \bar{G}_{IJ,K} (\bar{e}_\sigma^K \delta\sigma + \bar{e}_s^K \delta s)\tag{B.9}$$

at linear order, and

$$\begin{aligned}\delta G_{IJ}^{(2)} &= \bar{G}_{IJ,K} \left[ \bar{e}_\sigma^K \left( \delta\sigma^{(2)} - \frac{1}{2\bar{\sigma}'} \delta s \delta s' \right) + \bar{e}_s^K \left( \delta s^{(2)} + \frac{\delta\sigma}{\bar{\sigma}'} \left( \delta s' + \frac{\bar{\theta}'}{2} \delta\sigma \right) \right) \right. \\ &\quad \left. - \frac{1}{2} \bar{\Gamma}_{MN}^K (\bar{e}_\sigma^M \delta\sigma + \bar{e}_s^M \delta s) (\bar{e}_\sigma^N \delta\sigma + \bar{e}_s^N \delta s) \right] \\ &\quad + \frac{1}{2} \bar{G}_{IJ,KL} (\bar{e}_\sigma^K \delta\sigma + \bar{e}_s^K \delta s) (\bar{e}_\sigma^L \delta\sigma + \bar{e}_s^L \delta s)\end{aligned}\tag{B.10}$$

<sup>1</sup>This includes the term  $T = \frac{1}{6\bar{\sigma}'^2} \delta s \delta s'^2$  from the new defintion of  $\delta s^{(3)}$ .

at second order.

**Riemann tensor:** The Riemann tensor with all indices downstairs is given by

$$\begin{aligned}\bar{R}_{IKJL} &= \bar{G}_{IM}\bar{R}^M_{KJL} = \bar{G}_{IM}(\partial_J\bar{\Gamma}^M_{LK} - \partial_L\bar{\Gamma}^M_{JK} + \bar{\Gamma}^M_{JP}\bar{\Gamma}^P_{LK} - \bar{\Gamma}^M_{LP}\bar{\Gamma}^P_{JK}) \\ &= \frac{1}{2}(\bar{G}_{JK,IL} - \bar{G}_{KL,IJ} - \bar{G}_{IJ,KL} + \bar{G}_{IL,KJ}) + \bar{\Gamma}_{PIL}\bar{\Gamma}^P_{JK} - \bar{\Gamma}_{PIJ}\bar{\Gamma}^P_{LK},\end{aligned}\quad (\text{B.11})$$

where the Christoffel symbol with all indices downstairs is defined as

$$\bar{\Gamma}_{IJK} \equiv \bar{G}_{IP}\bar{\Gamma}^P_{JK} = \frac{1}{2}(\bar{G}_{IJ,K} + \bar{G}_{IK,J} - \bar{G}_{JK,I}). \quad (\text{B.12})$$

**Vielbeine:** Expanding the  $\sigma$ -vielbein,  $e_\sigma^J \equiv \frac{\dot{\phi}^J}{\dot{\sigma}}$ , up to second order, we obtain at linear order

$$\delta e_\sigma^J = \bar{\sigma}'^{-1}(\delta s' + \bar{\theta}'\delta\sigma)\bar{e}_s^J - \bar{\Gamma}_{KL}^J\bar{e}_\sigma^K(\bar{e}_\sigma^K\delta\sigma + \bar{e}_s^K\delta s), \quad (\text{B.13})$$

and with field space index lowered

$$\delta e_{\sigma I} = \bar{\sigma}'^{-1}(\delta s' + \bar{\theta}'\delta\sigma)\bar{e}_{sI} + \bar{\Gamma}_{LKI}\bar{e}_\sigma^L(\bar{e}_\sigma^K\delta\sigma + \bar{e}_s^K\delta s). \quad (\text{B.14})$$

At second order we have

$$\begin{aligned}\delta e_\sigma^{(2)J} &= -\frac{1}{2\bar{\sigma}'^2}\bar{e}_\sigma^J(\delta s' + \bar{\theta}'\delta\sigma)^2 + \frac{1}{\bar{\sigma}'}\bar{e}_s^J\left[-\bar{\sigma}'^{-1}(\delta\sigma' - \bar{\theta}'\delta s)(\delta s' + \bar{\theta}'\delta\sigma)\right. \\ &\quad \left. + \left(\delta s^{(2)} + \frac{\delta\sigma}{\bar{\sigma}'}\left(\delta s' + \frac{\bar{\theta}'}{2}\delta\sigma\right)\right)' + \bar{\theta}'\left(\delta\sigma^{(2)} - \frac{1}{2\bar{\sigma}'}\delta s\delta s'\right)\right] \\ &\quad + \frac{1}{2}\bar{e}_\sigma^J\bar{e}_s^M\bar{e}_s^N\bar{e}_\sigma^K\bar{e}_\sigma^L\bar{R}_{MKNL}\delta s^2 - \bar{\Gamma}_{KL}^J\left[\bar{e}_\sigma^L\left[\bar{e}_\sigma^K\left(\delta\sigma^{(2)} - \frac{1}{2\bar{\sigma}'}\delta s\delta s'\right)\right.\right. \\ &\quad \left.\left. + \bar{e}_s^K\left(\delta s^{(2)} + \frac{\delta\sigma}{\bar{\sigma}'}\left(\delta s' + \frac{\bar{\theta}'}{2}\delta\sigma\right)\right)\right] + \frac{1}{\bar{\sigma}'}\bar{e}_s^L(\bar{e}_\sigma^K\delta\sigma + \bar{e}_s^K\delta s)(\delta s' + \bar{\theta}'\delta\sigma)\right] \\ &\quad + \bar{e}_\sigma^M(\bar{e}_\sigma^K\delta\sigma + \bar{e}_s^K\delta s)(\bar{e}_\sigma^L\delta\sigma + \bar{e}_s^L\delta s)\left[-\frac{1}{2}\partial_M\bar{\Gamma}_{KL}^J + \bar{\Gamma}_{LN}^J\bar{\Gamma}_{MK}^N\right],\end{aligned}\quad (\text{B.15})$$

and

$$\begin{aligned}
\delta e_{\sigma I}^{(2)} = & -\frac{1}{2\bar{\sigma}'^2} \bar{e}_{\sigma I} (\delta s' + \bar{\theta}' \delta \sigma)^2 + \frac{1}{\bar{\sigma}'} \bar{e}_{sI} \left[ -\bar{\sigma}'^{-1} (\delta \sigma' - \bar{\theta}' \delta s) (\delta s' + \bar{\theta}' \delta \sigma) \right. \\
& + \left( \delta s^{(2)} + \frac{\delta \sigma}{\bar{\sigma}'} \left( \delta s' + \frac{\bar{\theta}'}{2} \delta \sigma \right) \right)' + \bar{\theta}' \left( \delta \sigma^{(2)} - \frac{1}{2\bar{\sigma}'} \delta s \delta s' \right) \left. \right] \\
& + \frac{1}{2} \bar{e}_{\sigma I} \bar{e}_s^M \bar{e}_s^N \bar{e}_\sigma^K \bar{e}_\sigma^L \bar{R}_{MKNL} \delta s^2 + \bar{\Gamma}_{LKI} \left[ \bar{e}_\sigma^L \left[ \bar{e}_\sigma^K \left( \delta \sigma^{(2)} - \frac{1}{2\bar{\sigma}'} \delta s \delta s' \right) \right. \right. \\
& \left. \left. + \bar{e}_s^K \left( \delta s^{(2)} + \frac{\delta \sigma}{\bar{\sigma}'} \left( \delta s' + \frac{\bar{\theta}'}{2} \delta \sigma \right) \right) \right] + \frac{1}{\bar{\sigma}'} \bar{e}_s^L (\bar{e}_\sigma^K \delta \sigma + \bar{e}_s^K \delta s) (\delta s' + \bar{\theta}' \delta \sigma) \right] \\
& + \bar{e}_\sigma^M (\bar{e}_\sigma^K \delta \sigma + \bar{e}_s^K \delta s) (\bar{e}_\sigma^L \delta \sigma + \bar{e}_s^L \delta s) \left[ \frac{1}{2} (\bar{G}_{IP,M} - \bar{G}_{IM,P}) \bar{\Gamma}_{KL}^P \right. \\
& \left. - \bar{\Gamma}_{PIK} \bar{\Gamma}_{ML}^P + \frac{1}{4} (\bar{G}_{KL,IM} - \bar{G}_{IK,LM} - \bar{G}_{IL,KM} + 2\bar{G}_{IM,KL}) \right], \tag{B.16}
\end{aligned}$$

In order to obtain the  $s$ -vielbeine we note that

$$e_s^J = \delta_I^J e_s^I = (\bar{e}_\sigma^J \bar{e}_{\sigma I} + \bar{e}_s^J \bar{e}_{sI}) e_s^I. \tag{B.17}$$

Expanding and rearranging the definitions

$$G_{IJ} e_\sigma^I e_\sigma^J = G_{IJ} e_s^I e_s^J \equiv 1 \quad \text{and} \quad G_{IJ} e_\sigma^I e_s^J \equiv 0 \tag{B.18}$$

up to second order, we obtain

$$\delta e_s^J = (\bar{e}_\sigma^J \bar{e}_{\sigma I} + \bar{e}_s^J \bar{e}_{sI}) \delta e_s^I = -\bar{\sigma}'^{-1} (\delta s' + \bar{\theta}' \delta \sigma) \bar{e}_\sigma^J - \bar{\Gamma}_{KL}^J \bar{e}_s^L (\bar{e}_\sigma^K \delta \sigma + \bar{e}_s^K \delta s) \tag{B.19}$$

at linear order. Lowering the field space index gives

$$\delta e_{sI} = -\bar{\sigma}'^{-1} (\delta s' + \bar{\theta}' \delta \sigma) \bar{e}_{\sigma I} + \bar{\Gamma}_{LKI} \bar{e}_s^L (\bar{e}_\sigma^K \delta \sigma + \bar{e}_s^K \delta s). \tag{B.20}$$

At second order we have

$$\begin{aligned}
\delta e_s^{(2)J} &= (\bar{e}_\sigma^J \bar{e}_{\sigma I} + \bar{e}_s^J \bar{e}_{sI}) \delta e_s^{(2)I} \\
&= -\frac{1}{2\bar{\sigma}'^2} \bar{e}_s^J (\delta s' + \bar{\theta}' \delta \sigma)^2 - \frac{1}{\bar{\sigma}'} \bar{e}_\sigma^J \left[ -\bar{\sigma}'^{-1} (\delta \sigma' - \bar{\theta}' \delta s) (\delta s' + \bar{\theta}' \delta \sigma) \right. \\
&\quad \left. + \left( \delta s^{(2)} + \frac{\delta \sigma}{\bar{\sigma}'} \left( \delta s' + \frac{\bar{\theta}'}{2} \delta \sigma \right) \right)' + \bar{\theta}' \left( \delta \sigma^{(2)} - \frac{1}{2\bar{\sigma}'} \delta s \delta s' \right) \right] \\
&\quad + \bar{e}_s^M \bar{e}_\sigma^K \left( \frac{1}{2} \bar{e}_s^J \bar{e}_s^N \bar{e}_\sigma^L \delta \sigma^2 + \bar{e}_\sigma^J \bar{e}_\sigma^N \bar{e}_s^L \delta \sigma \delta s \right) \bar{R}_{MKNL} - \bar{\Gamma}_{KL}^J \bar{e}_s^L \left[ \bar{e}_\sigma^K \left( \delta \sigma^{(2)} - \frac{1}{2\bar{\sigma}'} \delta s \delta s' \right) \right. \\
&\quad \left. + \bar{e}_s^K \left( \delta s^{(2)} + \frac{\delta \sigma}{\bar{\sigma}'} \left( \delta s' + \frac{\bar{\theta}'}{2} \delta \sigma \right) \right) \right] + \bar{\sigma}'^{-1} \bar{\Gamma}_{KL}^J (\bar{e}_\sigma^L \delta \sigma + \bar{e}_s^L \delta s) \bar{e}_\sigma^K (\delta s' + \bar{\theta}' \delta \sigma) \\
&\quad + \bar{e}_s^M (\bar{e}_\sigma^K \delta \sigma + \bar{e}_s^K \delta s) (\bar{e}_\sigma^L \delta \sigma + \bar{e}_s^L \delta s) \left[ -\frac{1}{2} \partial_M \bar{\Gamma}_{KL}^J + \bar{\Gamma}_{LN}^J \bar{\Gamma}_{MK}^N \right]. \tag{B.21}
\end{aligned}$$

Lowering the field space index gives

$$\begin{aligned}
\delta e_{sI}^{(2)} &= -\frac{1}{2\bar{\sigma}'^2} \bar{e}_{sI} (\delta s' + \bar{\theta}' \delta \sigma)^2 - \frac{1}{\bar{\sigma}'} \bar{e}_{\sigma I} \left[ -\bar{\sigma}'^{-1} (\delta \sigma' - \bar{\theta}' \delta s) (\delta s' + \bar{\theta}' \delta \sigma) \right. \\
&\quad \left. + \left( \delta s^{(2)} + \frac{\delta \sigma}{\bar{\sigma}'} \left( \delta s' + \frac{\bar{\theta}'}{2} \delta \sigma \right) \right)' + \bar{\theta}' \left( \delta \sigma^{(2)} - \frac{1}{2\bar{\sigma}'} \delta s \delta s' \right) \right] \\
&\quad + \bar{e}_s^M \bar{e}_\sigma^K \left( \frac{1}{2} \bar{e}_{sI} \bar{e}_s^N \bar{e}_\sigma^L \delta \sigma^2 + \bar{e}_{\sigma I} \bar{e}_\sigma^N \bar{e}_s^L \delta \sigma \delta s \right) \bar{R}_{MKNL} + \bar{\Gamma}_{LIK} \bar{e}_s^L \left[ \bar{e}_\sigma^K \left( \delta \sigma^{(2)} - \frac{1}{2\bar{\sigma}'} \delta s \delta s' \right) \right. \\
&\quad \left. + \bar{e}_s^K \left( \delta s^{(2)} + \frac{\delta \sigma}{\bar{\sigma}'} \left( \delta s' + \frac{\bar{\theta}'}{2} \delta \sigma \right) \right) \right] - \bar{\sigma}'^{-1} \bar{\Gamma}_{LIK} (\bar{e}_\sigma^K \delta \sigma + \bar{e}_s^K \delta s) \bar{e}_\sigma^L (\delta s' + \bar{\theta}' \delta \sigma) \\
&\quad + \bar{e}_s^M (\bar{e}_\sigma^K \delta \sigma + \bar{e}_s^K \delta s) (\bar{e}_\sigma^L \delta \sigma + \bar{e}_s^L \delta s) \left[ \frac{1}{2} (\bar{G}_{IP,M} - \bar{G}_{IM,P}) \bar{\Gamma}_{KL}^P \right. \\
&\quad \left. - \bar{\Gamma}_{PIK} \bar{\Gamma}_{ML}^P + \frac{1}{4} (\bar{G}_{KL,IM} - \bar{G}_{IK,LM} - \bar{G}_{IL,KM} + 2\bar{G}_{IM,KL}) \right]. \tag{B.22}
\end{aligned}$$

**Lie derivative expansions:** Expanding the Lie derivative up to second order, we have for the fields

$$\dot{\phi}^I = u^0 \partial_0 \phi^I = \bar{\phi}^I + \delta \phi^I - \bar{\phi}^I A^{(1)} + \delta \phi^{(2)I} - \delta \phi^I A^{(1)} - \bar{\phi}^I A^{(2)} + \frac{3}{2} \bar{\phi}^I A^{(1)2}. \tag{B.23}$$

Similarly, expanding  $\dot{\sigma}^2$ :

$$\begin{aligned}
\dot{\sigma}^2 &\equiv G_{IJ}\dot{\phi}^I\dot{\phi}^J = \bar{\sigma}'^2 + 2\bar{\sigma}' \left( \delta\sigma' - \bar{\theta}'\delta s - \bar{\sigma}'A^{(1)} \right) \\
&\quad + \bar{\sigma}'^2 \left( 4A^{(1)2} - 2A^{(2)} \right) - 4\bar{\sigma}'A^{(1)}(\delta\sigma' - \bar{\theta}'\delta s) + (\delta\sigma' - \bar{\theta}'\delta s)^2 + (\delta s' + \bar{\theta}'\delta\sigma)^2 \\
&\quad + 2\bar{\sigma}' \left[ \delta\sigma^{(2)} - \frac{1}{2\bar{\sigma}'}\delta s\delta s' \right]' - 2\bar{\sigma}'\bar{\theta}' \left[ \delta s^{(2)} + \frac{\delta\sigma}{\bar{\sigma}'} \left( \delta s' + \frac{\bar{\theta}'}{2}\delta\sigma \right) \right] - \bar{\sigma}'^2 \bar{e}_s^I \bar{e}_s^J \bar{e}_\sigma^K \bar{e}_\sigma^L \bar{R}_{IKJL} \delta s^2 \\
&\stackrel{\delta\sigma=0}{\approx} \bar{\sigma}'^2 + 2\bar{\sigma}'\bar{\theta}'\delta s + 2\bar{\sigma}'\bar{\theta}'\delta s^{(2)} - \bar{V}_{;ss}\delta s^2 + \frac{\bar{V}_{,\sigma}}{\bar{\sigma}'}\delta s\delta s', 
\end{aligned} \tag{B.24}$$

where the last expression is valid on large scales and in comoving gauge and where we have used the expressions for  $A^{(1)}$  and  $A^{(2)}$  given in (B.31) and (B.32), respectively.

We can then compute the perturbation expansion in  $\dot{\sigma} = \dot{\sigma}^{(0)} + \delta\dot{\sigma}^{(1)} + \delta\dot{\sigma}^{(2)} + \dots$ :

$$\dot{\sigma}^{(0)} = \sqrt{(\dot{\sigma}^2)^{(0)}} = \sqrt{\bar{G}_{IJ}\bar{\phi}^I\bar{\phi}^J} \equiv \bar{\sigma}' \tag{B.25}$$

at zeroth order,

$$\delta\dot{\sigma}^{(1)} = \frac{\delta(\dot{\sigma}^2)^{(1)}}{2\dot{\sigma}^{(0)}} = \delta\sigma' - \bar{\theta}'\delta s - \bar{\sigma}'A^{(1)} \stackrel{\delta\sigma=0}{\approx} \bar{\theta}'\delta s \tag{B.26}$$

at linear order, and

$$\begin{aligned}
\delta\dot{\sigma}^{(2)} &= \frac{\delta(\dot{\sigma}^2)^{(2)} - (\delta\dot{\sigma}^{(1)})^2}{2\dot{\sigma}^{(0)}} \\
&= \left[ \delta\sigma^{(2)} - \frac{1}{2\bar{\sigma}'}\delta s\delta s' \right]' - \bar{\theta}' \left[ \delta s^{(2)} + \frac{\delta\sigma}{\bar{\sigma}'} \left( \delta s' + \frac{\bar{\theta}'}{2}\delta\sigma \right) \right] + \frac{1}{2}\bar{\sigma}'^{-1}(\delta s' + \bar{\theta}'\delta\sigma)^2 \\
&\quad - (\delta\sigma' - \bar{\theta}'\delta s)A^{(1)} - \bar{\sigma}'A^{(2)} + \frac{3}{2}\bar{\sigma}'A^{(1)2} - \frac{1}{2}\bar{\sigma}'^2 \bar{e}_s^I \bar{e}_s^J \bar{e}_\sigma^K \bar{e}_\sigma^L \bar{R}_{IKJL} \delta s^2 \\
&\stackrel{\delta\sigma=0}{\approx} \bar{\theta}'\delta s^{(2)} + \frac{\bar{V}_{,\sigma}}{2\bar{\sigma}'^2}\delta s\delta s' - \frac{1}{2\bar{\sigma}'}(\bar{V}_{;ss} + \bar{\theta}'^2)\delta s^2 
\end{aligned} \tag{B.27}$$

at quadratic order.

**Metric perturbations  $A^{(1)}$  and  $A^{(2)}$ :** To determine  $A^{(1)}$  and  $A^{(2)}$  we make use of the fact that on large scales the comoving energy density perturbation is zero,  $\delta\epsilon \approx 0$ . Moreover, in comoving gauge, it simplifies to  $\delta\rho$ :

$$\delta\epsilon \equiv \delta\rho - \frac{\bar{\rho}'}{\bar{\sigma}'}\delta\sigma \stackrel{\delta\sigma=0}{\approx} \delta\rho \approx 0 \tag{B.28}$$

at first order, and

$$\delta\epsilon^{(2)} \equiv \delta\rho^{(2)} - \frac{\bar{\rho}'}{\bar{\sigma}'}\delta\sigma^{(2)} - \frac{\delta\sigma}{\bar{\sigma}'} \left[ \delta\epsilon' + \frac{1}{2} \left( \frac{\bar{\rho}'}{\bar{\sigma}'} \right)' \delta\sigma + \frac{\bar{\rho}'}{\bar{\sigma}'} \bar{\theta}' \delta s \right] \stackrel{\delta\sigma=0}{=} \delta\rho^{(2)} \approx 0 \quad (\text{B.29})$$

at second order.

The comoving energy density is given by (3.13), and can be expanded up to second order:

$$\begin{aligned} \rho &= \frac{1}{2} G_{IJ} \dot{\phi}^I \dot{\phi}^J + \frac{1}{2} G_{IJ} g^{ij} \nabla_i \phi^I \nabla_j \phi^J + V \approx \frac{1}{2} \dot{\sigma}^2 + V \\ \therefore \bar{\rho} &\approx \frac{1}{2} \bar{\sigma}'^2 + \bar{V} \\ \therefore \delta\rho &\approx -2\bar{\sigma}'\bar{\theta}'\delta s - \bar{\sigma}'^2 A^{(1)} \\ \therefore \delta\rho^{(2)} &\approx -2\bar{\sigma}'\bar{\theta}'\delta s^{(2)} - \bar{\sigma}'^2 A^{(2)} - \frac{\bar{V}_{,\sigma}}{\bar{\sigma}'} \delta s \delta s' + (\bar{V}_{;ss} + 2\bar{\theta}'^2) \delta s^2 + 2\bar{\sigma}' A^{(1)} (\bar{\theta}' \delta s + \bar{\sigma}' A^{(1)}) \end{aligned} \quad (\text{B.30})$$

where we have neglected spatial gradients.

At linear order, we thus have

$$A^{(1)} \approx -2 \frac{\bar{\theta}'}{\bar{\sigma}'} \delta s, \quad (\text{B.31})$$

and at second order

$$\begin{aligned} A^{(2)} &\approx -2 \frac{\bar{\theta}'}{\bar{\sigma}'} \delta s^{(2)} + \frac{1}{\bar{\sigma}'^2} (\bar{V}_{;ss} + 2\bar{\theta}'^2) \delta s^2 - \frac{\bar{V}_{,\sigma}}{\bar{\sigma}'^3} \delta s \delta s' + 2A^{(1)} \left( \frac{\bar{\theta}'}{\bar{\sigma}'} \delta s + A^{(1)} \right) \\ &\approx -2 \frac{\bar{\theta}'}{\bar{\sigma}'} \delta s^{(2)} + \frac{1}{\bar{\sigma}'^2} (\bar{V}_{;ss} + 6\bar{\theta}'^2) \delta s^2 - \frac{\bar{V}_{,\sigma}}{\bar{\sigma}'^3} \delta s \delta s'. \end{aligned} \quad (\text{B.32})$$

### Perturbations of other important quantities:

$$\delta V^{(1)} = \bar{V}_{,\sigma} \delta\sigma - \bar{\sigma}' \bar{\theta}' \delta s \stackrel{\delta\sigma=0}{\approx} -\bar{\sigma}' \bar{\theta}' \delta s \quad (\text{B.33})$$

$$\begin{aligned} \delta V^{(2)} &= \bar{V}_{,\sigma} \left[ \delta\sigma^{(2)} - \frac{1}{2\bar{\sigma}'} \delta s \delta s' \right] - \bar{\sigma}' \bar{\theta}' \left[ \delta s^{(2)} + \frac{\delta\sigma}{\bar{\sigma}'} \left( \delta s' + \frac{\bar{\theta}'}{2} \delta\sigma \right) \right] \\ &\quad + \frac{1}{2} \bar{V}_{;\sigma\sigma} \delta\sigma^2 + \bar{V}_{;s\sigma} \delta\sigma \delta s + \frac{1}{2} \bar{V}_{;ss} \delta s^2 \\ &\stackrel{\delta\sigma=0}{\approx} -\bar{\sigma}' \bar{\theta}' \delta s^{(2)} - \frac{\bar{V}_{,\sigma}}{2\bar{\sigma}'} \delta s \delta s' + \frac{1}{2} \bar{V}_{;ss} \delta s^2 \end{aligned} \quad (\text{B.34})$$

$$\begin{aligned} \delta V^{(3)} &\stackrel{\delta\sigma=0}{\approx} -\bar{\sigma}'\bar{\theta}' \left[ \delta s^{(3)} - \frac{1}{6\bar{\sigma}'^2} \delta s \delta s'^2 \right] - \bar{V}_{;\sigma} \left[ \frac{1}{2\bar{\sigma}'} \left( \delta s \delta s^{(2)} \right)' + \frac{\bar{\theta}'}{6\bar{\sigma}'^2} \delta s^2 \delta s' \right] \\ &+ \frac{1}{6} \bar{V}_{;sss} \delta s^3 + \bar{V}_{;ss} \delta s \delta s^{(2)} - \frac{1}{2\bar{\sigma}'} \bar{V}_{;s\sigma} \delta s^2 \delta s' \end{aligned} \quad (\text{B.35})$$

$$\delta V_{;ss} = \bar{V}_{;sss} \delta s - 2 \frac{\bar{V}_{;s\sigma}}{\bar{\sigma}'} \delta s', \quad (\text{B.36})$$

with  $\bar{V}_{;sss} = \bar{e}_s^I \bar{e}_s^J \bar{e}_s^K \bar{V}_{;IJK}$ .

$$\begin{aligned} \delta V_{;ss}^{(2)} &\approx \bar{V}_{;sss} \delta s^{(2)} + \frac{1}{2} \bar{V}_{;ssss} \delta s^2 - \frac{5}{2\bar{\sigma}'} \bar{V}_{;ss\sigma} \delta s \delta s' + \frac{\bar{V}_{;\sigma\sigma} - \bar{V}_{;ss}}{\bar{\sigma}'^2} \delta s'^2 \\ &- \frac{2}{\bar{\sigma}'} \bar{V}_{;s\sigma} \left( \delta s^{(2)'} + \frac{\bar{\theta}'}{2\bar{\sigma}'} \delta s \delta s' \right) - \frac{2\bar{V}_{;\sigma}}{\bar{\sigma}'} \bar{e}_s^I \bar{e}_s^J \bar{e}_s^K \bar{e}_\sigma^L \bar{R}_{IJKL} \delta s \delta s', \end{aligned} \quad (\text{B.37})$$

with  $\bar{V}_{;ssss} = \bar{e}_s^I \bar{e}_s^J \bar{e}_s^K \bar{e}_s^L \bar{V}_{;IJKL}$ .

$$\delta \dot{\theta} \approx -\frac{\bar{V}_{;ss}}{\bar{\sigma}'} \delta s + \frac{\bar{V}_{;\sigma}}{\bar{\sigma}'^2} \delta s' - \frac{\bar{\theta}'^2}{\bar{\sigma}'} \delta s. \quad (\text{B.38})$$

$$\begin{aligned} \delta \dot{\theta}^{(2)} &\approx \frac{\bar{V}_{;\sigma}}{\bar{\sigma}'^2} \delta s^{(2)'} - \frac{1}{\bar{\sigma}'} \left( \bar{V}_{;ss} + \bar{\theta}'^2 \right) \delta s^{(2)} - \frac{\bar{\theta}'}{2\bar{\sigma}'^2} \delta s'^2 + \frac{1}{2\bar{\sigma}'^2} \left( 4 \frac{\bar{\theta}' \bar{V}_{;\sigma}}{\bar{\sigma}'} - 3\bar{\theta}'' + 9H\bar{\theta}' \right) \delta s \delta s' \\ &+ \frac{1}{2\bar{\sigma}'^2} \left( -\bar{\sigma}' \bar{V}_{;sss} + 3\bar{V}_{;ss} \bar{\theta}' + \bar{\theta}'^3 \right) \delta s^2. \end{aligned} \quad (\text{B.39})$$

$$\delta \left[ \dot{\sigma}^2 \bar{e}_s^I \bar{e}_s^J \bar{e}_\sigma^K \bar{e}_\sigma^L \bar{R}_{IJKL} \right] \approx \bar{e}_s^I \bar{e}_s^J \bar{e}_\sigma^K \bar{e}_\sigma^L \left[ 2\bar{\sigma}' \bar{\theta}' \bar{R}_{IJKL} + \bar{\sigma}'^2 \bar{e}_s^N \mathcal{D}_N \bar{R}_{IJKL} \right] \delta s \quad (\text{B.40})$$

$$\begin{aligned} \delta \left[ \dot{\sigma}^2 \bar{e}_s^I \bar{e}_s^J \bar{e}_\sigma^K \bar{e}_\sigma^L \bar{R}_{IJKL} \right]^{(2)} &\approx \bar{e}_s^I \bar{e}_s^J \bar{e}_\sigma^K \bar{e}_\sigma^L \left[ \bar{R}_{IJKL} \left( 2\bar{\sigma}' \bar{\theta}' \delta s^{(2)} + \frac{\bar{V}_{;\sigma}}{\bar{\sigma}'} \delta s \delta s' - \bar{V}_{;ss} \delta s^2 \right) \right. \\ &+ \mathcal{D}_N \bar{R}_{IJKL} \left( \bar{\sigma}'^2 \bar{e}_s^N \delta s^{(2)} - \frac{\bar{\sigma}'}{2} \bar{e}_\sigma^N \delta s \delta s' + 2\bar{\sigma}' \bar{\theta}' \bar{e}_s^N \delta s^2 \right) \\ &+ \bar{\sigma}'^2 \bar{e}_s^N \bar{e}_s^Q \left( \frac{1}{2} \mathcal{D}_Q \mathcal{D}_N \bar{R}_{IJKL} - \bar{R}_{IJKP} \bar{R}_{NLQ}^P \right. \\ &\left. \left. + \bar{R}_{IJKL} \bar{R}_{NPQ}^P \right) \delta s^2 \right] \end{aligned} \quad (\text{B.41})$$

**Useful derivatives:**

$$\bar{\theta}'' = -\bar{V}_{;s\sigma} + 3H\bar{\theta}' + 2 \frac{\bar{\theta}' \bar{V}_{;\sigma}}{\bar{\sigma}'} \quad (\text{B.42})$$

$$\bar{V}'_{,\sigma} = \bar{\sigma}' (\bar{V}_{;\sigma\sigma} - \bar{\theta}'^2) \quad (\text{B.43})$$

$$\bar{V}'_{;ss} = \bar{\sigma}' \bar{V}_{;ss\sigma} - 2\bar{\theta}' \bar{V}_{;s\sigma} \quad (\text{B.44})$$

$$\bar{e}_s^{J'} = -\bar{\theta}' \bar{e}_\sigma^J - \bar{\Gamma}_{KL}^J \bar{\sigma}' \bar{e}_s^K \bar{e}_\sigma^L \quad (\text{B.45})$$

$$[\bar{e}_s^I \bar{e}_s^J \bar{e}_\sigma^K \bar{e}_\sigma^L \bar{R}_{IKJL}]' = \bar{e}_s^I \bar{e}_s^J \bar{e}_\sigma^K \bar{e}_\sigma^L \bar{\sigma}' \bar{e}_\sigma^M \mathcal{D}_M \bar{R}_{IKJL} \quad (\text{B.46})$$

## Appendix C

# Simplifications for our specific non-minimal model

In our specific model, the metric and its inverse are given by

$$G_{IJ} = \begin{pmatrix} 1 & 0 \\ 0 & \Omega(\phi)^2 \end{pmatrix}, \quad \text{and} \quad G^{IJ} = \begin{pmatrix} 1 & 0 \\ 0 & \Omega(\phi)^{-2} \end{pmatrix}. \quad (\text{C.1})$$

The non-trivial connections derived from this metric are then

$$\bar{\Gamma}_{\chi\chi}^\phi = -\Omega\Omega_{,\phi} \quad (\text{C.2})$$

and

$$\bar{\Gamma}_{\phi\chi}^\chi = \Omega^{-1}\Omega_{,\phi}, \quad (\text{C.3})$$

while the only non-trivial component (up to those related by symmetry) of the Riemann tensor is

$$\bar{R}_{\phi\chi\phi\chi} = -\Omega\Omega_{,\phi\phi}. \quad (\text{C.4})$$

The covariant derivatives of the Riemann tensor in our model are

$$\mathcal{D}_\chi \bar{R}_{\phi\chi\phi\chi} = 0, \quad (\text{C.5})$$

$$\mathcal{D}_\phi \bar{R}_{\phi\chi\phi\chi} = \Omega_{,\phi}\Omega_{,\phi\phi} - \Omega\Omega_{,\phi\phi\phi}, \quad (\text{C.6})$$

$$\mathcal{D}_\phi \mathcal{D}_\phi \bar{R}_{\phi\chi\phi\chi} = -\Omega\Omega_{,\phi\phi\phi\phi} + 2\Omega_{,\phi}\Omega_{,\phi\phi\phi} + \Omega_{,\phi\phi}^2 - 2\Omega^{-1}\Omega_{,\phi}^2\Omega_{,\phi\phi}, \quad (\text{C.7})$$

$$\mathcal{D}_\chi \mathcal{D}_\chi \bar{R}_{\phi\chi\phi\chi} = -\Omega^2\Omega_{,\phi}\Omega_{,\phi\phi\phi} + \Omega\Omega_{,\phi}^2\Omega_{,\phi\phi}, \quad (\text{C.8})$$

$$\mathcal{D}_\phi \mathcal{D}_\chi \bar{R}_{\phi\chi\phi\chi} = \mathcal{D}_\chi \mathcal{D}_\phi \bar{R}_{\phi\chi\phi\chi} = 0. \quad (\text{C.9})$$

We can define the zweibeine, via  $e_\sigma^I \equiv \frac{\dot{\phi}^J}{\dot{\sigma}}$ , such that

$$\bar{e}_\sigma^\phi = \frac{\bar{\phi}'}{\bar{\sigma}'}, \quad \bar{e}_\sigma^\chi = \frac{\bar{\chi}'}{\bar{\sigma}'}, \quad (\text{C.10})$$

$$\bar{e}_s^\phi = -\Omega \frac{\bar{\chi}'}{\bar{\sigma}'}, \quad \bar{e}_s^\chi = \Omega^{-1} \frac{\bar{\phi}'}{\bar{\sigma}'}, \quad (\text{C.11})$$

$$\bar{e}_{\sigma\phi} = \frac{\bar{\phi}'}{\bar{\sigma}'}, \quad \bar{e}_{\sigma\chi} = \Omega^2 \frac{\bar{\chi}'}{\bar{\sigma}'}, \quad (\text{C.12})$$

$$\bar{e}_{s\phi} = -\Omega \frac{\bar{\chi}'}{\bar{\sigma}'}, \quad \bar{e}_{s\chi} = \Omega \frac{\bar{\phi}'}{\bar{\sigma}'}, \quad (\text{C.13})$$

where a dot denotes a Lie derivative and a prime a derivative w.r.t. coordinate time  $t$ . Note that within this setup we must take  $\bar{e}_\sigma^\phi = -1$  during the ekpyrotic phase; this is because  $\sigma$  is defined to increase along the background trajectory [19] and thus  $\bar{\sigma}' = -\bar{\phi}'$  is the velocity on the background trajectory in the constant  $\chi$  backgrounds that we are interested in.

**Simplifications during the ekpyrotic phase:**

$$\delta s|_{\text{ekp}} = -\Omega \delta \chi, \quad (\text{C.14})$$

$$\delta s'|_{\text{ekp}} = -\bar{\phi}' \Omega_{,\phi} \delta \chi = -\bar{\sigma}' \Omega^{-1} \Omega_{,\phi} \delta s \quad \therefore \quad \delta \chi'|_{\text{ekp}} = 0, \quad (\text{C.15})$$

$$\delta s^{(2)}|_{\text{ekp}} = 0, \quad (\text{C.16})$$

$$\bar{V}_{,\sigma}|_{\text{ekp}} = -\bar{V}_{,\phi}, \quad (\text{C.17})$$

$$\bar{V}_{,s}|_{\text{ekp}} = \bar{\theta}' = 0, \quad (\text{C.18})$$

$$\bar{V}_{;\sigma\sigma}|_{\text{ekp}} = \bar{V}_{,\phi\phi}, \quad (\text{C.19})$$

$$\bar{V}_{;s\sigma}|_{\text{ekp}} = 0, \quad (\text{C.20})$$

$$\bar{V}_{;ss}|_{\text{ekp}} = \Omega^{-1} \Omega_{,\phi} \bar{V}_{,\phi}, \quad (\text{C.21})$$

$$\bar{V}_{;ss\sigma}|_{\text{ekp}} = (-\Omega^{-1} \Omega_{,\phi\phi} + \Omega^{-2} \Omega_{,\phi}^2) \bar{V}_{,\phi} - \Omega^{-1} \Omega_{,\phi} \bar{V}_{,\phi\phi}, \quad (\text{C.22})$$

$$\bar{V}_{;sss}|_{\text{ekp}} = 0, \quad (\text{C.23})$$

$$\bar{V}_{;ssss}|_{\text{ekp}} = -3\Omega^{-3} \Omega_{,\phi}^3 \bar{V}_{,\phi} + 3\Omega^{-2} \Omega_{,\phi}^2 \bar{V}_{,\phi\phi} + \Omega^{-2} \Omega_{,\phi} \Omega_{,\phi\phi} \bar{V}_{,\phi}, \quad (\text{C.24})$$

$$\mathcal{D}_\chi \bar{R}_{\chi\phi\chi\phi}|_{\text{ekp}} = 0, \quad (\text{C.25})$$

$$\mathcal{D}_\phi \bar{R}_{\chi\phi\chi\phi}|_{\text{ekp}} = \Omega_{,\phi} \Omega_{,\phi\phi} - \Omega \Omega_{,\phi\phi\phi}, \quad (\text{C.26})$$

$$\mathcal{D}_\chi \mathcal{D}_\chi \bar{R}_{\chi\phi\chi\phi}|_{\text{ekp}} = \Omega \Omega_{,\phi} (\Omega_{,\phi} \Omega_{,\phi\phi} - \Omega \Omega_{,\phi\phi\phi}), \quad (\text{C.27})$$

$$A^{(1)}|_{\text{ekp}} = A^{(2)}|_{\text{ekp}} = 0, \quad (\text{C.28})$$

$$\delta \dot{\sigma}^2|_{\text{ekp}} = \delta (\dot{\sigma}^2)^{(2)}|_{\text{ekp}} = 0, \quad (\text{C.29})$$

$$\bar{\Theta} = 3H, \quad \delta \Theta|_{\text{ekp}} = \delta \Theta^{(2)}|_{\text{ekp}} = 0, \quad (\text{C.30})$$

$$\delta V_{;ss}|_{\text{ekp}} = \delta V_{;ss}^{(2)}|_{\text{ekp}} = 0, \quad (\text{C.31})$$

$$\delta \dot{\theta}|_{\text{ekp}} = \delta \dot{\theta}^{(2)}|_{\text{ekp}} = 0, \quad (\text{C.32})$$

$$\delta [\dot{\sigma}^2 e_s^I e_s^J e_\sigma^K e_\sigma^L R_{IKJL}]|_{\text{ekp}} = \delta [\dot{\sigma}^2 e_s^I e_s^J e_\sigma^K e_\sigma^L R_{IKJL}]^{(2)}|_{\text{ekp}} = 0, \quad (\text{C.33})$$

$$\delta s_i^{(2)}|_{\text{ekp}} = \partial_i \delta s^{(2)}|_{\text{ekp}} = 0, \quad (\text{C.34})$$

$$\delta s_i^{(3)}|_{\text{ekp}} = \delta \dot{s}_i^{(3)}|_{\text{ekp}} = \delta \ddot{s}_i^{(3)}|_{\text{ekp}} = 0, \quad (\text{C.35})$$

$$\delta e_\sigma^\phi|_{\text{ekp}} = \delta e_{\sigma\phi}|_{\text{ekp}} = 0, \quad (\text{C.36})$$

$$\delta e_\sigma^\chi|_{\text{ekp}} = \delta e_{\sigma\chi}|_{\text{ekp}} = 0, \quad (\text{C.37})$$

$$\delta e_s^\phi|_{\text{ekp}} = \delta e_{s\phi}|_{\text{ekp}} = 0, \quad (\text{C.38})$$

$$\delta e_s^\chi|_{\text{ekp}} = \delta e_{s\chi}|_{\text{ekp}} = 0, \quad (\text{C.39})$$

$$\delta e_\sigma^{\phi(2)}|_{\text{ekp}} = \delta e_{\sigma\phi}^{(2)}|_{\text{ekp}} = 0, \quad (\text{C.40})$$

$$\delta e_\sigma^{\chi(2)}|_{\text{ekp}} = \frac{\bar{\theta}'}{2\bar{\sigma}'} \Omega^{-2} \Omega_{,\phi} \delta s^2, \quad \delta e_{\sigma\chi}^{(2)}|_{\text{ekp}} = \frac{\bar{\theta}'}{2\bar{\sigma}'} \Omega_{,\phi} \delta s^2, \quad (\text{C.41})$$

$$\delta e_s^{\phi(2)}|_{\text{ekp}} = \delta e_{s\phi}^{(2)}|_{\text{ekp}} = -\frac{\bar{\theta}'}{2\bar{\sigma}'} \Omega^{-1} \Omega_{,\phi} \delta s^2, \quad (\text{C.42})$$

$$\delta e_s^{\chi(2)}|_{\text{ekp}} = \delta e_{s\chi}^{(2)}|_{\text{ekp}} = 0. \quad (\text{C.43})$$

$$\delta G_{IJ}|_{\text{ekp}} = 0, \quad (\text{C.44})$$

$$\delta G_{IJ}^{(2)}|_{\text{ekp}} = 0. \quad (\text{C.45})$$

# Bibliography

- [1] European Space Agency, “PLANCK CMB.”  
[http://www.esa.int/spaceinimages/Images/2013/03/Planck\\_CMB](http://www.esa.int/spaceinimages/Images/2013/03/Planck_CMB), 2013  
(accessed 2016-03-05).
- [2] J. Schombert, “James Schombert v7.0.”  
[http://abyss.uoregon.edu/~js/images/universe\\_geometry.gif](http://abyss.uoregon.edu/~js/images/universe_geometry.gif), 2015  
(accessed 2016-02-02).
- [3] D. Baumann, “Inflation,” [0907.5424](#).
- [4] **Planck** Collaboration, P. A. R. Ade *et. al.*, “Planck 2015 results. XX. Constraints on inflation,” [1502.02114](#).
- [5] J.-L. Lehners, “Ekpyrotic and Cyclic Cosmology,” *Phys. Rept.* **465** (2008) 223–263, [0806.1245](#).
- [6] C. Gordon, D. Wands, B. A. Bassett, and R. Maartens, “Adiabatic and entropy perturbations from inflation,” *Phys. Rev.* **D63** (2001) 023506, [astro-ph/0009131](#).
- [7] J.-L. Lehners, “Ekpyrotic Non-Gaussianity: A Review,” *Adv. Astron.* **2010** (2010) 903907, [1001.3125](#).
- [8] A. A. Penzias and R. W. Wilson, “A Measurement of excess antenna temperature at 4080-Mc/s,” *Astrophys. J.* **142** (1965) 419–421.
- [9] **Planck** Collaboration, P. A. R. Ade *et. al.*, “Planck 2015 results. XIII. Cosmological parameters,” [1502.01589](#).
- [10] **Planck** Collaboration, P. A. R. Ade *et. al.*, “Planck 2015 results. XVII. Constraints on primordial non-Gaussianity,” [1502.01592](#).

- [11] M. Alvarez *et. al.*, “Testing Inflation with Large Scale Structure: Connecting Hopes with Reality,” [1412.4671](https://arxiv.org/abs/1412.4671).
- [12] C. M. Will, “The Confrontation between General Relativity and Experiment,” *Living Rev. Rel.* **17** (2014) 4, [1403.7377](https://arxiv.org/abs/1403.7377).
- [13] **Supernova Search Team** Collaboration, A. G. Riess *et. al.*, “Observational evidence from supernovae for an accelerating universe and a cosmological constant,” *Astron. J.* **116** (1998) 1009–1038, [astro-ph/9805201](https://arxiv.org/abs/astro-ph/9805201).
- [14] E. J. Copeland, M. Sami, and S. Tsujikawa, “Dynamics of dark energy,” *Int. J. Mod. Phys. D* **15** (2006) 1753–1936, [hep-th/0603057](https://arxiv.org/abs/hep-th/0603057).
- [15] **BICEP2** Collaboration, P. A. R. Ade *et. al.*, “Detection of  $B$ -Mode Polarization at Degree Angular Scales by BICEP2,” *Phys. Rev. Lett.* **112** (2014), no. 24 241101, [1403.3985](https://arxiv.org/abs/1403.3985).
- [16] **BICEP2, Planck** Collaboration, P. A. R. Ade *et. al.*, “A Joint Analysis of BICEP2/Keck Array and Planck Data,” *Phys. Rev. Lett.* **114** (2015) 101301, [1502.00612](https://arxiv.org/abs/1502.00612).
- [17] A. Ijjas, P. J. Steinhardt, and A. Loeb, “Inflationary paradigm in trouble after Planck2013,” *Phys. Lett. B* **723** (2013) 261–266, [1304.2785](https://arxiv.org/abs/1304.2785).
- [18] A. Fertig and J.-L. Lehners, “The Non-Minimal Ekpyrotic Trispectrum,” *JCAP* **1601** (2016) 026, [1510.03439](https://arxiv.org/abs/1510.03439).
- [19] S. Renaux-Petel and G. Tasinato, “Nonlinear perturbations of cosmological scalar fields with non-standard kinetic terms,” *JCAP* **0901** (2009) 012, [0810.2405](https://arxiv.org/abs/0810.2405).
- [20] J.-L. Lehners and S. Renaux-Petel, “Multifield Cosmological Perturbations at Third Order and the Ekpyrotic Trispectrum,” *Phys. Rev. D* **80** (2009) 063503, [0906.0530](https://arxiv.org/abs/0906.0530).
- [21] T. Qiu, X. Gao, and E. N. Saridakis, “Towards Anisotropy-Free and Non-Singular Bounce Cosmology with Scale-invariant Perturbations,” *Phys. Rev. D* **88** (2013) 043525, [1303.2372](https://arxiv.org/abs/1303.2372).
- [22] M. Li, “Note on the production of scale-invariant entropy perturbation in the Ekpyrotic universe,” *Phys. Lett. B* **724** (2013) 192–197, [1306.0191](https://arxiv.org/abs/1306.0191).

- [23] A. Ijjas, J.-L. Lehners, and P. J. Steinhardt, “General mechanism for producing scale-invariant perturbations and small non-Gaussianity in ekpyrotic models,” *Phys. Rev.* **D89** (2014), no. 12 123520, [1404.1265](#).
- [24] A. Fertig, J.-L. Lehners, and E. Mallwitz, “Ekpyrotic Perturbations With Small Non-Gaussian Corrections,” *Phys. Rev.* **D89** (2014), no. 10 103537, [1310.8133](#).
- [25] A. H. Guth, “The Inflationary Universe: A Possible Solution to the Horizon and Flatness Problems,” *Phys. Rev.* **D23** (1981) 347–356.
- [26] J. K. Erickson, D. H. Wesley, P. J. Steinhardt, and N. Turok, “Kasner and mixmaster behavior in universes with equation of state  $w \geq 1$ ,” *Phys. Rev.* **D69** (2004) 063514, [hep-th/0312009](#).
- [27] V. F. Mukhanov and G. V. Chibisov, “Quantum Fluctuation and Nonsingular Universe. (In Russian),” *JETP Lett.* **33** (1981) 532–535.
- [28] J.-L. Lehners, P. McFadden, N. Turok, and P. J. Steinhardt, “Generating ekpyrotic curvature perturbations before the big bang,” *Phys. Rev.* **D76** (2007) 103501, [hep-th/0702153](#).
- [29] J.-L. Lehners, “Classical Inflationary and Ekpyrotic Universes in the No-Boundary Wavefunction,” *Phys. Rev.* **D91** (2015), no. 8 083525, [1502.00629](#).
- [30] J. Martin, C. Ringeval, R. Trotta, and V. Vennin, “The Best Inflationary Models After Planck,” *JCAP* **1403** (2014) 039, [1312.3529](#).
- [31] J.-L. Lehners and P. J. Steinhardt, “Planck 2013 results support the cyclic universe,” *Phys. Rev.* **D87** (2013), no. 12 123533, [1304.3122](#).
- [32] J.-L. Lehners, “Cosmic Bounces and Cyclic Universes,” *Class. Quant. Grav.* **28** (2011) 204004, [1106.0172](#).
- [33] A. Fertig, J.-L. Lehners, and E. Mallwitz, “Conflation: a new type of accelerated expansion,” [1507.04742](#).
- [34] A. Einstein, “The Foundation of the General Theory of Relativity,” *Annalen Phys.* **49** (1916) 769–822. [Annalen Phys. 14, 517 (2005)].

- [35] A. Einstein, “Cosmological Considerations in the General Theory of Relativity,” *Sitzungsber. Preuss. Akad. Wiss. Berlin (Math. Phys.)* **1917** (1917) 142–152.
- [36] A. Friedmann, “On the Curvature of space,” *Z. Phys.* **10** (1922) 377–386. [Gen. Rel. Grav. 31, 1991 (1999)].
- [37] A. Friedmann, “On the Possibility of a World with Constant Negative Curvature of Space,” *Z. Phys.* **21** (1924) 326–332. [Gen. Rel. Grav. 31, 2001 (1999)].
- [38] G. Lemaitre, “A homogeneous Universe of constant mass and growing radius accounting for the radial velocity of extragalactic nebulae,” *Annales Soc. Sci. Brux. Ser. I Sci. Math. Astron. Phys.* **A47** (1927) 49–59.
- [39] G. Lemaitre, “Republication of: The beginning of the world from the point of view of quantum theory,” *Nature* **127** (1931) 706. [Gen. Rel. Grav. 43, 2929 (2011)].
- [40] E. Hubble, “A relation between distance and radial velocity among extra-galactic nebulae,” *Proc. Nat. Acad. Sci.* **15** (1929) 168–173.
- [41] G. Gamow, “Expanding universe and the origin of elements,” *Phys. Rev.* **70** (1946) 572–573.
- [42] R. A. Alpher, H. Bethe, and G. Gamow, “The origin of chemical elements,” *Phys. Rev.* **73** (1948) 803–804.
- [43] G. F. Smoot *et. al.*, “Structure in the COBE differential microwave radiometer first year maps,” *Astrophys. J.* **396** (1992) L1–L5.
- [44] S. Weinberg, “The Cosmological Constant Problem,” *Rev. Mod. Phys.* **61** (1989) 1–23.
- [45] T. W. B. Kibble, “Topology of Cosmic Domains and Strings,” *J. Phys.* **A9** (1976) 1387–1398.
- [46] T. W. B. Kibble, “Some Implications of a Cosmological Phase Transition,” *Phys. Rept.* **67** (1980) 183.

- [47] A. H. Guth and S. H. H. Tye, “Phase Transitions and Magnetic Monopole Production in the Very Early Universe,” *Phys. Rev. Lett.* **44** (1980) 631. [Erratum: Phys. Rev. Lett. 44, 963 (1980)].
- [48] M. B. Einhorn, D. L. Stein, and D. Toussaint, “Are Grand Unified Theories Compatible with Standard Cosmology?,” *Phys. Rev.* **D21** (1980) 3295.
- [49] Ya. B. Zeldovich and M. Yu. Khlopov, “On the Concentration of Relic Magnetic Monopoles in the Universe,” *Phys. Lett.* **B79** (1978) 239–241.
- [50] J. Preskill, “Cosmological Production of Superheavy Magnetic Monopoles,” *Phys. Rev. Lett.* **43** (1979) 1365.
- [51] **Particle Data Group** Collaboration, K. A. Olive *et. al.*, “Review of Particle Physics,” *Chin. Phys.* **C38** (2014) 090001.
- [52] S. W. Hawking and R. Penrose, “The Singularities of gravitational collapse and cosmology,” *Proc. Roy. Soc. Lond.* **A314** (1970) 529–548.
- [53] R. H. Dicke and P. J. E. Peebles, “The big bang cosmology – enigmas and nostrums,” in *General Relativity: An Einstein Centenary Survey* (S. W. Hawking and W. Israel, eds.), ch. 9, pp. 504–517. Cambridge University Press, 1979.
- [54] R. Brout, F. Englert, and E. Gunzig, “The Causal Universe,” *Gen. Rel. Grav.* **10** (1979) 1–6.
- [55] A. A. Starobinsky, “Spectrum of relict gravitational radiation and the early state of the universe,” *JETP Lett.* **30** (1979) 682–685. [Pisma Zh. Eksp. Teor. Fiz. 30, 719 (1979)].
- [56] A. A. Starobinsky, “A New Type of Isotropic Cosmological Models Without Singularity,” *Phys. Lett.* **B91** (1980) 99–102.
- [57] K. Sato, “Cosmological Baryon Number Domain Structure and the First Order Phase Transition of a Vacuum,” *Phys. Lett.* **B99** (1981) 66–70.
- [58] D. Kazanas, “Dynamics of the Universe and Spontaneous Symmetry Breaking,” *Astrophys. J.* **241** (1980) L59–L63.

[59] A. D. Linde, “A New Inflationary Universe Scenario: A Possible Solution of the Horizon, Flatness, Homogeneity, Isotropy and Primordial Monopole Problems,” *Phys. Lett.* **B108** (1982) 389–393.

[60] A. Albrecht and P. J. Steinhardt, “Cosmology for Grand Unified Theories with Radiatively Induced Symmetry Breaking,” *Phys. Rev. Lett.* **48** (1982) 1220–1223.

[61] S. R. Coleman and E. J. Weinberg, “Radiative Corrections as the Origin of Spontaneous Symmetry Breaking,” *Phys. Rev.* **D7** (1973) 1888–1910.

[62] A. D. Linde, “Chaotic Inflation,” *Phys. Lett.* **B129** (1983) 177–181.

[63] S. W. Hawking, “The Development of Irregularities in a Single Bubble Inflationary Universe,” *Phys. Lett.* **B115** (1982) 295.

[64] A. A. Starobinsky, “Dynamics of Phase Transition in the New Inflationary Universe Scenario and Generation of Perturbations,” *Phys. Lett.* **B117** (1982) 175–178.

[65] A. H. Guth and S. Y. Pi, “Fluctuations in the New Inflationary Universe,” *Phys. Rev. Lett.* **49** (1982) 1110–1113.

[66] J. M. Bardeen, P. J. Steinhardt, and M. S. Turner, “Spontaneous Creation of Almost Scale - Free Density Perturbations in an Inflationary Universe,” *Phys. Rev.* **D28** (1983) 679.

[67] R. L. Arnowitt, S. Deser, and C. W. Misner, “The Dynamics of general relativity,” *Gen. Rel. Grav.* **40** (2008) 1997–2027, [gr-qc/0405109](https://arxiv.org/abs/gr-qc/0405109).

[68] J. M. Maldacena, “Non-Gaussian features of primordial fluctuations in single field inflationary models,” *JHEP* **05** (2003) 013, [astro-ph/0210603](https://arxiv.org/abs/astro-ph/0210603).

[69] M. Sasaki, “Large Scale Quantum Fluctuations in the Inflationary Universe,” *Prog. Theor. Phys.* **76** (1986) 1036.

[70] V. F. Mukhanov, “Quantum Theory of Gauge Invariant Cosmological Perturbations,” *Sov. Phys. JETP* **67** (1988) 1297–1302. [Zh. Eksp. Teor. Fiz. 94N7,1(1988)].

[71] C. T. Byrnes, M. Sasaki, and D. Wands, “The primordial trispectrum from inflation,” *Phys. Rev.* **D74** (2006) 123519, [astro-ph/0611075](https://arxiv.org/abs/astro-ph/0611075).

[72] J. M. Bardeen, “Gauge Invariant Cosmological Perturbations,” *Phys. Rev.* **D22** (1980) 1882–1905.

[73] D. Seery and J. E. Lidsey, “Non-Gaussianity from the inflationary trispectrum,” *JCAP* **0701** (2007) 008, [astro-ph/0611034](#).

[74] R. Penrose, “Difficulties with inflationary cosmology,” *Annals N. Y. Acad. Sci.* **571** (1989) 249–264.

[75] G. W. Gibbons and N. Turok, “The Measure Problem in Cosmology,” *Phys. Rev.* **D77** (2008) 063516, [hep-th/0609095](#).

[76] D. Baumann and L. McAllister, *Inflation and String Theory*. Cambridge University Press, 2015.

[77] K. Dasgupta, R. Gwyn, E. McDonough, M. Mia, and R. Tatar, “de Sitter Vacua in Type IIB String Theory: Classical Solutions and Quantum Corrections,” *JHEP* **1407** (2014) 054, [1402.5112](#).

[78] P. J. Steinhardt, “Natural inflation,” in *The Very Early Universe* (G. Gibbons, S. Hawking, and S. Siklos, eds.), pp. 251–266. Cambridge University Press, 1983.

[79] A. Vilenkin, “The Birth of Inflationary Universes,” *Phys. Rev.* **D27** (1983) 2848.

[80] A. De Simone, A. H. Guth, M. P. Salem, and A. Vilenkin, “Predicting the cosmological constant with the scale-factor cutoff measure,” *Phys. Rev.* **D78** (2008) 063520, [0805.2173](#).

[81] J. Garriga and A. Vilenkin, “Watchers of the multiverse,” *JCAP* **1305** (2013) 037, [1210.7540](#).

[82] A. Borde, A. H. Guth, and A. Vilenkin, “Inflationary space-times are incomplete in past directions,” *Phys. Rev. Lett.* **90** (2003) 151301, [gr-qc/0110012](#).

[83] J. Khoury, B. A. Ovrut, P. J. Steinhardt, and N. Turok, “The Ekpyrotic universe: Colliding branes and the origin of the hot big bang,” *Phys. Rev.* **D64** (2001) 123522, [hep-th/0103239](#).

- [84] V. Belinsky, I. Khalatnikov, and E. Lifshitz, “Oscillatory approach to a singular point in the relativistic cosmology,” *Adv. Phys.* **19** (1970) 525–573.
- [85] C. W. Misner, “Mixmaster universe,” *Phys. Rev. Lett.* **22** (1969) 1071–1074.
- [86] C. W. Misner, K. S. Thorne, and J. A. Wheeler, *Gravitation*. W. H. Freeman, San Francisco, 1973.
- [87] A. Notari and A. Riotto, “Isocurvature perturbations in the ekpyrotic universe,” *Nucl. Phys.* **B644** (2002) 371–382, [hep-th/0205019](https://arxiv.org/abs/hep-th/0205019).
- [88] L. Battarra and J.-L. Lehners, “Quantum-to-classical transition for ekpyrotic perturbations,” *Phys. Rev.* **D89** (2014), no. 6 063516, [1309.2281](https://arxiv.org/abs/1309.2281).
- [89] K. Koyama and D. Wands, “Ekpyrotic collapse with multiple fields,” *JCAP* **0704** (2007) 008, [hep-th/0703040](https://arxiv.org/abs/hep-th/0703040).
- [90] K. Koyama, S. Mizuno, and D. Wands, “Curvature perturbations from ekpyrotic collapse with multiple fields,” *Class. Quant. Grav.* **24** (2007) 3919–3932, [0704.1152](https://arxiv.org/abs/0704.1152).
- [91] J. M. Stewart and M. Walker, “Perturbations of spacetimes in general relativity,” *Proc. Roy. Soc. Lond.* **A341** (1974) 49–74.
- [92] A. J. Tolley and D. H. Wesley, “Scale-invariance in expanding and contracting universes from two-field models,” *JCAP* **0705** (2007) 006, [hep-th/0703101](https://arxiv.org/abs/hep-th/0703101).
- [93] E. I. Buchbinder, J. Khoury, and B. A. Ovrut, “On the initial conditions in new ekpyrotic cosmology,” *JHEP* **11** (2007) 076, [0706.3903](https://arxiv.org/abs/0706.3903).
- [94] J.-L. Lehners and P. J. Steinhardt, “Dark Energy and the Return of the Phoenix Universe,” *Phys. Rev.* **D79** (2009) 063503, [0812.3388](https://arxiv.org/abs/0812.3388).
- [95] J. Khoury, P. J. Steinhardt, and N. Turok, “Inflation versus cyclic predictions for spectral tilt,” *Phys. Rev. Lett.* **91** (2003) 161301, [astro-ph/0302012](https://arxiv.org/abs/astro-ph/0302012).
- [96] D. H. Lyth, K. A. Malik, and M. Sasaki, “A General proof of the conservation of the curvature perturbation,” *JCAP* **0505** (2005) 004, [astro-ph/0411220](https://arxiv.org/abs/astro-ph/0411220).
- [97] E. I. Buchbinder, J. Khoury, and B. A. Ovrut, “Non-Gaussianities in new ekpyrotic cosmology,” *Phys. Rev. Lett.* **100** (2008) 171302, [0710.5172](https://arxiv.org/abs/0710.5172).

[98] J.-L. Lehners and P. J. Steinhardt, “Non-Gaussianity Generated by the Entropic Mechanism in Bouncing Cosmologies Made Simple,” *Phys. Rev.* **D80** (2009) 103520, [0909.2558](#).

[99] E. I. Buchbinder, J. Khoury, and B. A. Ovrut, “New Ekpyrotic cosmology,” *Phys. Rev.* **D76** (2007) 123503, [hep-th/0702154](#).

[100] J.-L. Lehners, P. McFadden, and N. Turok, “Colliding Branes in Heterotic M-theory,” *Phys. Rev.* **D75** (2007) 103510, [hep-th/0611259](#).

[101] J.-L. Lehners and N. Turok, “Bouncing Negative-Tension Branes,” *Phys. Rev.* **D77** (2008) 023516, [0708.0743](#).

[102] P. Creminelli, A. Nicolis, and M. Zaldarriaga, “Perturbations in bouncing cosmologies: Dynamical attractor versus scale invariance,” *Phys. Rev.* **D71** (2005) 063505, [hep-th/0411270](#).

[103] M. Koehn, J.-L. Lehners, and B. Ovrut, “Non-Singular Bouncing Cosmology: Consistency of the Effective Description,” [1512.03807](#).

[104] T. Battefeld, “Modulated Perturbations from Instant Preheating after new Ekpyrosis,” *Phys. Rev.* **D77** (2008) 063503, [0710.2540](#).

[105] J.-L. Lehners, P. McFadden, and N. Turok, “Effective Actions for Heterotic M-Theory,” *Phys. Rev.* **D76** (2007) 023501, [hep-th/0612026](#).

[106] M. Alishahiha, E. Silverstein, and D. Tong, “DBI in the sky,” *Phys. Rev.* **D70** (2004) 123505, [hep-th/0404084](#).

[107] X. Chen, M.-x. Huang, S. Kachru, and G. Shiu, “Observational signatures and non-Gaussianities of general single field inflation,” *JCAP* **0701** (2007) 002, [hep-th/0605045](#).

[108] D. H. Lyth, “The Primordial curvature perturbation in the ekpyrotic universe,” *Phys. Lett.* **B524** (2002) 1–4, [hep-ph/0106153](#).

[109] L. A. Boyle, P. J. Steinhardt, and N. Turok, “The Cosmic gravitational wave background in a cyclic universe,” *Phys. Rev.* **D69** (2004) 127302, [hep-th/0307170](#).

[110] D. Baumann, P. J. Steinhardt, K. Takahashi, and K. Ichiki, “Gravitational Wave Spectrum Induced by Primordial Scalar Perturbations,” *Phys. Rev.* **D76** (2007) 084019, [hep-th/0703290](#).

[111] D. Battefeld and P. Peter, “A Critical Review of Classical Bouncing Cosmologies,” *Phys. Rept.* **571** (2015) 1–66, [1406.2790](#).

[112] N. Turok, M. Perry, and P. J. Steinhardt, “M theory model of a big crunch / big bang transition,” *Phys. Rev.* **D70** (2004) 106004, [hep-th/0408083](#).

[113] I. Bars, S.-H. Chen, P. J. Steinhardt, and N. Turok, “Antigravity and the Big Crunch/Big Bang Transition,” *Phys. Lett.* **B715** (2012) 278–281, [1112.2470](#).

[114] S. Gielen and N. Turok, “A Perfect Bounce,” [1510.00699](#).

[115] P. Creminelli and L. Senatore, “A Smooth bouncing cosmology with scale invariant spectrum,” *JCAP* **0711** (2007) 010, [hep-th/0702165](#).

[116] D. A. Easson, I. Sawicki, and A. Vikman, “G-Bounce,” *JCAP* **1111** (2011) 021, [1109.1047](#).

[117] Y.-F. Cai, D. A. Easson, and R. Brandenberger, “Towards a Nonsingular Bouncing Cosmology,” *JCAP* **1208** (2012) 020, [1206.2382](#).

[118] N. Arkani-Hamed, H.-C. Cheng, M. A. Luty, and S. Mukohyama, “Ghost condensation and a consistent infrared modification of gravity,” *JHEP* **05** (2004) 074, [hep-th/0312099](#).

[119] A. Nicolis, R. Rattazzi, and E. Trincherini, “The Galileon as a local modification of gravity,” *Phys. Rev.* **D79** (2009) 064036, [0811.2197](#).

[120] B. Xue, D. Garfinkle, F. Pretorius, and P. J. Steinhardt, “Nonperturbative analysis of the evolution of cosmological perturbations through a nonsingular bounce,” *Phys. Rev.* **D88** (2013) 083509, [1308.3044](#).

[121] L. Battarra, M. Koehn, J.-L. Lehners, and B. A. Ovrut, “Cosmological Perturbations Through a Non-Singular Ghost-Condensate/Galileon Bounce,” *JCAP* **1407** (2014) 007, [1404.5067](#).

[122] M. Koehn, J.-L. Lehners, and B. A. Ovrut, “Cosmological super-bounce,” *Phys. Rev.* **D90** (2014), no. 2 025005, [1310.7577](#).

- [123] D. Langlois and F. Vernizzi, “Evolution of non-linear cosmological perturbations,” *Phys. Rev. Lett.* **95** (2005) 091303, [astro-ph/0503416](#).
- [124] D. Langlois and F. Vernizzi, “Conserved non-linear quantities in cosmology,” *Phys. Rev.* **D72** (2005) 103501, [astro-ph/0509078](#).
- [125] D. Langlois and F. Vernizzi, “Nonlinear perturbations for dissipative and interacting relativistic fluids,” *JCAP* **0602** (2006) 014, [astro-ph/0601271](#).
- [126] D. Langlois and F. Vernizzi, “Nonlinear perturbations of cosmological scalar fields,” *JCAP* **0702** (2007) 017, [astro-ph/0610064](#).
- [127] G. F. R. Ellis and M. Bruni, “Covariant and Gauge Invariant Approach to Cosmological Density Fluctuations,” *Phys. Rev.* **D40** (1989) 1804–1818.
- [128] M. Bruni, G. F. R. Ellis, and P. K. S. Dunsby, “Gauge invariant perturbations in a scalar field dominated universe,” *Class. Quant. Grav.* **9** (1992) 921–946.
- [129] S. W. Hawking, “Perturbations of an expanding universe,” *Astrophys. J.* **145** (1966) 544–554.
- [130] R. M. Wald, *General Relativity*. The University of Chicago Press, 1984.
- [131] D. Langlois and S. Renaux-Petel, “Perturbations in generalized multi-field inflation,” *JCAP* **0804** (2008) 017, [0801.1085](#).
- [132] S. Groot Nibbelink and B. J. W. van Tent, “Density perturbations arising from multiple field slow roll inflation,” [hep-ph/0011325](#).
- [133] G. I. Rigopoulos, E. P. S. Shellard, and B. J. W. van Tent, “Non-linear perturbations in multiple-field inflation,” *Phys. Rev.* **D73** (2006) 083521, [astro-ph/0504508](#).
- [134] D. Wands, K. A. Malik, D. H. Lyth, and A. R. Liddle, “A New approach to the evolution of cosmological perturbations on large scales,” *Phys. Rev.* **D62** (2000) 043527, [astro-ph/0003278](#).
- [135] K. A. Malik and D. Wands, “Cosmological perturbations,” *Phys. Rept.* **475** (2009) 1–51, [0809.4944](#).
- [136] M. Bruni, S. Matarrese, S. Mollerach, and S. Sonego, “Perturbations of space-time: Gauge transformations and gauge invariance at second order and beyond,” *Class. Quant. Grav.* **14** (1997) 2585–2606, [gr-qc/9609040](#).

- [137] L. Battarra and J.-L. Lehners, “On the Creation of the Universe via Ekpyrotic Instantons,” *Phys. Lett.* **B742** (2015) 167–171, [1406.5896](#).
- [138] L. Battarra and J.-L. Lehners, “On the No-Boundary Proposal for Ekpyrotic and Cyclic Cosmologies,” *JCAP* **1412** (2014) 023, [1407.4814](#).
- [139] J.-L. Lehners, “New Ekpyrotic Quantum Cosmology,” *Phys. Lett.* **B750** (2015) 242–246, [1504.02467](#).
- [140] V. Rubakov, “Harrison-Zeldovich spectrum from conformal invariance,” *JCAP* **0909** (2009) 030, [0906.3693](#).
- [141] K. Hinterbichler and J. Khoury, “The Pseudo-Conformal Universe: Scale Invariance from Spontaneous Breaking of Conformal Symmetry,” *JCAP* **1204** (2012) 023, [1106.1428](#).
- [142] P. Creminelli, A. Nicolis, and E. Trincherini, “Galilean Genesis: An Alternative to inflation,” *JCAP* **1011** (2010) 021, [1007.0027](#).
- [143] F. Di Marco, F. Finelli, and R. Brandenberger, “Adiabatic and isocurvature perturbations for multifield generalized Einstein models,” *Phys. Rev.* **D67** (2003) 063512, [astro-ph/0211276](#).
- [144] C.-Y. Tseng, “Decoherence problem in an ekpyrotic phase,” *Phys. Rev.* **D87** (2013), no. 2 023518, [1210.0581](#).
- [145] K. Koyama, S. Mizuno, F. Vernizzi, and D. Wands, “Non-Gaussianities from ekpyrotic collapse with multiple fields,” *JCAP* **0711** (2007) 024, [0708.4321](#).
- [146] J.-L. Lehners and P. J. Steinhardt, “Non-Gaussian density fluctuations from entropically generated curvature perturbations in Ekpyrotic models,” *Phys. Rev.* **D77** (2008) 063533, [0712.3779](#). [Erratum: *Phys. Rev.* D79, 129903 (2009)].
- [147] J.-L. Lehners and P. J. Steinhardt, “Intuitive understanding of non-gaussianity in ekpyrotic and cyclic models,” *Phys. Rev.* **D78** (2008) 023506, [0804.1293](#). [Erratum: *Phys. Rev.* D79, 129902 (2009)].
- [148] F. Finelli, “Assisted contraction,” *Phys. Lett.* **B545** (2002) 1–7, [hep-th/0206112](#).

- [149] A. Ijjas and P. J. Steinhardt, “The anamorphic universe,” *JCAP* **1510** (2015) 001, [1507.03875](#).
- [150] Y.-S. Piao, “Conformally Dual to Inflation,” [1112.3737](#).
- [151] C. Wetterich, “Hot big bang or slow freeze?,” *Phys. Lett.* **B736** (2014) 506–514, [1401.5313](#).
- [152] M. Li, “Generating scale-invariant tensor perturbations in the non-inflationary universe,” *Phys. Lett.* **B736** (2014) 488–493, [1405.0211](#). [Erratum: *Phys. Lett.* B747, 562 (2015)].
- [153] G. Domenech and M. Sasaki, “Conformal Frame Dependence of Inflation,” *JCAP* **1504** (2015) 022, [1501.07699](#).
- [154] R. Blumenhagen, D. Lust, and S. Theisen, “Basic concepts of string theory,” *Basic concepts of string theory*, Springer Verlag (2013).
- [155] F. Finelli, A. Tronconi, and G. Venturi, “Dark Energy, Induced Gravity and Broken Scale Invariance,” *Phys. Lett.* **B659** (2008) 466–470, [0710.2741](#).
- [156] J. D. Barrow and K.-i. Maeda, “Extended inflationary universes,” *Nucl. Phys.* **B341** (1990) 294–308.
- [157] L. Amendola, M. Litterio, and F. Occhionero, “The Phase space view of inflation. 1: The nonminimally coupled scalar field,” *Int. J. Mod. Phys.* **A5** (1990) 3861–3886.
- [158] A. Y. Kamenshchik, A. Tronconi, and G. Venturi, “Reconstruction of Scalar Potentials in Induced Gravity and Cosmology,” *Phys. Lett.* **B702** (2011) 191–196, [1104.2125](#).
- [159] T. Qiu, J. Evslin, Y.-F. Cai, M. Li, and X. Zhang, “Bouncing Galileon Cosmologies,” *JCAP* **1110** (2011) 036, [1108.0593](#).
- [160] T. Qiu and Y.-T. Wang, “G-Bounce Inflation: Towards Nonsingular Inflation Cosmology with Galileon Field,” *JHEP* **04** (2015) 130, [1501.03568](#).
- [161] A. M. Levy, A. Ijjas, and P. J. Steinhardt, “Scale-invariant perturbations in ekpyrotic cosmologies without fine-tuning of initial conditions,” *Phys. Rev.* **D92** (2015), no. 6 063524, [1506.01011](#).

- [162] J.-L. Lehners and E. Wilson-Ewing, “Running of the scalar spectral index in bouncing cosmologies,” *JCAP* **1510** (2015) 038, [1507.08112](#).
- [163] M. C. Johnson and J.-L. Lehners, “Cycles in the Multiverse,” *Phys. Rev.* **D85** (2012) 103509, [1112.3360](#).
- [164] J.-L. Lehners, “Eternal Inflation With Non-Inflationary Pocket Universes,” *Phys. Rev.* **D86** (2012) 043518, [1206.1081](#).
- [165] J. Khoury, J.-L. Lehners, and B. Ovrut, “Supersymmetric  $P(X,\phi)$  and the Ghost Condensate,” *Phys. Rev.* **D83** (2011) 125031, [1012.3748](#).
- [166] M. Koehn, J.-L. Lehners, and B. A. Ovrut, “Higher-Derivative Chiral Superfield Actions Coupled to  $N=1$  Supergravity,” *Phys. Rev.* **D86** (2012) 085019, [1207.3798](#).
- [167] J.-L. Lehners, “Diversity in the Phoenix Universe,” *Phys. Rev.* **D84** (2011) 103518, [1107.4551](#).

## **Selbstständigkeitserklärung**

Hiermit erkläre ich meine Dissertation selbstständig ohne fremde Hilfe verfasst zu haben und nur die angegebene Literatur und Hilfsmittel verwendet zu haben.

Angelika Fertig  
Potsdam, 21. März 2016